SUPERCRITICAL FLUID SPRAY APPLICATION PROCESS FOR ADHESIVES AND PRIMERS

SERDP Project PP-1118

Marc D. Donohue

Principal Investigator

Johns Hopkins University

March 2003

Report Documentation Page

Form Approved
OMB No. 0704-0188

1. REPORT DATE	2. REPORT TYPE	3. DATES COVERED
MAR 2003		**00-00-2003 to 00-00-2003**

4. TITLE AND SUBTITLE	5a. CONTRACT NUMBER
Supercritical Fluid Spray Application Process for Adhesives and Primers	5b. GRANT NUMBER
	5c. PROGRAM ELEMENT NUMBER
6. AUTHOR(S)	5d. PROJECT NUMBER
	5e. TASK NUMBER
	5f. WORK UNIT NUMBER
7. PERFORMING ORGANIZATION NAME(S) AND ADDRESS(ES) **Johns Hopkins University,Laurel,MD,20723-6099**	8. PERFORMING ORGANIZATION REPORT NUMBER
9. SPONSORING/MONITORING AGENCY NAME(S) AND ADDRESS(ES)	10. SPONSOR/MONITOR'S ACRONYM(S)
	11. SPONSOR/MONITOR'S REPORT NUMBER(S)

12. DISTRIBUTION/AVAILABILITY STATEMENT
Approved for public release; distribution unlimited

13. SUPPLEMENTARY NOTES

14. ABSTRACT

15. SUBJECT TERMS

16. SECURITY CLASSIFICATION OF:			17. LIMITATION OF ABSTRACT	18. NUMBER OF PAGES	19a. NAME OF RESPONSIBLE PERSON
a. REPORT **unclassified**	b. ABSTRACT **unclassified**	c. THIS PAGE **unclassified**	**Same as Report (SAR)**	**207**	

Preface

Project Background

In this project, we reformulated various solvent borne, high volatile organic compound (VOC) adhesives and adhesive primers, as cited in SERDP's Statement of Need, for application by a supercritical carbon dioxide spray process. Over the last several years, a new spray application process has been developed for polymeric based paints and other coatings that can reduce solvent VOC emissions up to 80%. This process was conceived by the principal investigator of this project and has been commercialized by the Dow Chemical Company. This unique process (known as the UNICARB® process) is based on the use of supercritical carbon dioxide as a replacement for organic solvents in multi-component spray coating formulations. By adapting this process to adhesives and adhesive primer applications, stringent compliance standards can be achieved respective to environmental, toxicological, materials compatibility, and, physical property performance characteristics as outlined in the original proposal and Statement of Need. Furthermore, by employing this process to apply adhesives that are presently used in the military, the costs incurred for developing and testing new (different) low/no-VOC, non-structural adhesives will be negated.

To accomplish this task, a systematic program was implemented aimed at understanding the thermodynamic and rheological properties of adhesive-solvent-carbon dioxide mixtures for each type of adhesive and primer. Additionally, optimal conditions of temperature, pressure, and polymer/solvent ratio were determined for each adhesive and primer type such that proper atomization and film formation was achieved while simultaneously VOC emissions are minimized. Concurrent with this project was a design and engineering effort to miniaturize this process to make it portable and versatile for the many different military applications and contractor venues.

Advantages of adopting this process include but are not limited to: reduction in VOC emissions; reduction in solvent costs; use of existing and proven adhesives and primers; more evenly distributed coatings; reduction in labor costs; reduction of worker health and safety costs; and, reduction of costs associated with hazardous material management respective to permits and emission control equipment.

Objective

The overall objective of this project was to provide to the military an adhesive application spray process that minimizes VOC emissions and reduces costs associated with the use of organic solvents. In doing so, this application process was constructed to be both a permanent process for use in a high volume manufacturing operation and a portable process for use in a repair or small volume manufacturing setting. To accomplish this, this project addressed six key areas that fulfilled this objective. They were as follows:

- Reformulated adhesives and adhesive primers such that they were adapted to this process;
- Developed phenomenological understanding of multi-phase thermodynamic and rheological properties;
- Determined optimal spray application properties;
- Developed a hand-held, high pressure, refillable spray device;
- Performed bench and mil-spec testing of adhesion and other physical properties; and,
- Performed assessment of reduction in environmental impacts.

The primary objective of this research effort was to determine the single-phase region of temperature and pressure where the polymer-solvent-carbon dioxide mixture coexists for each type of adhesive and adhesive primer. It is the existence of this low-pressure, one-phase region where the supercritical carbon dioxide spray process becomes possible. To determine this

operating window, a systematic experimental procedure was employed to map out phase diagrams for each mixture while at the same time a phenomenological understanding was created respective to thermodynamic and rheological properties. By employing a dual experimental and phenomenological approach, each successive effort to adapt this process to a different adhesive or adhesive primer was accomplished in a more efficient manner. Furthermore, a design and engineering effort was implemented which miniaturized the UNICARB® process to make it portable. In doing so, modifications to the process and operating conditions were made such that it can be used in a two-phase, semi-batch mode.

There are two important physical properties that will determine whether a particular polymeric based adhesive can be reformulated to adapt to the UNICARB® process. The first is whether or not the one phase region exists at low pressures (between 1000 psi and 2000 psi) and the second is that the viscosity of the mixture in the one-phase region must be low enough to achieve good atomization.

At the genesis of this project, there had been few experimental studies of polymer-solvent-carbon dioxide mixtures on which to base a reformulation of existing adhesive/solvent mixtures for adaptation to the supercritical spray process. Similarly, our knowledge of phenomenological behavior was inadequate in predicting when solids would precipitate in the system and how to change process conditions to eliminate them once they had formed. Phase diagrams for polymer-solvent-carbon dioxide systems are considerably more complicated than for typical systems of liquid-liquid immiscibilities. Specifically, more information was needed respective to the phase behavior of polymer-solvent-supercritical fluid mixtures, particularly those where solid phases can form. Once this was understood, adaptation of the process for different types of adhesives was possible.

To accomplish the above task, a parallel effort was made to develop a phenomenological understanding related to thermodynamic and rheological properties of these mixtures and the

process in general. This consisted of developing models that enabled correlation of the existing data and resulting qualitative prediction of the behavior for new systems. The emphasis was on understanding: 1) the effects of hydrogen bonding on the liquid-liquid phase behavior; 2) the effects of solids precipitation on the overall phase diagram; and, 3) the effects of density and pressure on the phase diagrams using an equation of state.

Similarly, development of the hand-held device was made easier once these effects were understood. Consider that this device is a semi-batch, closed system where the pressure and chemical species concentrations are dynamically changing as the mixture is being sprayed onto a substrate. This makes operation of the system more complex in that the operating window of temperature and pressure as well as the operating line must be clearly understood for this to perform correctly. Also, the spray nozzle needed to be designed and engineered to exploit this effect over the duration of the spray operation.

Technical Approach

Background

A new process has been developed which has significantly reduced VOC emissions during spray-coating operations by using high-pressure carbon dioxide to replace much of the solvent in paint formulations (1-5). This process, know as the UNICARB® process (UNICARB® is a registered trademark of the Union Carbide Corporation) was both patented and commercialized in 1990. Its first commercial uses were found in the application of cellulose nitrate coatings on fine wood furniture, and application of acrylic paints at the General Motors' plant in Saginaw, Michigan. A simple schematic of the process, configured for continuous operation, can be found in Figure 1.

Though carbon dioxide is a "green-house" gas, its use in the UNICARB® process actually reduces the total amount of carbon dioxide emitted. In the UNICARB® process, carbon dioxide replaces solvent on approximately a pound for pound basis. Since organic solvents emitted to the atmosphere eventually oxidize to produce about three pounds of carbon dioxide, there is a direct reduction of CO_2 that is emitted to the atmosphere. Furthermore, in addition to being environmentally compatible, carbon dioxide has other advantages that make it ideal for coating applications which include: 1) A low critical temperature (31°C); 2) a low critical pressure (1070 psi); 3) exceedingly slight health and toxicological effects (TLV for exposure is 5000 ppm); 4) inherent nonflammable and inert physical properties; and, 5) its low-cost (approximately $0.09 per pound) and availability (four billion pounds are marketed yearly in the United States).

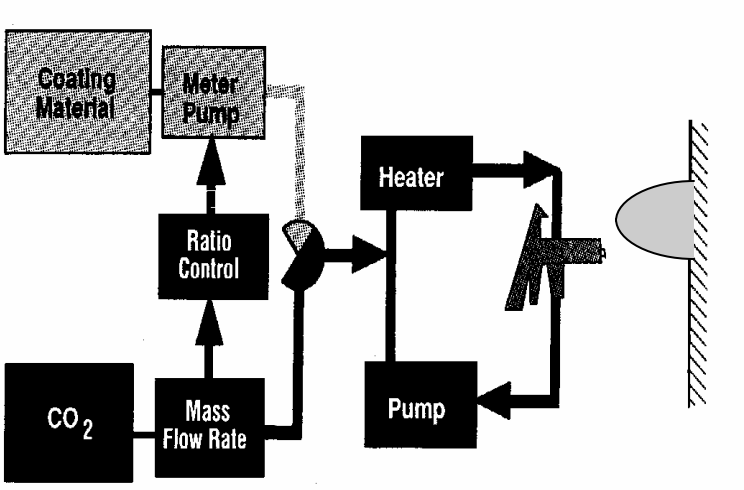

Figure 1 Simplified schematic of the UNICARB® spray process

Conceptually, the UNICARB® process is straightforward in that a concentrated solution of polymeric materials, pigments, and other additives are mixed in situ with high-pressure carbon dioxide and then sprayed. In practice, the process is complicated by the fact that one is mixing an incompressible, highly viscous material (polymeric material and solvent) with a highly compressible fluid of very low viscosity (supercritical carbon dioxide).

Consider that polymeric based paint formulations are complex mixtures that often contain thirty or more components including binders, pigments, surfactants, flow-control agents, and organic solvents. Similarly, solvent-based adhesives can be considered to be a solid polymeric resin dissolved in a solvent. The solvents used for both paints and adhesives are mixtures of volatile organic compounds which are specifically chosen for their ability to dissolve a given material and also to reduce its viscosity. The organic solvents are a combination of "fast" and "slow" evaporating solvents which serve a variety of purposes related to viscosity reduction, film formation, and adhesion. In spraying paints and coatings, the primary function of organic solvents are to: a) reduce viscosity enabling atomization of the material being sprayed; and, b) to facilitate in droplet coalescence on the substrate surface thereby providing a coherent, uniform film. In the supercritical spray process, supercritical carbon dioxide replaces that fraction of the organic solvent that is needed to give the viscosity reduction necessary for spray atomization. While some solvent is still needed for film formation, VOC emissions can be reduced substantially.

Methods

Before a polymeric material can be adapted to the UNICARB® process, the phase behavior of that material (i.e. the adhesive) with carbon dioxide has to be known. Mixtures of high-pressure carbon dioxide with the adhesive concentrate must exist as a single phase at elevated pressures for the UNICARB® process to work. Furthermore, on depressuriztion of the mixture, it is necessary for the mixture to pass through two phase boundaries to obtain enhanced atomization. The process occurs in a flow regime that is

known as “choked flow” whereby the coating material exits the spray nozzle at a pressure of several hundred pounds per square inch. This phenomena is what allows for enhanced atomization, even for highly viscous materials. Conversely, in typical airless spray application process, the coating material exits the spray nozzle at atmospheric pressure.

To-date little is known of the phase behavior of polymer-solvent-carbon dioxide mixtures, and determining the underlying thermodynamic and rheological behavior is an arduous trial and error process. Additionally, precipitation of solids in solution have been encountered and need to be avoided for when using this process. References 6 through 11 describe some of the work in the field as well as the general thermodynamic behavior of these systems.

Another operating parameter that needs to be considered is the “slow” solvent to polymer ratio. For the UNICARB® process, one wants the minimum amount of solvent possible and hence would like polymer to solvent ratios preferably in the range of three to five. While the work in the references stated above is of great value, all of the experimental data in the open literature are for polymer to solvent ratios less than 0.2 and most of this data is for solvent to polymer ratios in the range of 0.05 to 0.01. Recent experimental work at Johns Hopkins Univeristy consists of a comprehensive experimental program to measure the behavior of polymer-solvent-carbon dioxide systems at low solvent concentrations. Furthermore, there have been several systems investigated where the polymer-solvent combinations are relevant to the adhesive industry and the phase diagrams have been mapped. All of the polymer-solvent-carbon dioxide systems that have been investigated at Johns Hopkins are listed in Table 1 in the Appendix. It should be noted that some of the polymers investigated are used in adhesive

formulations (12), namely acrylic polymer, poly (methyl methacrylate), and, cellulose acetate butyrate.

As noted above, mixtures of high-pressure carbon dioxide with the paint concentrate must exist as a single phase. Polymer-solvent-carbon dioxide mixtures generally have phase diagrams of types III and IV (6), but in the pressure - temperature projections of systems containing polymers, the Liquid-Liquid-Vapor lines tend to fall on top of the vapor pressure curve of the solvent. This results in phase diagrams that look like Figure 2.

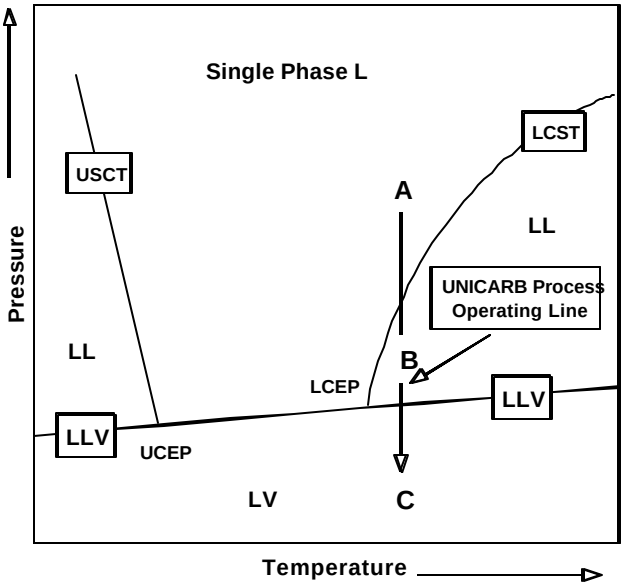

Figure 2 Schematic phase diagram for a polymer/solvent/ supercritical fluid mixture. The process conditions for the UNICARB® process are shown, starting from about 100 PSI above the LCST curve (Point A), the mixture first forms a liquid-liquid mixture (Point B, inside the nozzle) before forming a Liquid-Vapor binary (Point C, outside the spray nozzle).

The single phase region (L) is bounded by the upper critical solution temperature (UCST) curve at temperatures lower then the upper critical end point (UCEP), by the vapor-liquid (LV) equilibrium line for temperatures between the UCEP and lower critical end point (LCEP) and the lower critical solution temperature (LCST) line for temperatures greater then the LCEP. The high temperature liquid-liquid (LL) region contains a polymer-rich liquid phase and a carbon dioxide-rich phase with the solvent distributed between them. It is bounded by the LCST curve as pressure is increased and a liquid-liquid-vapor (LLV)

phase boundary as pressure is decreased. The LV region is bordered by the LV or LLV curve over the entire range of temperature as pressure is increased. As the carbon dioxide concentration is increased, the bubble point curve shifts to higher pressures and the temperature, at which the LL region appears shifts to lower temperatures. The exact shape of the diagram depends on the polymer, the solvent and the polymer concentration.

In the UNICARB® process, the liquid spray mixture must pass from the single phase region (Point A) through the LL (Point B) region during depressurization in order to obtain good atomization. Enhanced atomization occurs because the dissolved carbon dioxide nucleates to form a liquid phase before forming the gas phase (Point C). Figure 3, in the Appendix, shows phase behavior of mixtures of supercritical carbon dioxide with; a) Poly (methyl methacrylate) in methyl ethyl ketone; acrylic-melamine at 70% polymer level; cellulose acetate butyrate in methyl amyl ketone; and, polystyrene in tetrahydrofurane. The lines that are nearly horizontal are LV curves and the steeper lines are curves representing the locus of lower critical solution temperatures (LCST).

A high pressure view cell is used to determine the phase behavior of supercritical carbon dioxide-solvent-polymer mixtures and will be used to obtain data for this project. Information which may be obtained include densities, viscosities, solubilities and equilibrium phase boundaries. The cell (on loan from Union Carbide) is rated for pressures up to 3300 PSI at 350F, but higher rated cells can be built if necessary. In Figure 4, in the Appendix, a cross section of the high pressure cell is shown. The cell content is well mixed by an electro-magnetically driven stirring bar. Carbon dioxide is supplied via a feed line from a carbon dioxide feed cylinder. The carbon dioxide content can be increased during the experiment. Phase changes inside the cell are viewed by a

camera and displayed on a monitor with the potential to capture phase behavior on a video recorder. Light is supplied at the top of the cell from a halogen light source .

As stated above, though there have been several experimental studies (6-11) of polymer-solvent- carbon dioxide mixtures, our knowledge base still is inadequate to provide the heuristics necessary to reformulate existing commercial adhesive compositions so they can be used in the UNICARB® process. Our knowledge also is inadequate to predict when solids will precipitate in the system or how to change process conditions to eliminate them once they have formed. We performed a combination of experiments that provided this information and therefore facilitate widespread implementation of this spray technology to adhesives. While the UNICARB® process was developed as a continuously operating process, we additionally have to developed a portable version using supercritical carbon dioxide to replace VOC's based on the UNICARB® technology.

Specifically, in the experimental part of the project, we measured phase diagrams and solution viscosities for polymer-solvent-carbon dioxide mixtures. As illustrated in Table 1, we already have considerable experience in performing these measurements. The measurements focused on polymer formulations (e.g., rubber-based adhesives) relevant to the DOD's needs. The key variables to measure lie on the boundaries of the one-phase region shown in Figure 2. Measurements of pressure, temperature, composition, and viscosity were made. The equipment outlined above, to be used in these experiments is shown schematically in Figure 2. In addition to being able to measure the phase diagrams, this apparatus is able to measure solution viscosities in situ for single-phase systems.

Noting that there are two important physical properties that will need to be determined as to whether a particular polymeric based adhesive can be reformulated to adapt to the UNICARB® process; i.e., does the one phase region exist at low pressures as depicted in Figures 2; and, the viscosity of the mixture in the one-phase region low enough. For the UNICARB® process to work, the viscosity at point A in Figure 2 cannot be much greater than ten poise (1000 cP).

For polymer-solvent-carbon dioxide mixtures, the viscosity depends strongly on the carbon dioxide concentration and on the polymer/solvent ratio. The key for minimizing VOC emissions is determining the optimal conditions of temperature, pressure, and polymer/solvent ratio that give the proper viscosity for both atomization and film formation. Since this must be done by trial and error for each different formulation, it takes a substantial amount of time. However, while the mechanistic understanding has been developed for the physical phenomena respective to paint mixtures which, in turn, has given rise to phase diagrams like Figure 2, the same path has been followed for existing adhesives such that they can be reformulated to adapt to the process within this project. In summary, these measurements allow for reformulation of existing adhesive mixtures to the UNICARB® spray technology, replacing VOCs with supercritical carbon dioxide, which not only is environmentally benign but also will resolve other disadvantages using solvent or water based adhesives as outlined above.

The UNICARB® process was developed as a continuously operating process requiring a single phase polymer/solvent/supercritical fluid to start the process. While, as outlined above, adhesives can be reformulated to this process, we also have "miniaturized" this technology and made it portable.

This portable system operates in the following manner. The vessel is filled with approximately 140 cubic centimeters of concentrated adhesive (i.e., polymer and "slow" solvent). After securing the lid, supercritical carbon dioxide is loaded until the can is pressurized to approximately 2000 psi (the exact pressure was be determined for each adhesive during the course of the research project). A substantial amount of the carbon dioxide will dissolve in the polymeric material. This is in contrast to traditional hand-held spray cans where the gas's function is a propellant to force material out of the canister (usually butane or nitrogen) and does not dissolve appreciably in the adhesive (or paint). Essentially, this miniature UNICARB® system starts with a two phase system (i.e., carbon dioxide-rich and polymer-rich phase), and in this case, it is crucial to know, how much of the carbon dioxide dissolves in the polymer phase and how much of the usually heavy (slow) solvent of the adhesive concentrate is extracted into the carbon dioxide phase. To gain a better understanding for this type of mixture behavior, and to find proper operating conditions for the devise proposed, ternary mixture (polymer-solvent-carbon dioxide) diagrams were measured and mapped.

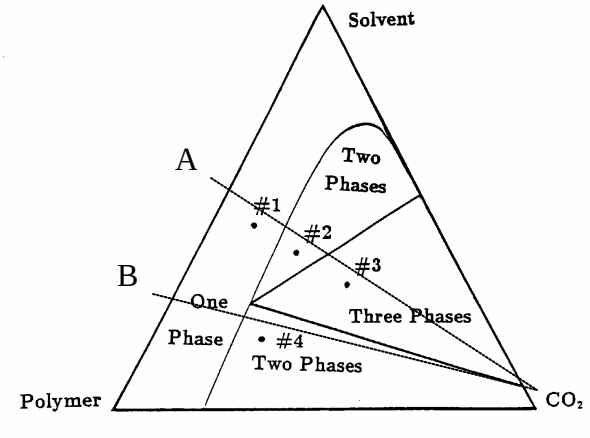

Figure 4 - Ternary phase diagram.

Figure 4 shows a ternary diagram for a polymer-solvent-supercritical fluid mixture at constant temperature and pressure containing one-, two- and three-phase regions. It is bounded on the left by a curve that detaches very close to the high solvent concentration and then moves almost parallel to the polymer-solvent axis until it intersects with the

polymer-supercritical fluid axis. Note that for the self-contained miniaturized UNICARB® system, the concentrations of the chemical species in the vessel changes as the volume of the adhesive left in the can changes with spraying. This results in a dynamic shift in the phase boundaries and miscibilities of the species as the process continues. As such an extended operating window needs to be delineated respective to the phase diagrams for this process.

Starting with a low to medium concentrated polymer/solvent binary (Point A), the mixture exists in the single phase region for low supercritical fluid concentrations (Point #1). An increase in the SCF concentration (i.e. one moves on a straight line drawn through the lower left hand corner) brings the system into the two phase region (solvent-rich and polymer-rich phase, LL or LF, Point #2). At SCF concentrations typically above 90%, a predominantly carbon dioxide vapor phase is formed, that is, three phases coexist (LLV or LLF, Point #3). Starting with a highly concentrated polymer/solvent binary (Point B), adding SCF will bring the system into the two phase region (LV, Point #4). As temperature or pressure increases, the lines in the ternary diagram shift.

Figure 5 shows a model ternary phase diagram. Tie-lines relate the liquid mixture composition to the gas phase composition which essentially is a pure gas. Starting out with a highly concentrated polymer solution (Point A), the addition of a substantial amount of supercritical fluid would lead to point B in the diagram, which means that the gas phase is essentially pure SCF and the liquid phase leaving the spray can has a composition indicated by C. Using up adhesive concentrate, the composition will change and from point B one would move to point D. However, since the tie lines are essentially flat, the composition of the liquid adhesive concentrate leaving the can is still very much

like the one before, as indicated by point E. The slope of the tie-lines and the ternary diagram itself very much depend on the polymer system and solvent used, that is, it is possible to have tie-lines with the opposite slope. Therefore, it is important for the hand-held device to work within the boundaries of the tie-lines to maintain the same concentration and quality of material over the duration of the spraying procedure.

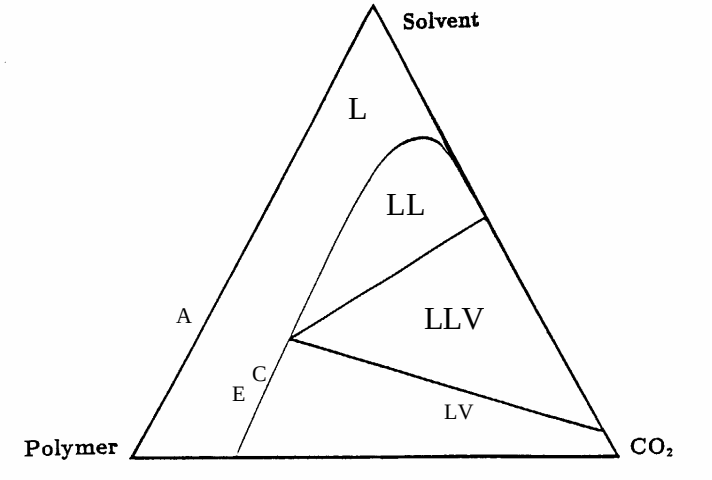

Figure 5 Ternary diagram as it relates to the new process. Tie-lines are drawn to relate the liquid mixture composition to the gas phase composition which essentially is a pure gas. Load concentrated adhesive (A) and add SCF (B), mixture sprayed is C; as devices is emptied one would move to D, mixture sprayed is E.

Additionally to the development of the device itself, we performed measurements of ternary phase diagrams for adhesive concentrates. The temperature and pressure dependence was determined since the pressure in the vessel decreases when adhesive is sprayed. The temperature dependence is important because the solubility of the supercritical carbon dioxide fluid in the polymer phase depends on temperature as well. Once operating ranges for prospective adhesives have been determined, the new spray prototype was built and tested.

A parallel aspect to this research effort was to develop a phenomenological understanding of thermodynamic and rheological properties. Though this is not necessary for initial studies, it greatly enhanced our ability to adapt other existing adhesives as well as formulate for entirely new adhesive materials. However, each successive iteration of the experimental phase of this project respective to each type of

adhesive was accomplished in a much shorter time frame. Similarly, new adhesives which are developed at some future date and incorporated into military uses can be adapted readily.

To obtain understanding of thermodynamic and rheological properties, models were developed that enable correlation of the existing data and at least qualitative prediction of the behavior for new systems. The emphasis was on modeling the effects of hydrogen bonding on the liquid-liquid phase behavior and on modeling the effects of solids precipitation on the overall phase diagram. Our modeling efforts began with lattice theories (the Lattice Cluster Theory of Freed and coworkers (13-15)) so that we could understand the effects of molecular weight, molecular structure, and melting point. When we were confident that we can model the solid-liquid equilibria for polymer-solvent mixtures, we will begin working with an equation of state to model the effects of density and pressure on the phase diagrams. We began this using the Simplified-Perturbed Hard Chain (SPHCT) equation (16). Peters et al. (17, 18) and Gasem and Robinson (19) have found that the SPHCT equation is superior to cubic equations commonly used in engineering calculations for long chain molecules. Van Pelt et al. (20) also have shown that the SPHCT is able to predict the types of phase diagrams exhibited by polymer/solvent/supercritical fluid mixtures.

Research Team

This project involved collaboration among scientists and engineers at several organizations. Briefly, the organizations involved, the key personnel, and their contributions were:

- Johns Hopkins University
  Marc D. Donohue, Department of Chemical Engineering
  Glen D Gaddy, Department of Chemical Engineering

- Army Research Laboratories (Aberdeen, MD)
  Gumersindo Rodriguez, Polymers Research Branch, Materials Division

- Airforce (Wright-Patterson Airforce Base, OH)
  Alan J. Fletcher, Systems Support Division, Materials Directorate

- Army Tank-automotive and Armaments Command (Warren, MI)
  Thomas Landy, Integrated Process Team Chair

- Army Aviation and Missle Command, Redstone Arsenal
  Steven F. Carr, Materials Directorate

- Dow Chemical Company
  Kenneth Nielsen, UNICARB Division
  Jeffrey Goad, UNICARB Division

- Thar Designs
  Lalit Chordia, President

- 3M Corporation
  Brian Johnson, Adhesives Research Division

Summary

The overall objective of this project was to provide to the military an adhesive application spray process that minimizes VOC emissions and reduces costs associated with the use of organic solvents. In doing so, this application process was constructed to be both a permanent process for use in a high volume manufacturing operation and a portable process for use in a repair or small volume manufacturing setting. Six key areas were addressed to fulfill this task. They are as follows:

- Reformulation of adhesives and adhesive primers such that the can be adapted to this process;
- Develop phenomenological understanding of multi-phase thermodynamic and rheological properties;
- Determine optimal spray application properties;
- Develop hand-held, high pressure, refillable spray device;
- Perform bench and mil-spec testing of adhesion and other physical properties; and,
- Perform assessment of reduction in environmental impacts.

As a result, this report contains the output of each of the efforts above including data sets, formulations, and equipment descriptions.

Table of Contents

1. Supercritical Carbon Dioxide: Poor Solvent, Good Solute

1.1 Introduction

Supercritical carbon dioxide can be used in a variety of chemical processes. Processes such as spraying of paint coatings and adhesives (1-3), synthesis of polymers with microcellular structures (4), and drying of silica aerogel (5-11) already have been developed into commercial applications. The growing popularity of using supercritical carbon dioxide also has been documented in the literature for supercritical fluid extraction (SFE) (12-14), pharmaceutical applications (15-16), supercritical fluid cleaning technology (17-26), and polymer synthesis (27-29). Nevertheless, despite the substantial interest in developing applications using supercritical carbon dioxide, the specific roles and properties of carbon dioxide that make a supercritical process possible and advantageous often have been misunderstood. The consideration of supercritical carbon dioxide being only a solvent is a common stereotype. The fact is that supercritical carbon dioxide can behave as a solvent or a solute, but it is a poor solvent and a good solute. In applications such as spraying paint, coatings, and adhesives, aerogel-making, and impregnations, carbon dioxide can behave either as a solute, or in a mixed role of solute and solvent, but not solely as a solvent. By understanding how supercritical carbon dioxide behaves in a particular process, efforts will not be wasted on improving its solvent properties if supercritical carbon dioxide were meant to behave as a solute. Thus, this introduction will provide a review on the spectrum of technologies using

supercritical carbon dioxide with emphasis on clarifying the role of supercritical carbon dioxide in each process.

1.2 Supercritical Fluids

A supercritical fluid is defined as a substance existing above its critical temperature and pressure, as illustrated in the simple P-T phase diagram shown in Figure 1.1. Supercritical fluids have a number of properties that make them useful in industrial processes. Table 1.1 compares some properties of a supercritical fluid with those of a liquid and a gas (30). In the supercritical region, fluids can have near liquid-like density and near gas-like transport properties. Density is an important factor in determining solubility of solutes in supercritical fluids, and it can be 700 times higher than the density of a gas. The density of a supercritical fluid also depends strongly on pressure. Figure 1.2 shows the density of a supercritical fluid as a function of pressure. In the region near the critical point, a slight increase in pressure can cause the density to increase by a factor of 2, which can cause a significant change in the solubility behavior of the supercritical fluid. Contrary to density and solubility behavior, the transport properties of supercritical fluids typically are gas-like, and are not as sensitive as density to pressure changes. Gas-like transport properties are desirable for processes limited by diffusivity or viscosity.

1.3 Supercritical Fluid as a Solvent

Supercritical carbon dioxide is particularly attractive in comparison to other supercritical fluids because it is inexpensive, non-reactive, has low toxicity and low

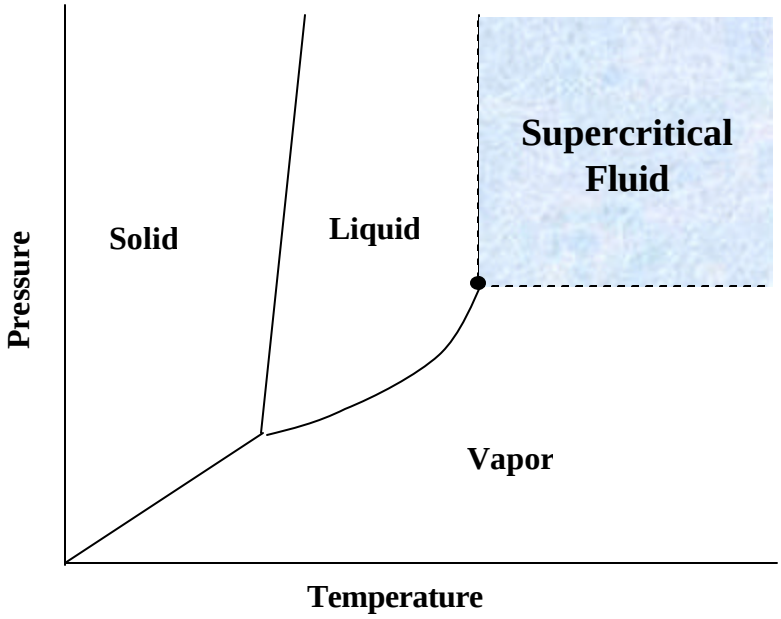

Figure 1.1: Phase diagram showing supercritical region.

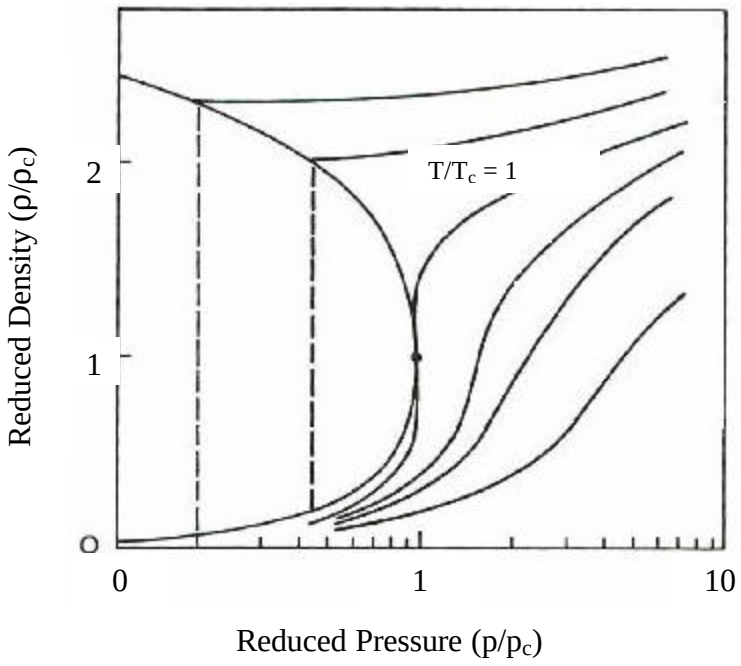

Figure 1.2: Density as function of temperature and pressure.

critical temperature (31 °C). Much of today's work focuses on applications that use supercritical carbon dioxide as a solvent, despite the fact that carbon dioxide is a poor solvent. Although supercritical carbon dioxide's density is much higher than that of a gas, it is a poor solvent because its density is not as high as a typical organic liquid. However, the properties of variable density, gas-like diffusivity and viscosity, and no surface tension can compensate for the poor solubility and allow supercritical processes to be viable alternatives to technologies using liquid solvents.

Property	Gas	SCF	Liquid
Density (kg/m^3)	1	700	1000
Viscosity (ns/m^2)	10^{-5}	10^{-4}	10^{-3}
Diffusion Coefficient (cm^2/s)	10^{-1}	10^{-4}	10^{-5}

Table 1.1: A comparison of properties of gas, SCF, and liquid (30).

1.3.1 Supercritical Fluid Extraction (SFE)

The basic scheme of SFE process consists of three steps. A solvent, typically carbon dioxide, first is heated and pressurized to a supercritical state before it enters the extraction vessel. Inside the extraction vessel, the desired chemical is extracted by supercritical carbon dioxide from either a solid matrix or a liquid feed, and is carried out of the extractor. The exit stream then is depressurized, allowing the supercritical carbon

dioxide to expand, thereby reducing its solvent power. As a result, the extracted heavy product is precipitated and carbon dioxide is recycled for reuse.

In such processes, supercritical carbon dioxide behaves as a solvent. SFE has attracted interest over the last three decades from the separation science community because it offers the advantages of reducing toxic solvent usage, easy solvent regeneration, and no solvent residue in the extract. By replacing toxic organic solvents in conventional liquid extraction processes, carbon dioxide considerably reduces the harmful effects on both the workers and the environment. Supercritical carbon dioxide also allows easy solvent separation and regeneration due to its variable density and solubility. Schultze and Donohue. (31) have shown that solubility in supercritical fluid can be correlated to solvent density. Figure 1.3 shows the solubility of naphthalene in carbon dioxide. The log-linear behavior shows that solubility is a very sensitive function of density. For example, as solvent density is increased from 2 to 6 mol/L, the solubility is increased by one order of magnitude. Therefore, easy separation of the solvent from the extract in SFE can be achieved by a simple depressurization step, in which low solubility in the solvent is caused by reduced density. The separation step in SFE processes is much more efficient in comparison to conventional liquid extraction process where the solvent separation regeneration usually involves distillation.

Although changing pressure can vary the solubility of solute in supercritical carbon dioxide, the fact remains that supercritical carbon dioxide still is a poor solvent for polar substances and macromolecules due to low density compared to liquid solvents. As a result, other solutes (cosolvents), which are called entrainers or modifiers, often are added to the supercritical fluid to make carbon dioxide a better solvent, increase

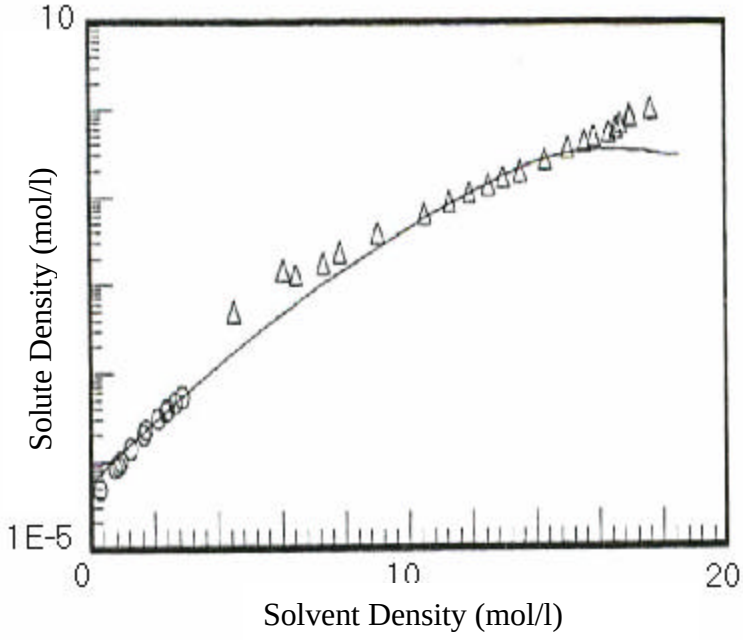

Figure 1.3: Solubility of naphthalene in carbon dioxide plotted as function of density.

the extraction efficiency, and reduce extraction time. Walsh and Donohue (32) have shown that hydrogen bonding of the cosolvent with the desired extraction solute can enhance solubility significantly. Choices of modifiers and the methods of introducing modifiers are summarized in a review by Lang and Wang (33). Some of the possible methods of introducing modifiers include a second separate stream, premixed with carbon dioxide in a single stream, and direct spiking.

The applications of SFE have been discussed widely over the past decades. According McHugh and Krukonis (34), there has been large-scale industrial success in coffee, tea, spices, and hops. High pressure equipment manufacturers for SFE, such as Uhde Hochdrucktechnik, make equipment for SFE applications ranging from extracting caffeine from coffee beans and tea, decontaminating ginseng extract, to extracting fat from tortilla chips and brewer's barley. In addition to the commercial applications mentioned, SFE is the subject of many different extraction research projects. When searched by Chemical Abstracts, more than 1000 listings were found describing SFE-related subjects. Here, the discussion of the roles of supercritical fluid is limited to only three areas of research that have been reviewed extensively by Reverchon (12), Lehotay (13), and Wai (14).

Studies have been discussed by Reverchon (12) on 37 flavor and fragrance compounds that were extracted from root, seed, leaf, flower, fruit, herb, peel, bulb, berry and rhizome using supercritical fluids. SFE of flavor and fragrance compound involves the penetration of supercritical fluid into a solid matrix, and subsequently the extraction of all compounds that can be dissolved by the supercritical fluid. Most of these studies compare the chemical characterizatics of the extract obtained by SFE to those produced

by steam distillation or solvent extraction. Product characterizatics are important to consider because essential oils are made up of many compounds, and the presence or the concentration of certain contaminants can alter the quality of the extract significantly. In general, product characterizatics are evaluated at different extraction conditions such as process pressure, temperature, extraction time, and solvent flow rate. Reverchon concluded that SFE improves quality of products by reducing artifacts and better reproducing the original flavor or fragrance.

A review by Lehotay (13) summarizes research developments and findings involving analytical methods for SFE of pesticide residue in foods. Although supercritical carbon dioxide in SFE has limited polarity range for simultaneous extraction of possible pesticide analytes when compared to the liquid solvent in traditional multiresidue method, it still offers the advantages of non-toxicity and higher selectivity. In this area of research, focus has been put on developing multiresidue methods, which are analysis techniques that are sensitive to multiple analytes. Findings in various studies identified the four categories of important parameters to be controlled in multiresidue SFE method development: choice of analytical method, trapping parameters, extraction conditions, and sample preparation. The effects of these SFE parameters on pesticide extraction in celite, soils, grains, and produce were reported by Lehotay (13).

Extraction of metal ions is another growing area of SFE research. SFE of metal-ions is a new technique that has the advantages of minimizing organic waste generation and allows direct extraction of solute from a solid matrix. SFE of metal ions can be applied to the treatment of metal contaminated waste material and mineral processing, and is an example of a SFE application that requires the use of modifiers. Due to the lack

of solubility in supercritical carbon dioxide, metal ions cannot be extracted directly. Instead, metal ions are chelated with an appropriate ligand to neutralize their charge and allow them to become soluble in carbon dioxide. A review by Wai and Wang (14) examines the important factors controlling SFE of metal species: solubility of chelating agents and metal chelates in supercritical fluid, the presence of water, pH, temperature, pressure, chemical forms of the metal species, and the solid matrix. Collectively, these parameters determine the feasibility and efficiency for SFE of metal species. The review article also examines the progress made on SFE of organometallic compounds, toxic metals, lanthanides and actinides.

1.3.2 Cleaning

Using supercritical carbon dioxide as a cleaning agent is an application based on the principles of SFE. The major advantages of this process are the reductions of conventional ozone-depleting solvent usage and time required for solvent removal. Because non-wetting surfaces are difficult to reach for most liquids due to their surface tension, the absence of surface tension for supercritical carbon dioxide also can be an advantage, even though it usually is not important in SFE. Similar to its behavior in SFE, supercritical carbon dioxide first comes into contact with solutes, then solubilizes contaminants, and finally carries them away. Thus, the solvent power of supercritical carbon dioxide changes with density so that solute first can be extracted and later can be released. The solutes in this case are usually traces of oil and inorganic contaminants.

Supercritical carbon dioxide has been used to clean metal surfaces, pharmaceutical products, and delicate electronic parts in a number of studies. In

particular, the use of supercritical carbon dioxide has been investigated in the removal of hydrocarbons from aluminum surfaces (17), lubricant residues from aluminum sheets and foil (18), metal oxides and radioactive oxides (19), and water- and oil-soluble contaminants from metal coupons (20). Pharmaceutical products such as anterior cruciated ligament prostheses (21) and elastomeric articles (22) also have been cleaned by supercritical carbon dioxide. Electronic components cleaned by supercritical carbon dioxide include optical fiber preforms (23), micromechanical devices (e.g. landing electrode of a digital micromirror device) (24), wafers (25), and chip resistors (26). Although the basic concepts of these cleaning processes are the same in each case, the process details vary from one application to another in order meet different cleaning requirements. In the production of optical fiber preforms described by Evans *et al.* (23), residual oil is removed in one chamber and separated in another chamber. In the process patented by Wallace and Douglas (24), a micromechanical device is placed and kept in a chamber of supercritical carbon dioxide until a subsequent passivation step to remove contaminants and to prevent recontamination. Bok *et al.* (25) describe a pressure pulsation mechanism to stimulate improved mixing and dissolution of the contaminants from wafers. In addition to active research in this area, developments in cleaning with supercritical carbon dioxide also have spread to commercial applications. AT&T installed a supercritical carbon dioxide cleaning system in 1994 to remove traces of oil from long quartz rods (35). Praxair, Inc., and Supercritical Systems, Inc. jointly are developing a semiconductor wafer cleaning system that uses supercritical fluids to remove photoresist (36).

1.3.3 Supercritical Fluid Chromatography

SFC is another area of separation science that uses a supercritical fluid as solvent. In comparison to high performance liquid chromatography (HPLC), SFC can offer faster analysis time, better resolution, and the ability to separate thermally unstable compounds. SFC and HPLC share similar concepts but differ in the materials used as the mobile phase. SFC uses a supercritical fluid as the mobile phase whereas HPLC uses a liquid. In the first step of SFC, compressed carbon dioxide is pumped in as a liquid, and then it is heated to above its critical temperature to become a supercritical fluid. The sample is injected and dissolved into the supercritical carbon dioxide, which subsequently carries the sample through the stationary phase. The temperature is held above the critical temperature at both the injector and the column using an oven. Studies and challenges regarding capillary column SFC and packed column SFC have been reviewed recently by several authors (37-39).

Capillary column SFC has attracted interest because some non-volatile samples can be separated with high efficiency. However, success has been limited to the separation of non-polar polymers or mixtures of analytes whose polarities are similar, in which separation is dependent on size and volatility instead of differences in polarity. In the review by Smith (37), the separation of mixtures of alkanes from C_{20} to $C_{>100}$ and the separation of natural and synthetic waxes are discussed. In normal-phase separation mode, packed column SFC is a faster analytical method than HPLC. The retention mechanism in normal-phase mode of separation is the interaction of the polar analyte with the polar stationary phase, where as in reversed-phase mode, the retention mechanism is the interaction of the nonpolar analyte with the nonpolar stationary phase.

Because supercritical carbon dioxide does not have high polarity, it is a poor choice of solvent for nonpolar analytes in the reversed-phase separation mode. Thus, applications of SFC generally are limited to normal-phase method. Smith reviews separations favoring this mode, such as enantioseparation of chiral analytes (37). Due to the success and popularity gained in the recent years, enantiomer separations by packed column SFC have been reviewed in a number of publications (38-42). In addition to reviewing enantioseparation by packed column SFC, Terfloth (40) discusses enantioseparation by capillary column SFC. Other packed column SFC applications such as basic, neutral, and acidic analytes are reviewed by Berger (39). Additionally, SFC applications for natural products, agrochemicals, fossil fuels, lubricants, waxes, polymer-related materials, and pharmaceutical compounds are reviewed by Chester (38) and SFC applications for carbohydrates are reviewed by Lafosse (42).

1.3.4 Polymerizations

Supercritical carbon dioxide offers several advantages over traditional solvents as a polymerization reaction medium: energy-intensive drying requirements are eliminated, the solvent is environmentally benign, and reaction kinetics often are improved due to the transport properties of supercritical fluids. Polymerizations are carried out either as homogeneous processes or heterogeneous processes; this is governed by the solubility of the different components of the reaction (monomer, catalyst, and polymer) in the supercritical solvent. Kiran (27), Kendall *et al.* (28), and Cooper (29) have reviewed both homogenous and heterogeneous polymerization processes in supercritical fluid media. Polymerization mechanisms using supercritical carbon dioxide as the solvent include free

radical, cationic, transition metal-catalyzed, thermal ring-opening polymerization reactions, and oxidative coupling.

As described in Kendall *et al.*, all components remain in solution with supercritical carbon dioxide in homogenous polymerization; whereas in heterogeneous polymerization, one or more components are insoluble in supercritical carbon dioxide. Applications of homogenous polymerization have been limited because most polymers have low solubilities in carbon dioxide. An exception is fluoropolymers, which have good solubilities in chlorofluorocarbons (CFC) and carbon dioxide. DeSimone *et al.* (43) reported that 1-1-dihydroperfluirooctyl acrylate (FOA) was synthesized by homogeneous free-radical polymerization in supercritical carbon dioxide. The kinetics of polymerization of FOA in supercritical carbon dioxide was studied in detail by Guan *et al.* (44) and van Herk *et al.* (45). Factors such as decomposition rate, initiator efficiency, and propagation rate were determined and compared to those reported for other solvents. The results showed that in carbon dioxide the decomposition rate is considerably lower (44) and the propagation rate is about the same (45). However, the initiator efficiency is 1.5 times higher (44). The higher initiator efficiency can be explained by the reduction of the solvent cage effect in carbon dioxide. Due to the gas-like diffusivity of supercritical carbon dioxide, the cage effect is greatly reduced and diffusion is enhanced. Other homogenous polymerizations reported include free-radical polymerization of styrene and cationic polymerization of fluorinated vinyl and cyclic ethers.

Literature reports on precipitation polymerization in supercritical carbon dioxide are more common in comparison to homogeneous polymerization because the polymer does not have to be soluble in carbon dioxide. In precipitation polymerization, an

initially homogeneous mixture of monomer, initiator, and solvent becomes heterogeneous during the reaction, as insoluble polymer chains aggregate to form a separate polymer phase. Studies on precipitation polymerization in carbon dioxide have been reviewed in two publications (28,29). Some of these studies are listed in Table 1.2, which includes reports on free-radical precipitation polymerization of acrylic acid, divinylbenzene (DVB), trimethlolpropane trimethacrylate (TRM), ethylene glycol dimethacrylate (EDMA), tetrafluoroethylene (TFE) and copolymerization of TFE with hexafuoropropene (HFP) and with perfluoro (propyl vinyl ether) (PPVE). Other mechanisms discussed include cationic polymerization of isobutyl vinyl ether (IBVE),

Monomers	Precipitation Polymerization Mechanisms	References
acrylic acid	Free-radical	(46-48)
TFE	Free-radical homopolymerization	(49)
TFE/PPVE copolymer	Free-radical copolymerization	(49)
TFE/HFP copolymer	Free-radical copolymerization	(49)
TRM	Free-radical	(50)
EDMA	Free-radical	(50,51)
DVB	Free-radical	(52)
IBVE	Cationic	(53)
norbornene	Ring opening metathesis	(54,55)
phenylacetylene	Transition metal catalysis	(56)
PO/CO2 copolymer	Transition metal catalysis	(57)
CHO/CO2 copolymer	Transition metal catalysis	(58)
phenylene oxide	Oxidative coupling	(59)
polypyrrole	Oxidative coupling	(60)

Table 1.2: Precipitation polymerization of different monomers via different reaction mechanisms.

transition metal catalysis for homopolymerization of norbornene, phenylacetylene, and for copolymerization of carbonates such as propylene oxide (PO) and cyclohexene oxide (CHO).

A dispersion polymerization begins as a homogeneous mixture because of the solubility of both monomer and initiator in the continuous phase. Once the growing oligomeric

radicals reach a critical molecular weight, the chains are no longer soluble in the reaction medium and phase separation occurs. At this point, a surface-active stabilizing molecule adsorbs to or becomes chemically attached to the polymer colloid and helps prevent coagulation or agglomeration of the particles. In contrast to dispersion polymerization, the reaction mixture in an emulsion polymerization is initially heterogeneous due to the low solubility of the monomer in the continuous phase. The initiator is dissolved in the continuous phase and not in the monomer phase. The insoluble polymer is stabilized as colloidal particles. A stabilized colloid is maintained by the repulsive forces resulting from surface charges imparted by ionic initiating species, small molecule ionic surfactant, amphiphilic macromolecular stabilizer, or a combination of these additives. Studies on dispersion and emulsion polymerization in carbon dioxide have focused on designing and developing optimal macromolecular stabilizers from different types of large molecules such as macromonomers, homopolymers, random copolymers, and block copolymers. There already have been detailed reviews on the progress of research in this field (28,29) which discuss the development of surfactants for the polymerization of monomers including acrylamide, 2,6 dimethylphenylene oxide, divinylbenzene, ethylvinylbenzene, methyl methacrylate, styrene, vinyl acetate, and ethylene.

1.3.5 Particle Formation

Recrystallization and precipitation of a desired product from solution are useful techniques in particle design. In particular, micron-sized particles with narrow size distribution can be formed by precipitation using supercritical carbon dioxide. Compared to conventional techniques such as milling, recrystallization with liquid antisolvents,

freeze drying, and spray drying, the use of supercritical carbon dioxide offers the advantages of solvent reduction, no trace residues, absence of thermal degradation, and controllable particle size. Recrystallization using supercritical carbon dioxide as solvent can be done in two ways: rapid expansion of supercritical fluid solution (RESS) and precipitation with compressed antisolvents. In RESS, solute is dissolved in supercritical carbon dioxide, forming a dilute solution. The supercritical solution is subsequently expanded through a small orifice, which results in a gas-like solvent density and thus a low solubility, which causes the formation of solute particles. The abrupt transition in solvent characteristics results in the nucleation and growth of the solute species in solution, which can have a number of different forms. Products can be micron-sized particles, thin films, and fine polymer fibers depending on the application of the process. The particle characteristics are affected by operating parameters such as temperature and pressure prior to and after expansion, and nozzle geometry. Nucleation mechanisms for inorganic compounds, organic compounds and polymers during RESS process are reviewed in detail by Palakodaty and York (61).

Another method of recrystallization using supercritical carbon dioxide is precipitation with compressed antisolvents (PCA). An antisolvent is a substance used to precipitate a solute from solution. Generally, an antisolvent is immiscible with the solute, but is completely miscible with the solvent. Supercritical carbon dioxide as antisolvent can behave as a solvent or a solute depending on the design of the antisolvent process. For example, in a PCA process, carbon dioxide can behave as a solvent and/or a solute. The process begins as a solution of solute dissolved in carbon dioxide-soluble solvent is sprayed into supercritical carbon dioxide. Subsequently, when a small solution droplet is

exposed to a large excess of supercritical carbon dioxide, two precipitation mechanisms can occur. In the first mechanism, only the carbon dioxide-soluble solvent is extracted from the solution, and thus precipitating dry solute particles. In the second precipitation mechanism, supercritical carbon dioxide diffuses into the solution droplet causing it to expand in volume. Consequently, the solute is precipitated as the solubility of the solute in solvent decreases due to low solvent density. In PCA processes, these two precipitation mechanisms compete with each other, and which dominates depends on the solubility of solvent in carbon dioxide, and the solubility of carbon dioxide in the solvent. Supercritical carbon dioxide behaves as a solvent if the first mechanism dominates but it behaves as a solute if the second mechanism dominates. It also is possible that neither precipitation mechanism dominates, and carbon dioxide exhibits both solute and solvent behaviors. In addition to PCA, there is another antisolvent recrystallization process called gas antisolvent recrystallization (GAS), in which carbon dioxide behaves just as a solute while functioning as an antisolvent. This technique will be discussed in section 1.4.1.

Applications of RESS and PCA processes include pharmaceuticals, inorganic compounds, and polymer particles and coatings. Extensive studies on the production of pharmaceutical compounds by RESS and PCA are reviewed by Subramaniam *et al.* (15) Most of the pharmaceuticals produced by RESS and PCA are micron-sized particles. In a modification of RESS, Young *et al.* report the production of suspensions of cyclosporine particles by RESS into aqueous surfactant solutions (16). The water-insoluble drug is sprayed into aqueous solution to prevent particle growth and agglomeration, this also results in smaller particle size than the normal RESS into air. Using a similar technique,

Sun *et al.* (62) report the production of metal and metal sulfide nano-sized particles in stable solution. Nanocrystalline particles prepared include silver sulfide (Ag_2S), cadmium sulfide (CdS), lead sulfide (PbS), silver metal and nickel metal (63). For polymer processing, Shim *et al.* (62) used RESS to create poly(2-ehylhexyl acrylate) aqueous latexes. The size of the particles ranges from 0.5 to 2.7 microns. Tepper and Levit (64) also demonstrated the deposition of microspheres of high molecular weight poly(dimethylsiloxane) onto the sensing surface of a microfabricated transducer using the RESS technique. Patent reviews and additional literature references for RESS and PCA have been summarized in a review by Jung and Perrut (65).

1.4 Supercritical Fluid as a Solute

Although supercritical carbon dioxide is a poor solvent for most large molecules and polymers, it is a good solute, dissolving readily into different substrates. Being a good solute, supercritical carbon dioxide can be a very effective plasticizer and swelling agent (66). Thus, the use of carbon dioxide can be advantageous for processes that require low glass transition temperatures or swollen polymers.

1.4.1 Gas Antisolvent (GAS) Recrystallization

Contrary to the PCA process discussed in section 1.3.5, supercritical carbon dioxide behaves solely as a solute in the GAS process. The property of supercritical carbon dioxide being a good swelling agent is exploited by the GAS process. In GAS, supercritical carbon dioxide is dissolved in a solvent containing the solute of interest forming a ternary system. The carbon dioxide then swells and expands the solvent, and

causes the density and thus the solvent power of the solvent to decrease. As a result, the solute of interest becomes supersaturated and precipitates from the solution forming micron-sized particles. Both GAS and PCA are antisolvent process, but they differ significantly in how supercritical carbon dioxide behaves in solution. Thus, it is important to recognize that the term antisolvent describes a substance that is used to precipitate solute from solvent, but it can behave either as a solute or solvent in different processes.

RESS, PCA, and GAS are all recrystallization techniques that use supercritical carbon dioxide to produce micron-sized particles. In comparison to RESS, pharmaceutical applications of GAS are more common because very few pharmaceutical compounds are soluble in supercritical carbon dioxide. Formation of microparticles for insulin (67), hyaluronic acid ethyl ester-11 (68), carbamazepine (69), b-carotene (70), sulfonamides or sulfones (71), and a solute developed by Novartis Pharmaceuticals (72) all have been reported. Formation of fine explosive particles is another area that benefits from GAS process. Studies have been done by Niehaus *et al*. and Gallagher *et al*. on recrystallization of RDX (73,74). Other studies of GAS include recrystallization of 1,3,5,7-tetranitro-1,3,5,6-tetraazacyclooctane (HMX) (75) and anthracene (76). A comprehensive summary of patents and reports on GAS is included in Perrut's review article (65).

1.4.2 Paint and Adhesive Spraying

Union Carbide Corporation patented a supercritical fluid process called UNICARB® for paint coating and adhesive spraying applications (77). The UNICARB®

process differs from the GAS process since the supercritical carbon dioxide does not precipitate solute particles. Rather, supercritical carbon dioxide serves multiple purposes: it is a plasticizer and a viscosity reducer, and it enhances atomization. In the UNICARB® process, supercritical carbon dioxide behaves as solute and acts as a diluent for paint coatings and adhesives (1-3). Polymeric material is combined with carbon dioxide immediately prior to spraying, and then the mixture is sprayed at 323 K and 1500 psia. This process involves an atomization mechanism called decompressive spray. During spraying, depressurization occurs quickly as the polymer and carbon dioxide pass through the orifice in the spray nozzle. Depressurization causes the dissolved carbon dioxide to undergo a phase transition and form gas bubbles that increases the compressibility of the system and decreases the speed of sound in the flow. A choked flow is reached when the flow rate through the orifice reaches the speed of sound, and causes a high-pressure zone outside the nozzle because the pressure drop cannot propagate faster than the speed of sound. The expansion of gas bubbles under high pressures overcomes liquid forces of viscosity, cohesion, and surface tension, and ejects droplets outward in all directions. This produces a feathered pattern spray with uniform interior and tapered edges.

Due to the inherent properties of supercritical carbon dioxide and the new spray mechanism, the UNICARB® process offers several advantages. First, supercritical carbon dioxide used in the process has gas-like viscosity and is a better viscosity reducer than liquid solvents. Second, the UNICARB® process reduces dry time as carbon dioxide evaporates instantaneously after being sprayed. Third, the UNICARB® process increases material transfer efficiency due to a well-defined spray pattern and uniform droplet size. Material transfer efficiency reflects the amount of material sprayed versus the amount of

material that actually adheres to the target. Having an uniform spray pattern enhances transfer efficiency by allowing accurate spray, thus less waste outside the target. Uniform droplet size enhances transfer efficiency due to the lack of droplets that are too small and thus swept away from the target by air currents. Lastly, formulations with supercritical carbon dioxide have been shown to result in improved material properties such as shear strength (78).

Other patents based on similar concepts have been reviewed by Perrut (65). In his review, Perrut classifies UNICARB® as well as these other applications under the general acronym: particles from gas-saturated solution (PGSS).

1.4.3 Microcellular Structures

Similar to the UNICARB® process, the supersaturation of supercritical carbon dioxide can be applied to the formation of microcellular polymers. Making microcellular polymers with supercritical carbon involves two steps. First, supercritical carbon dioxide is dissolved in the polymer. As a solute, supercritical carbon dioxide causes plasticization of the polymer and lowers the glass transition temperature, Tg. Then, the pressure of the system is rapidly decreased, causing the carbon dioxide to become supersaturated and to nucleate small bubbles. Eventually, the carbon dioxide escapes, leaving behind a porous polymer structure. In some cases where the plasticization caused by dissolving carbon dioxide is not enough to lower Tg to room temperature, then a temperature quench follows the pressure quench to allow nucleation of carbon dioxide gas bubbles inside the polymer.

Success of foaming processes using supercritical carbon dioxide has been seen both in laboratory studies and in commercial applications. Microcellular structures in poly(methyl methacrylate) (79,80), polystyrene (79,81), poly (vinyl chloride) (79), and polycarbonate (79) have been reported. In addition to homopolymers, Wang *et al.* (82) have investigated the microcellular structure of polystyrene/liquid crystalline polymer blend. Production of microcellular polystyrene using an injection mold machine and extruder have been reported and patented (83,84). In addition to research studies, the use of supercritical carbon dioxide in making microcellular polymers was commercialized by Trexel Inc. for extrusion and injection molding processes. In this patented process, known as the Mucell™ process, a supercritical fluid is introduced into the polymer melt in the barrel of the molding machine. When the polymer is injected into the mold, pressure drops, causing the formation of microcells. In addition, the dissolved fluid acts as a temporary plasticizer that lowers polymer viscosity. This causes a reduction in injection pressure and allows an increase in injection speed. According to a news release by E.I. duPont de Nemours and Company (85), studies have indicated that parts had smooth skins of solid polymer and cores with very small, uniformly distributed closed-cell voids. Other companies that have adapted this technology include Arburg, Battenfield, Engel North America, Ferromatik Milacron, Husky, JSW, Kraus, Maffei, and Van Dorn Demag Corporation.

1.5 Supercritical Fluid as a Solute and a Solvent

1.5.1 Aerogel Drying

The production of aerogels requires a technique known as supercritical fluid drying. In this technique, supercritical carbon dioxide usually is the fluid of choice, and plays a mixed role of solvent and solute. Silica gel is first formed as a wet gel from silicon alkoxide precursors in ethanol, which subsequently, must be dried. Direct drying of liquid ethanol is known to cause the collapse of the hollow silica network due to the surface tension of the ethanol. As a result, ethanol must undergo solvent exchange with supercritical carbon dioxide, which has no surface tension. Supercritical carbon dioxide first behaves as a solvent by dissolving and extracting ethanol. Simultaneously, as ethanol is being extracted from the silica network, carbon dioxide replaces ethanol and diffuses as solute. Eventually, carbon dioxide fills the entire silica network to keep it from collapsing. After extraction of ethanol, supercritical carbon dioxide is slowly vented, leaving only the silica network intact because supercritical carbon dioxide lacks surface tension.

Silica gel has been made for optoelectronic applications due to its strong photoluminescence (5). In addition to silica gel, other types of aerogels have been synthesized using similar techniques. Synthesis of an organic, low molecular weight aerogel of 2,3-didecyloxyanthracene (DDOA) is reported by Placin *et al* (6). This work shows that DDOA aerogel can be synthesized either in liquid solvent and then dried by supercritical fluid, or in supercritical medium without additional drying. Another organic aerogel synthesized from N-hydrxymethylacrylamide and resorcinol was reported by Wu *et al* (7). Inorganic aerogel of NiO/Al_2O_3 was synthesized to be used as aerogel catalyst

by Sunol *et al* (8). Humic acid is a biopolymer with many important biological uses. It was isolated in the form of aerogel by Willey *et al*. using the supercritical drying method (9). Other polymer-based aerogels synthesized include polyisocyanate aerogel (10) and melamine-formaldehyde copolymer aerogel (11), both of which have applications in thermal and sound insulation, and optics.

1.5.2 Composite Materials

As a solute, supercritical carbon dioxide has the ability to swell polymer substrates and act as a solvent, it can help carbon dioxide-soluble materials to penetrate polymer substrates and to be deposited into polymer substrates via absorption. This allows the polymerization processes described in section 3.3 to take place inside a substrate, forming composite materials. In a scheme proposed by Watkins and McCarthy (86,87), monomers and thermal initiators are first dissolved in supercritical carbon dioxide at a temperature in which initiators decompose slowly. In a reactor, this supercritical carbon dioxide solution is allowed to swell and diffuse into the polymer substrate, where the monomers are absorbed. Finally, the reactor is heated to begin free-radical polymerization inside the polymer substrate, and the supercritical carbon dioxide can be vented either before or after polymerization. Watkins and McCarthy investigated polystyrene/substrate blends for six semicrystalline and glassy polymer substrates: polyethylene, bisphenol A polycarbonate, poly(oxymethylene), nylon 66, poly(4-methyl-1-pentene), and poly(chlorotrifluoroethylene) (86). In a slightly modified process, Kung *et al*. (88) also reported the synthesis of poly(ethyl 2-cyanoacrylate), PECA, in swollen poly(tetrafluoroethylene-*co*-hexafluoropropylene), FEP, via anionic polymerization in

supercritical carbon dioxide. Although carbon dioxide is known to terminate most anionic polymerization, Kung *et al.* were able to demonstrate that PECA formed in carbon dioxide is comparable to that formed in a conventional solvent. In a report on unpublished works by Watkins and Krukonis, Gallagher-Wetmore *et al.* (89) describe the modification of the surfaces of polypropylene and polytetrafluoroethylene, by the impregnating vinyl pyridine via supercritical carbon dioxide into the polymer substrates. Vinyl pyridine subsequently is polymerized, rendering the surfaces of the hydrophobic polymers hydrophilic. In an investigation by Ma and Tomasko (90), hydrophilicity of high-density polyethylene also has been modified by impregnating nonionic surfactant (N, N-dimethyldodecylamine N-oxide) using supercritical carbon dioxide. Synthesis of metal complexes into polymer substrates are reported for the impregnations of $Mn_2(CO)_{10}$ into polyethylene matrix (91) and of copper/iron diiminate into polyacrylate films (92).

Synthesis of composite materials also can occur without reaction. To prevent degradation, materials often need to be impregnated with protective agents. Impregnations of hydrophobic UV-absorbers based on benxophenone-, coumarin- and stryrene derivatives in poly(ethylene terephthalate), polypropylene, and poly(ether ketone) synthetic fibers are reported by Knittel *et al.* (93). Anton *et al.* (94) have reported the impregnation of stones such as marble and bio-calcarenite with fluorinated urethane compounds in a patent. Impregnation of a biocide, tebuconazole into wood species has been reported in several publications (95-97). However, in the impregnation of an additive into a solid matrix such as stone or wood, supercritical carbon dioxide does not form a solution with the solid, and only behaves as a solvent medium.

1.6 References

1. Lee, C.; Hoy, K. L.; Donoue, M. D. Supercritical Fluids as Diluents in Liquid Spray Application of Coatings. *U.S. Patent 4,923,720*, May 8, 1990.
2. Cole, T.A.; Nielsen, K.A. Supercritical fluid as diluents in liquid spray applications of adhesive. *U.S. Patent 5,066,522*, Nov. 19, 1991.
3. Donohue, M. D.; Geiger, J. L.; Kiamos, A. A.; Nielsen, K. A. *ACS Symposium Series No. 626*, **1996**, *Ch.12*, 152-167.
4. Pierick, D.; Jacobsen, K. *Plastics Engineering* **2001**, *57(5)*, 46-51
5. Canham, L.T.; Cullis, A.G.; Pickering, C.; Dosser, O.D.; Cox, T.I.; Lynch, T.P. *Nature (London)* **1994**, *368(6467)*, 133-5.
6. Placin, F, Desvergne, J.-P.; Cansell, F. *J. Mater. Chem.* **2000**, *10*, 2147-2149.
7. Wu, Z.; Zhang, Z.; Zhang, M. *Chin. J. Polym. Sci.* **1996,** *14(2)*, 127-133.
8. Sunol, S. G.; Keskin, O.; Guey, O.; Sunol, A.K. *ACS Symp. Ser.* **1995**, *608(Innovations in Supercritical Fluids)*, 258-68.
9. Willey, R.J.; Radwan, A.; Vozzella, M.E.; Fataftah, A.; Davies, G.; Ghabbour, E.A. *J. Non-Cryst. Solids* **1998**, *225*, 30-35.
10. Biesmans, G.L.J.G. Polyisocyanate based aerogel. *US Patent 5,990,184*, 1999.
11. Pekala, R.W. Melamine-formaldehyde copolymer aerogels. *US Patent 5,081,163*, 1992.
12. Reverchon, E. *J. Supercrit. Fluids* **1997**, *10*, 1-37.
13. Lehotay, S.J. *J. Chromatogr. A* **1997**, *758*, 289-312.
14. Wai, C.M.; Wang, S. *J. Chromatogr. A* **1997**, *785*, 369-383.

15. Subramaniam, B.; Rajewski, R.A.; Snavely, K. *J. Pharma. Sci*. **1997**, *86(6)*, 885-890.

16. Young, T.J.; Mawson, S.; Johnston, K.P. *Biotechnol. Prog.* **2000**, *16*, 402-407.

17. Momose, T.; Yoshida, H.; Sherverni, Z.; Ebina, T.; Tatenuma, K.; Ikushima, Y. *J. Vac. Sci. Technol*, **1999**, *17(4)*, 1391.

18. Heenan, D.F.; Januszkiewicz, K.R.; Strtford, G. *Lubr. Eng.* **1999**, *55(12)*, 18-22.

19. Tomioka, O.; Enokida, Y.; Yamamoto, I.; Takahashi, T. *Prog. Nucl. Energy* **2000**, *37(1-4)*, 417-422.

20. Roberts, K.L.; Forbes, J.E.; Pritchard, V.B.; Saunders, K.B.; White, G.L. *Book of Abstracts, 218th ACS National Meeting, New Orleans,* Aug. 22-26, 1999.

21. Fages, J; Poddevin, N; King, M.W.; Marois, Y.; Bronner, J; Jakubiec, B.; Roy, R.; Mainard, D.; Laroche, G.; Delagoutte, J.P.; Guidoin, R. *ASIAO Journal* **1998**, *44(4)*, 278-88.

22. Barnes, P. Method of cleaning or purifying elastomers and elastomeric articles which are intended for medical or pharmaceutical use. *PCT Int. Appl. WO 9738044*, 1997.

23. Evans, J.J.; Hong, S.P.; Ray, Urmi; Thiele, T.M. Optical fiber perform cleaning method. *U.S. Patent 6,260,386*, July 17, 2001.

24. Wallace, R.M.; Douglas, M.A. Cleaning and treating a micromechanical device. *Eur. Pat. Appl., EP 746013*, 1997.

25. Bok, E.; Kelch, Dieter; Schumacher, K.S. *Solid State Technol.* **1992**, 117-120.

26. Wang, C.W.; Chang, R.T.; Lin, W.K.; Liang, M.T.;Yang, J.F.; Wang, J.B. *J. Electrochem. Soc.* **1999**, *146(9)*, 3485-3488.

27. Kiran, E. *NATO Sci. Ser. E*, **2000**, *366*, 253.

28. Kendall, J. L.; Canelas, D. A.; Young, J. L.; DeSimone, J. M. *Chem. Rev*. **1999**, *99*, 543-563.

29. Cooper, A.I. *J. Mater. Chem*., **2000**, *10*, 207-234.

30. Akerman, A.; Roop, R.K.; Hess, R.K.; Sang-Do Yeo Supercritical Fluid Technology, 1991, CRC Press, Inc.

31. Schultze, C; Donohue, M. *Fluid Phase Equilibria* **1996**, *116*, 465-472.

32. Walsh, G.D.; Donohue, M.D. *Fluid Phase Equilibria* **1989**, *52*, 295.

33. Lang, Q.; Wai, C.M. *Talanta* **2001**, *53*, 771-782.

34. McHugh, M.; Krukonis, V. Supercritical Fluid Extraction, Butterworth-Heinemann Series in Chemical Engineering; Butterworth-Heinemann: Stoneham, MA, 1994, 2nd edition, pp 4-9.

35. Krukonis, V.; Brunner, G.; Perrut, M. *Third International Symposium on Supercritical Fluids*, **1994**, 1-22

36. Praxair Technology, Press Release, September 28, 2000, "Praxair and Supercritical System to Develop Next Generation Wafer Cleaning Technology."

37. Smith, R.M. *J. Chromatogr, A* **1999**, *856*, 83-115.

38. Chester, T.L.; Pinkston, J.D. *Anal. Chem.* **2000**, *72*, 129R-135R.

39. Berger, T.A. *J. Chromatogr, A* **1997**, *785*, 3-33.

40. Terfloth, G. *J. Chromatogr. A* **2001**, *906*, 301-307.

41. Williams, K.L.; Sander, L.C. *J. Chromatogr. A* **1997**, *785*, 149-158.

42. Lafosse, M.; Herbreteau, B.; Morin-Allory, L *J. Chromatogr. A* **199**, *720*, 61-73.

43. DeSimone, J. M.; Guan, Z.; Elsbernd, C. S. *Science*, **1992**, *257*, 945-947.

44. Guan, Z.; Combes, J. R.; Menceloglu, Y. Z.; DeSimone, J. M. *Macromolecules*, **1993**, *26*, 2663-2669.

45. van Herk, A. M.; Manders, B. G.; Canelas, D. A.; Quadir, M.; DeSimone, J. M. *Macromolecules*, **1997**, *30*, 4780-4782.

46. Romack, T.J.; Maury, E.E.; DeSimone, J.M. *Macromolecules*, **1995**, *28*, 912.

47. Hu, H.Q.; Chen, M.C.; Li, J.; Cong, G.M. *Acta Polym. Sinica* **1998**, 740.

48. Dada, E.; Lau, W.; Merritt, R.F.; Paik, Y.H.; Swift, G. *Polym. Prepr.* **1996**, *74*, 427.

49. Romack, T.J.; DeSimone, J.M.; Treat, T.A. *Macromolecules*, **1995**, *28*,8429.

50. Cooper, A.I.; Hems, W.P.; Holmes, A.B. *Macromol. Rapid Commun.* **1999,** *32*, 2156.

51. Elliot, J.R.; Cheung, H.M. *ACS Symp. Ser.* **1993**, *514*, 271.

52. Cooper, A.I.; Hems, W.P.; Holmes, A.B. *Macromol. Rapid Commun.* **1999,** *32*, 2156.

53. Clark, M.R.; DeSimone, J.M. *Macromolecules*, **1995**, *28*,3002.

54. Mistele, C.D.; Thorp, H.H.; DeSimone, J.M. *J. Macromol. Sci., Pure Appl. Chem*. **1996**, *A33*, 953.

55. Fürstner, A.; Koch, D.; Langemann, K.; Leitner, W.; Six, C. *Angew. Ceh., Int. Ed. Engl.* **1997**, *36*, 2466.

56. Hori, H.; Six, C.; Leitner, W. *Macromolecules*, **1999**, *32*, 3178.

57. Darensburg, D.J.; Stafford, N. W.; Katsurao, T. *J. Mol. Catal. A, Chem.* **1995**, *104*, L1.

58. Darensburg, D.J.; Holtcamp, M.W. *Macromolecules*, **1995**, *28*, 7577.

59. Kappellen, K.K.; Mistele, C.D.; DeSimone, J.M. *Macromolecules*, **1996**, *29*, 495.

60. Kerton, F.M.; Lawless, G.A.; Armes, S.P. *J. Mater. Chem.* **1997**, *7*, 1965.

61. Palakodaty, S.; York, P. *Pharmaceutical Research* **1999**, *16(7)*, 976-985.

62. Sun, Y.P.; Riggs, J.E.; Rollins, H.W.; Radhakishan, G. *J. Phys. Chem. B* **1999**, *103*, 77-82.

63. Shim, J.J.; Yates, M.Z.; Johnston, K.P. *Ind. Eng. Chem. Res.* **2001**, *40*, 536-543.

64. Tepper, G.; Levit, N. *Ind. Eng. Chem. Res.* **2000**, *39*, 4445-4449.

65. Jung, J.; Perrut, Michel *J. Supercrit. Fluids* **2001**, *20*, 179-219.

66. Chapman, B.R.; Gochanour, C.R.; Paulaitis, M.E. *Macromolecules*, **1996**, *29*, 5635-5649.

67. Yeo, S.-D.; Debenedetti, P.G.; Radosz, M.; Schmidt, H.-W. *Macromolecules*, **1993**, *26*, 6207-6210.

68. Bertucco, A.; Pallado, P.; Benedetti, L. *In High Pressure Chemical Engineering*; Process Technology Proceedings, 12; von Rohr, P.R., Trepp, C., Eds.; Elsevier; Amsterdam, 1996; 217-222.

69. Moneghini, M.; Kikic, I.; Voinovich, d.; Perissutti, B.; Filipovic-Grcic, J. *Int. J. Pharm.* **2001**, *222(1)*, 129-138.

70. Chang, C.J.; Randolph, A.D.; Craft, N.E. *Biotechnol. Prog.* **1991**, *7(3)*, 275-8

71. Reverchon, E. Micronized pharmaceutical sulfonamides or sulfones. *PCT Int. Appl. WO 2001066090*, 2001.

72. Mueller, M.; Meier, U.; Kessler, A.; Mazzotti, M. *Ind. Eng. Chem. Res*. **2000**, *39(7)*, 2260-2268.

73. Niehaus, M.; Teipel, U.; Bunte, g.; Krause, H.; Weisweiler, W. *Process Technol. Proc.* **1996**, *12*, 345-350.

74. Gallagher, P.M.; Coffey, M.P.; Krukonis, V.J.; Hillstrom, W.W. *J. Supercrit. Fluids* **1992**, *5(2)*, 130-42.

75. Cai, J.; Zhou, Z.; Xiu, D. *Chin. J. Chem. Eng.* **2001**, *9(3)*, 258-261.

76. Liou, Y.; Chang, C.J. *Sep. Sci. Technol.* **1992**, *27(10)*, 1277-89.

77. Cole, T.A.; Nielsen, K.A. Supercritical Fluids as Diluents in Liquid Spray Application of Adhesives. U.S. Patent 5,066,522, November 19, 1991

78. Yang, C.C.; Gaddy, G.D.; Donohue, M.D. *Ind. Chem. Eng. Res.*, submitted for publication.

79. Chiou, J.S.; Barlow, J.W.; Paul, D.R. *J. Appl. Polym. Sci*. **1985**, *30(6)*, 2633-42

80. Beckman, E.J. *Adv. Sci. Technol*. **1995**, 4, 152-162.

81. Arora, K.A.; Lesser, A.J., McCarthy, T.J. *Macromolecules*, **1998**, *31*, 4614-20

82. Wang, J.; Cheng, X.; Yuan, M.; He, J. *Polymer* **2001**, *42*, 8265-8275.

83. Baumgartl, H; Dietzen, F.J.; Swoboda, J. *Ger. Offen. DE 4437860*, 1996.

84. Shimbo, M; Nishida, K.; Heraku, T.; Lijima, K.; Sekino, T.; Terayama, T. Foams '99, Int. Conf. Thermoplast. Foam, 1st (1999).

85. E.I. duPont de Nemours and Company, Press Release, March 2000, "Dupont to Support Customers in Gaining Benefits of Foaming Process."

86. Watkins, J.J.; McCarthy, T.J. *Macromolecules*, **1994**, *27*, 4845-4847.

87. Watkins, J.J.; McCarthy, T.J. *Macromolecules*, **1995**, *28*, 4067-4074.

88. Kung, E.; Lesser, J.J.; McCarthy, T.J. *Macromolecules*, **2000**, *33*, 8192-8199.

89. Gallagher-Wetmore, P.; Ober, C.K.; Gabor, A.H.; Allen, R.D. *Proc. SPIE-Int. Soc. Opt. Eng.* **1996**, *2725(Metrology, Inspection, and Process Control for Microlithography X),* 289-299.

90. Ma, X.; Tomasko, D.L. *Ind. Eng. Chem. Res.* **1997**, *36*, 1586-1597.

91. Clarke, M.J.; Howdle, S.M.; Jobling, M.; Poliakoff, M. *Inorg. Chem.* **1993**, *32*, 5643-5644.

92. Said-Galiyev, E.; Nikitin, L.; Vinokur, R.; Gallyamov, M.; Kurykin, M.; Petrova, O.; Lokshin, B.; Volkov, I.; Khokhlov, A.; Schaumburg, K. *Ind. Eng. Chem. Res.* **20**, *39*, 4891-4896.

93. Knittel, D.; Dugal, S.; Schollmeyer, E. *Chem. Fibers Int.* **1997**, *47(1)*, 46-48.

94. Anton, D.R.; Kirchner, J.R.; Tuminello, W.H. Protection of stones from water/air pollution degradation by impregnation with fluorinated urethanes in supercritical CO2 solution. *PCT Int. Appl. WO 2001062687*, 2001.

95. Acda, M.N.; Morrell, J.J.; Levien, K.L. *Mater. Org.* **1996**, *30(4)*, 293-300.

96. Acda, M.N.; Morrell, J.J.; Levien, K.L. *Wood Fiber Sci.* **1997**, *29(3)*, 282-290.

97. Acda, M.N.; Morrell, J.J.; Levien, K.L. *Wood Sci. Technol.* **2001**, *35(1-2)*, 127-136.

2. Experimental Objectives and Methods

2.1 Objectives

In traditional spray-applied solvent-based contact adhesives, polymer first is mixed with conventional "solvents" to form a solution. Additives are mixed in to give enhanced material properties. The solvents used in these formulations are classified into two categories, fast "solvents" and slow "solvents". Their role is to reduce the viscosity of the polymer, and usually they behave thermodynamically as solutes. In the spraying process, adhesive solution forms a laminar jet as it goes through a nozzle and the spray atomizes as the laminar jet is broken up due shear with surrounding air. The atomized adhesive droplets adhere to the substrate, and then form a film as solvents evaporates (1). This traditional spraying process is formulated with low molecular weight organic compounds (LMWOCs), and offers acceptable performance. However, most LMWOCs are volatile organic compounds (VOCs) that facilitate the production of ground-level ozone. LMWOCs also are harmful to the environment by contaminating drinking water (1) and causing land infertility (2). An alternative to conventional spraying process is to use the UNICARB® process to spray adhesives. Using the UNICARB® process, a contact adhesive needs to be reformulated because supercritical carbon dioxide is used as a viscosity reducer and replaces some of the conventional LMWOCs. To reformulate contact adhesives for the UNICARB® process, the thermodynamic behaviors of the potential base polymer systems mixed with supercritical carbon dioxide first must be investigated. This is necessary because the UNICARB® process requires the adhesive system to first undergo a liquid to liquid-liquid phase transition and then a liquid-liquid to

liquid-liquid-vapor phase transition. Thus, in order to apply the UNICARB® process to the spraying of adhesives, it is necessary to first characterize the phase behavior of base polymer, and then find the range of operating conditions in which the system can undergo the proper phase transitions. In this work, the supercritical phase behavior of three polymer systems are investigated to determine their potential for use in the UNICARB® process. The types of polymer investigated are styrenic block copolymers, polychloroprene, and polyacrylate.

2.2 Materials

SBS and SEBS block copolymers, Kraton® D-1107 and G-1652, were obtained from Shell Oil Inc. (now Kraton Inc.). Kraton® D-1107 was in the form of small spheroids and Kraton® G-1652 was in the form of flakes. Neoprene WRT, a polychloroprene, was obtained from E.I. DuPont de Nemours and Co. Desmocoll and Desmomelt polyurethanes were obtained from Bayer Corp. Acrylic-based Morstik® adhesive was obtained from Rohm&Haas Co. Polyalkylene glycol (MW~ 2500 g/mol), polyethyleneglycol (MW~4600 and ~8000 g/mol) were obtained from Dow Chemical. Liquid toluene was obtained from Sigma-Aldrich Chemicals and liquid carbon dioxide was obtained from BOC Gases.

Kraton® D-1107 block copolymer was mixed with toluene at three different ratios, 1:3, 17:33, and 2:3, which can be translated into 25%, 34%, and 40 wt. % polymer in toluene. Kraton® G-1652 also was mixed with toluene at three different ratios, 1:3, 1:2, and 2:3, which are equivalent to 25%, 33%, and 40 wt. % polymer in toluene. Neoprene WRT was mixed with toluene at two different ratios, 9:41, and 1:3, which can be

translated into 18 wt. % and 25 wt. % polymer in toluene. A polychloroprene-based contact adhesive was formulated by adding tacktifiers to and eliminating hexane from the base formulation published by Landrock (3). Morstik® was investigated with 8:1 Morstik®:toluene dilution, and without dilution. Polyalklene glycol and polyethylene glycol were characterized without dilution.

2.3 Apparatus

Volumetric data was obtained from a Phaser III supercritical phase analysis unit, which is shown schematically in Figure 3.1. The Phaser is a high-pressure cell adapting the concept of a piston and cylinder device. The system pressure is varied by changing the volume of the system at constant temperature. The change of the volume is made possible by moving the piston, which is connected to a hydraulic fluid pressure generator. When the hydraulic fluid is injected, it pushes the piston inward, causing the pressure in the system cell to increase. When the hydraulic fluid is withdrawn, the piston moves outward, allowing the pressure to decrease. The high-pressure cell has two windows to allow illumination by a light source and visual observations. A magnetic stirring bar is located in a small well at the bottom of the system cell in order to improve mixing and measure viscosity. A detailed description of the apparatus is given by Kiamos (4).

2.4 Procedure

Polymer samples were weighed and mixed with toluene to achieve desired concentrations. About 250 grams of the polymeric mixtures were loaded into the phaser cell, which subsequently was sealed, and then a measured amount of carbon dioxide was

added to the polymeric mixture using a pump. The mixture was pressurized to 2000 psia and left to equilibrate for at least 24 hours.

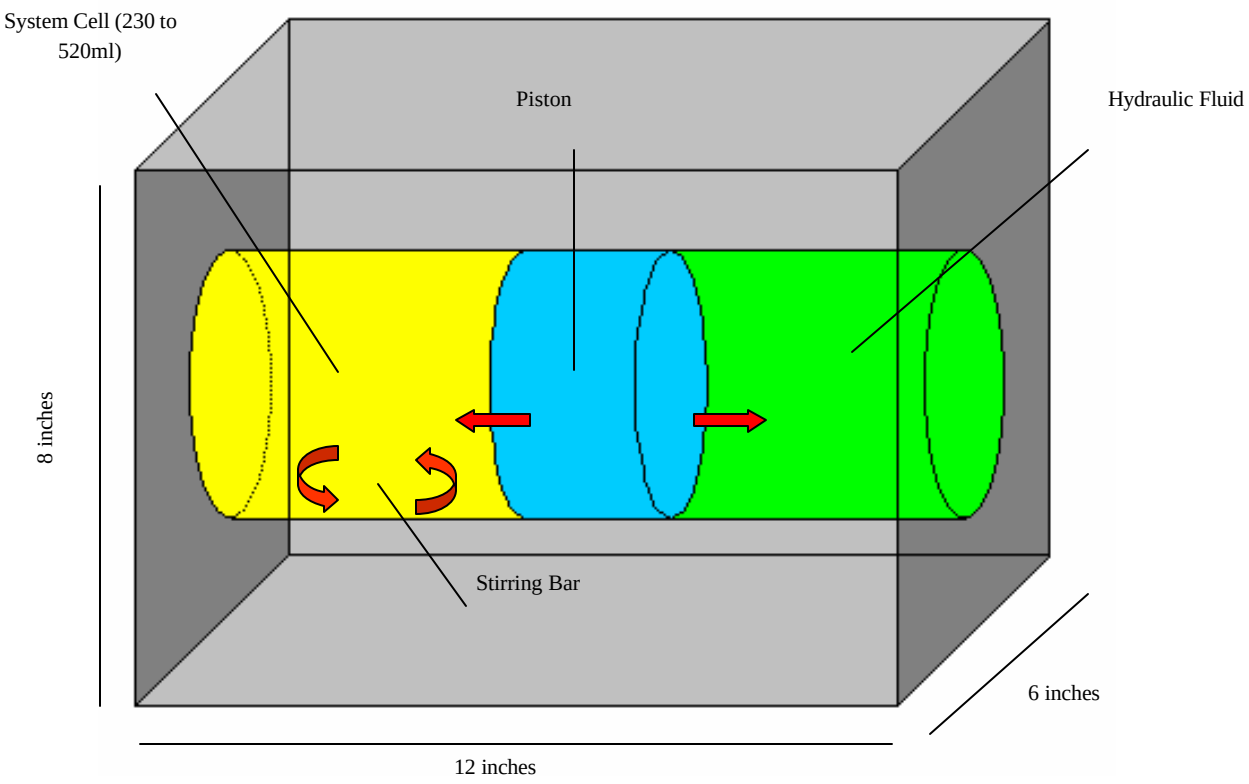

Pressures at which phase transitions occurred were determined statically and dynamically. To determine the phase boundaries statically, volumetric data were collected using the technique described by Muralidharan and Donohue. (5). The volume of the system first was increased a small amount, after which the system was allowed to sit for 5-15 minutes to equilibrate. Pressure and volume data then were recorded. This procedure was repeated many times to obtain a series of data points. In a dynamic experiment, the volume of the system was expanded rapidly. The phase boundaries then

were determined from the pressure profile as a function of time. Rapid expansion of the system was achieved by first closing a switch valve in the hydraulic line and then creating a vacuum behind it. In this setup, the system remained under pressure of 2000 psi. Once the switch valve was opened, the vacuum was filled rapidly by the outward moving piston and hydraulic fluid, thus resulting in a rapidly expanding system volume. Both the static and the dynamic experiments were repeated at various carbon dioxide concentrations and temperatures.

2.5 References

1. Donohue, M. D.; Geiger, J. L.; Kiamos, A. A.; Nielsen, K. A. *ACS Symposium Series No. 626*, **1996**, *Ch.12*, 152-167.
2. National Research Council, Division of Medical Science Assembly of Life Science. In Vapor-Phase Organic Pollutants; National Academy of Sciences: Washington, D.C., 1976; pp236-270.
3. Brinson, H.F. Adhesives and Sealants, 1990, Engineering Materials Handbook Vol. 3.
4. Kiamos, A. A. High Pressure Behavior of Polymer-solvent-Supercritical Fluid Mixtures. M.S. Thesis, The Johns Hopkins University, 1992.
5. Muralidharan, V.; Donohue, M.D. *The Journal of Supercritical Fluids*, **1994**, *7*, 275-281.

3. Phase Transitions in Polymer – Supercritical Fluid Mixtures

3.1 Introduction

According to Scott and van Konynenburg, there are six classifications of binary mixtures (1). In particular, the Type IV phase diagram is useful in describing the phase behavior of the polymer-supercritical fluid (SCF) mixtures studied here. A full understanding of the Type IV phase diagram can be very beneficial in developing polymer-processing applications that use supercritical fluids. Kirby and McHugh (2) recently have reviewed the phase behavior of different types of polymers in supercritical fluid solvents. Systems reviewed by Kirby and McHugh include homopolymer-SCF, copolymer-SCF, fluoropolymer-SCF, and polymer-CO_2 systems. Kiamos (3) and Schultze (4) also have reported phase diagrams for polymer-supercritical carbon dioxide systems from experimental results. Nevertheless, the understanding of the phase behavior of polymer-supercritical fluid mixtures is not yet complete due to the lack of understanding of an unusual liquid to liquid-fluid phase transition occurring at high solute concentrations. This chapter will review the Type IV phase diagram and address the unusual phase transition with experimental results.

3.2 Polymeric Solution Thermodynamics

A general phase diagram for polymer-solute mixtures can be constructed by first considering the phase behavior of the pure components in the mixture. On a pressure-

temperature-composition (P-T-X) three-dimensional phase diagram as shown in Figure 3.1, the two-dimensional P-T phase diagrams of the pure species are recovered at the concentration limits of pure solute and pure polymer. At both concentration limits, a solid-vapor equilibrium curve starts at the origin (P, T = 0), and extends to the triple point. Beginning at the triple points of pure polymer and pure solute, the solid-liquid equilibrium curves and the liquid-vapor equilibrium curves extend in two different directions. The liquid-vapor equilibrium curve also is called the vapor pressure curve. As the concentration varies from pure polymer to pure solute, the vapor pressure curves at each end of phase diagram extend toward each other and form a surface in P-T-X space as shown schematically in Figure 3.2. Close to the triple points, the shape of the surface is almost flat, and it then becomes increasingly concave as it extends toward the critical points. This surface formed by vapor pressure curves at various concentrations is a phase boundary that characterizes the evaporation of the mixture. Above the phase boundary, the mixture is a single-phase liquid or two liquids in equilibrium, which will be discussed in the next section. Along the phase boundary, an additional vapor phase is in equilibrium with the liquid phase. The phase transition crossing this boundary is called a bubble point.

In addition to describing the bubble point of the mixture, it also is necessary to describe the property of immiscibility that occurs when two different liquid species are mixed. Under certain thermodynamic conditions, the different species of a mixture become immiscible due to unfavorable interactions and phase separate into two liquid phases. The conditions under which immiscibility occurs are determined by the temperature, pressure, and composition of the system. The phase boundaries that

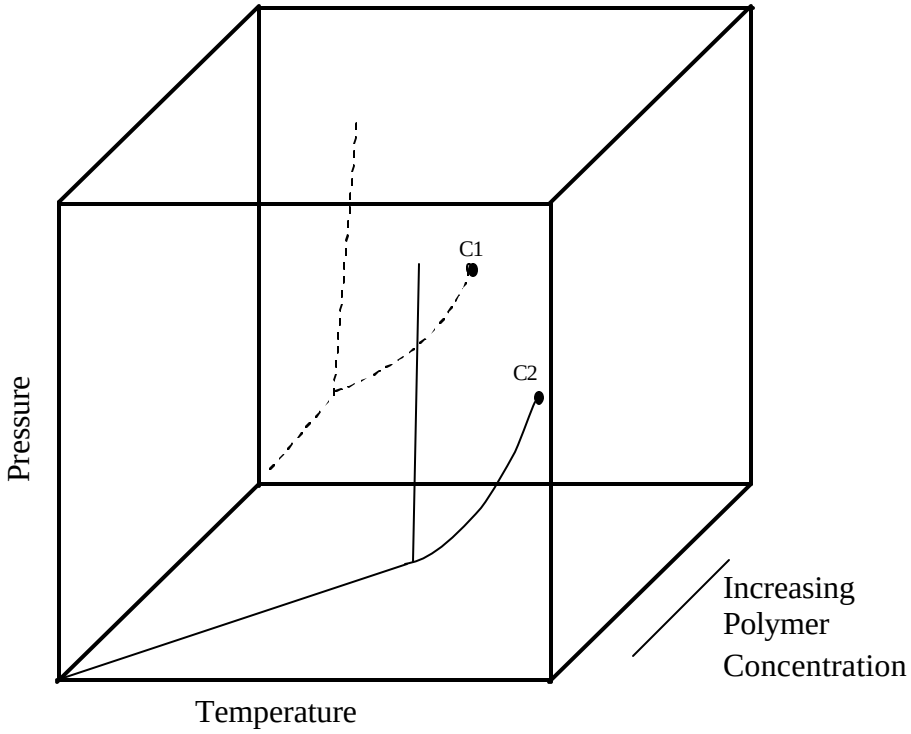

Figure 3.1: Schematic phase diagrams for a mixture at the concentration limits of pure solute and pure polymer.

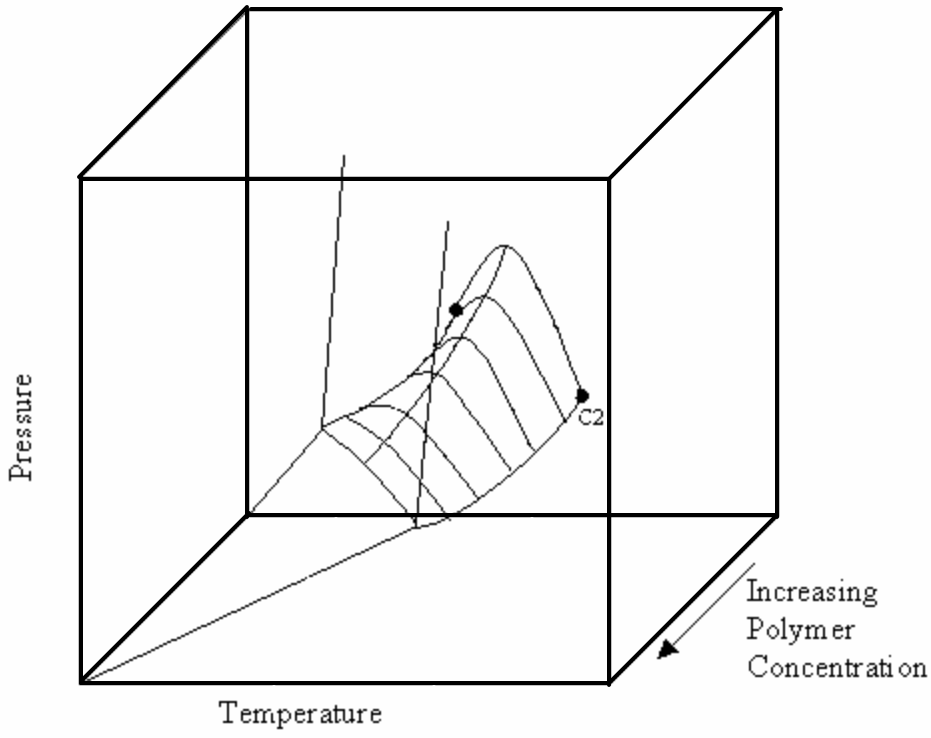

Figure 3.2: Schematic phase diagram for a mixture showing schematically the condensation/evaporation phase boundary surface.

correspond to the occurrence of immiscibility are called the upper and lower critical solution temperature (UCST/LCST) curves. Shown in Figure 3.3(a) is a qualitative P-T-X phase diagram for a monodisperse and amorphous polymer-solvent mixture exhibiting UCST/LCST critical loci. The Figure was adapted from an article by Folie and Radoz (5). The immiscible region is the shaded region and several T-X phase diagrams with immiscible regions are produced by taking slices of the P-T-X phase diagram at various pressures. At high pressures, the immiscible region exhibits a maximum temperature, which is known as the UCST. At intermediate pressures, there are two immiscible regions. The immiscible region at lower temperature exhibits UCST, while another immiscible region at high temperature exhibits a minimum temperature, known as the LCST. At low pressures, the immiscible region is hourglass-shaped and there is no critical temperature. A phase transition that occurs as the mixture becomes immiscible is called a cloud point.

By combining the phase diagrams in Figure 3.2 and Figure 3.3 and then projecting the critical loci into P-T space, a phase diagram for polymer-solute system is obtained. The resultant P-T phase diagram is shown in Figure 3.4(a), and is referred to as type IV in the classification of van Konynenburg and Scott (1). There are three sets of critical loci in this diagram. At low temperatures, the UCST curve extends from high pressure to the upper critical end point (UCEP), where a small liquid-liquid-vapor (LLV) three-phase region starts. The LLV region often is represented as a line because the LLV region usually is very small. The second set of critical loci start at high temperatures, as the LCST curve originates from the critical point of the less volatile component and extends to the lower critical end point (LCEP), where again a three-phase region starts.

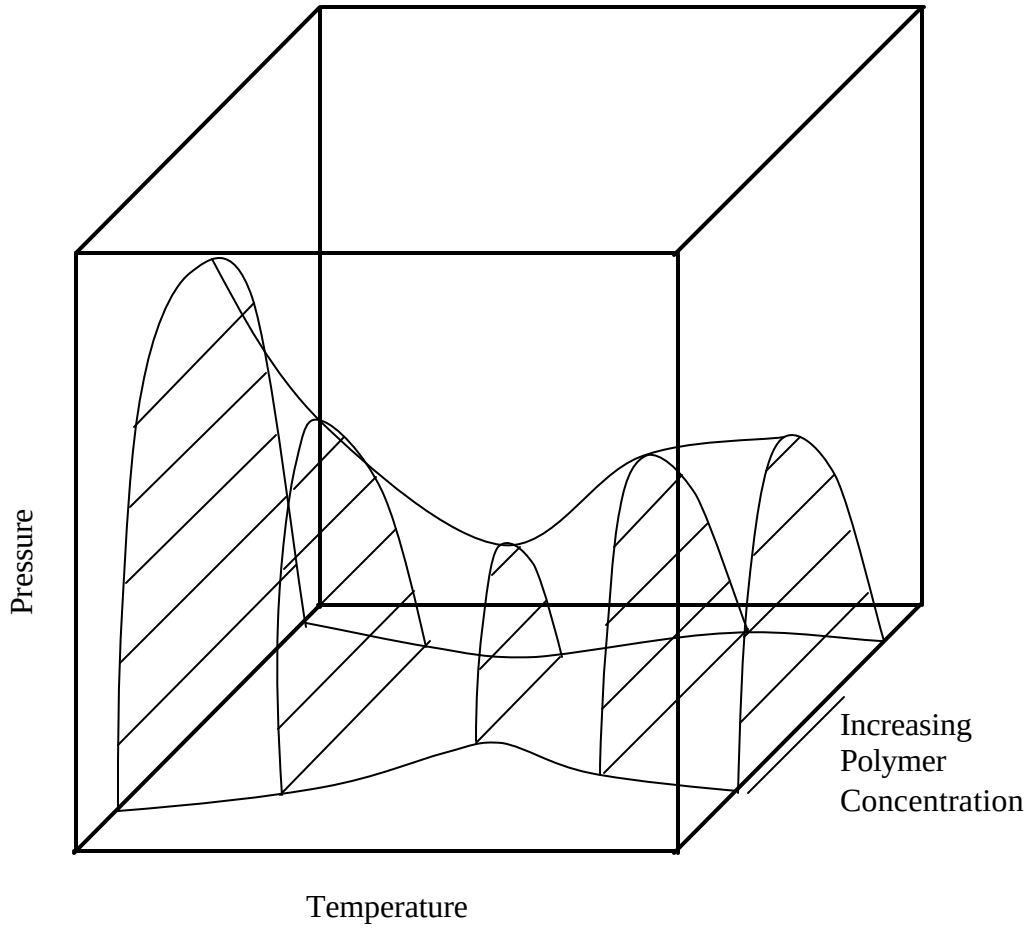

Figure 3.3: Phase diagram for a mixture showing schematically the region of immiscibility.

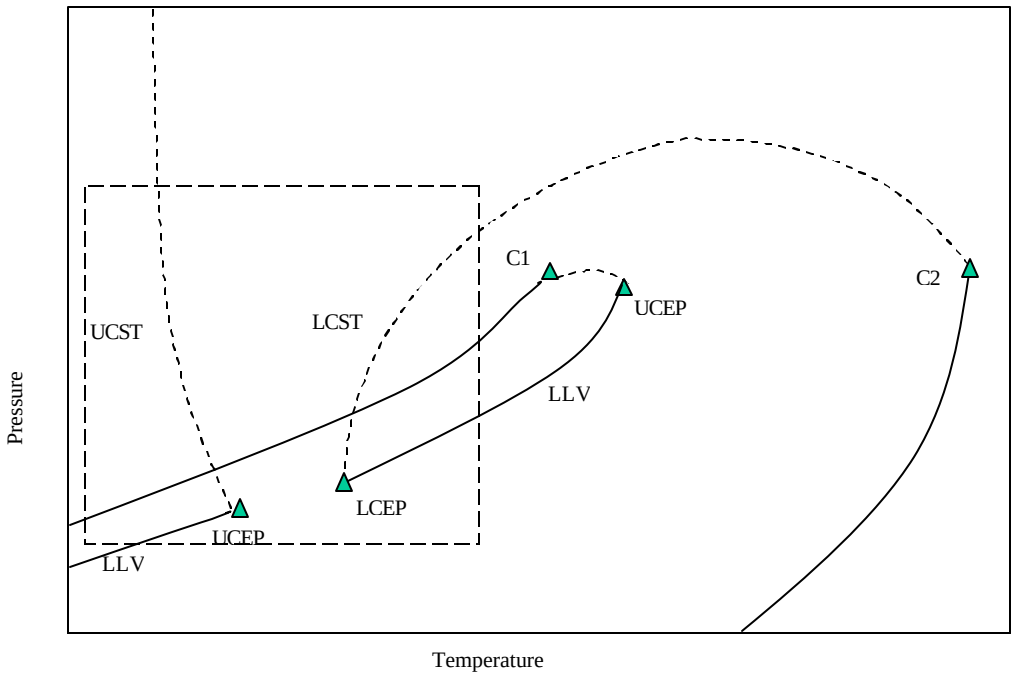

Figure 3.4(a): Type IV phase diagram.

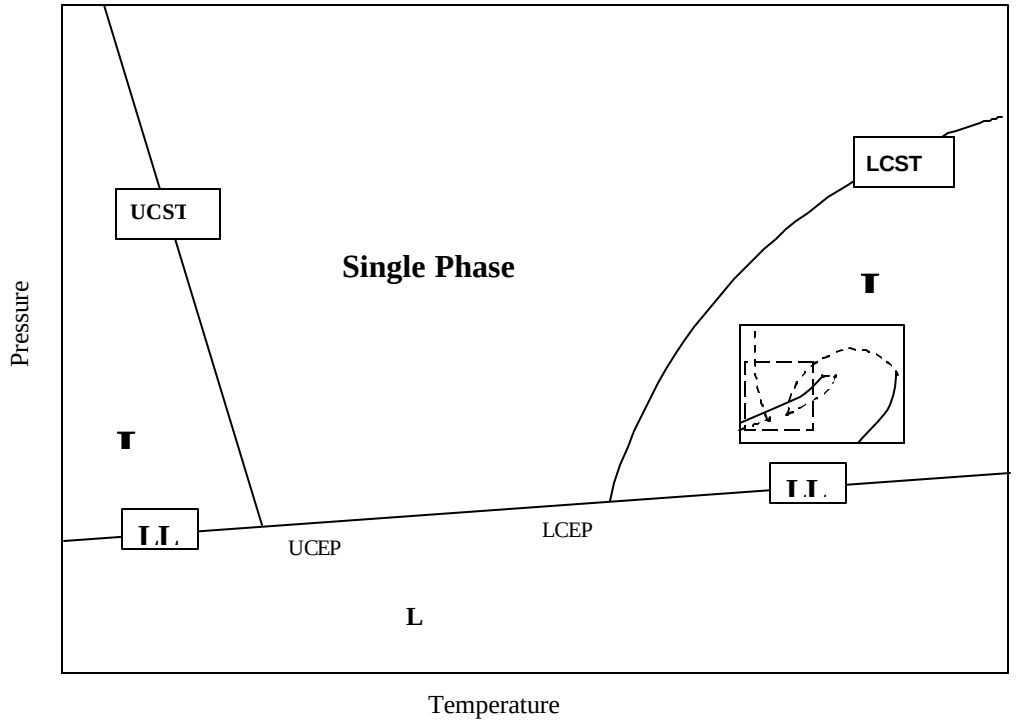

Figure 3.4(b): A section of type IV phase diagram.

A third critical curve begins at the critical point of the more volatile component and intersects the LLV region at another UCEP.

The temperature and pressure ranges of type IV phase diagrams can span several hundred degrees centigrade, and 10^6 psia. However, the focus of this discussion will only be put on the section of the phase diagram that corresponds to the temperature and pressure required in practical polymer processing applications. Additionally, when describing the phase behavior of a polymer-solute system in general, LLV curves are usually overlap with the vapor pressure curve. A modified portion of the type IV phase diagram is shown in Figure 3.4(b). In this phase diagram, a single-phase liquid region (L) is located in the gap between the two critical curves. The single-phase liquid region is bounded below by the bubble point curve; for the system studied here, this usually falls near the vapor pressure curve of the solute. Additionally, beneath the critical curves, there are two liquid-liquid regions (LL), in which two liquid phases are in equilibrium. The LL regions are bounded below by the LLV regions. The region beneath the vapor pressure and LLV regions is a liquid-vapor region (LV), in which a liquid and a vapor phase coexist.

The two-dimensional type IV phase diagram discussed so far is a projection of a three-dimensional phase diagram that describes the evaporation and the immiscibility of a mixture. In order to study the effect of increasing solute content, two-dimensional phase diagrams also can be constructed by taking slices of the three-dimensional phase diagram at constant composition. The phase diagram at constant composition appears very similar to the projected diagram. However, as the solute concentration increases, the UCST curve moves to higher temperatures and pressures, and the LCST curve moves to lower

temperatures and higher pressures. This causes the gap between UCST and LCST to shrink and then to merge into a single curve at high solute concentrations, as shown in Figure 3.5. The region beneath the merged critical curve is usually a LL region, but not always. This region will be analyzed in section 3.3.

3.3 Evidence for an Unusual L-LF Phase Transition

Polyalkylene glycol (MW~ 2500 g/mol) from Union Carbide Corporation was analyzed experimentally. Polyalkylene glycol is a clear liquid with low viscosity at room temperature. Solubility data were obtained as described in Chapter 2 over carbon dioxide concentrations ranging from 9 to 36 weight % at 50 °C. Phase transitions at each composition were determined from P-V isotherms, which are shown in Figure 3.6 (a-e). The phase transition pressures are summarized in Table 3.1. Three types of phase transitions were identified from the volumetric data. First, bubble points were found to occur at 8.5 wt. % carbon dioxide, in which the shape of P-V isotherm shown in Figure 3.6(a) began as a straight line, and then deviated from the initial slope in the form of a curve before turning into a flat line. The curvature in this P-V isotherm can be attributed to the close proximity of the mixture critical point in these measurements. As carbon dioxide concentrations were increased to 13.4%, a cloud point and then a bubble point were identified as the P-V isotherm changed from a very steep line into a less steep line, and then into a completely flat line. This data is presented in Figure 3.6(b). At high carbon dioxide concentrations, an unusual phase transition occurred. This phase transition was classified as neither bubble point nor cloud point because of the anomalous shape of the P-V isotherm, which is shown in Figures 3.6(c-e). The P-V isotherm begins

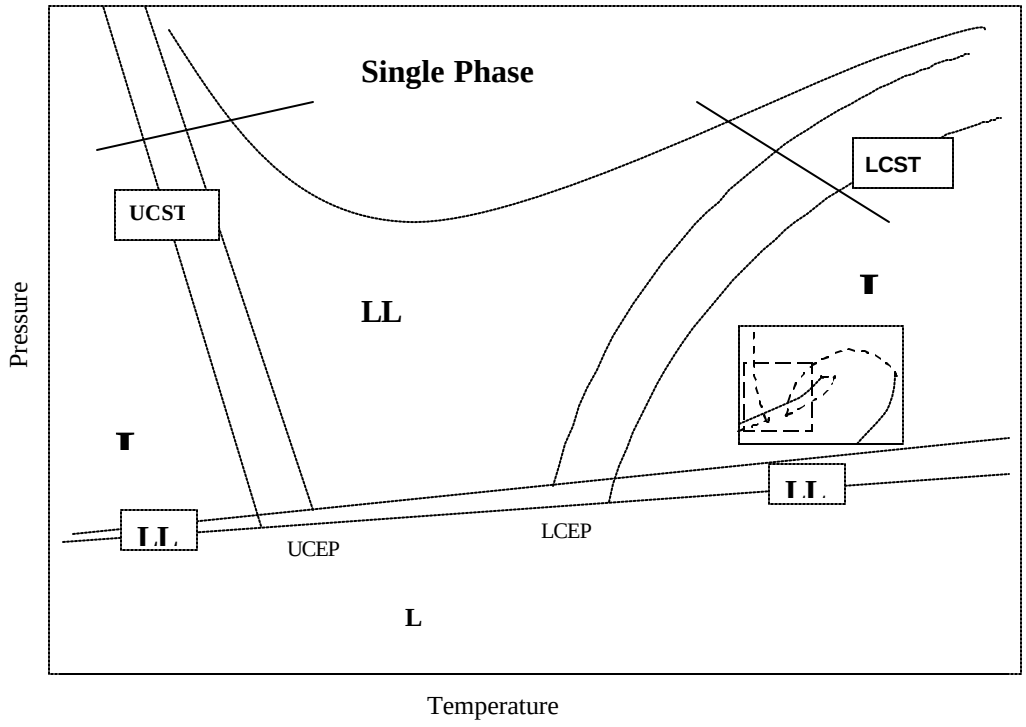

Figure 3.5: Effect of increasing solute concentration.

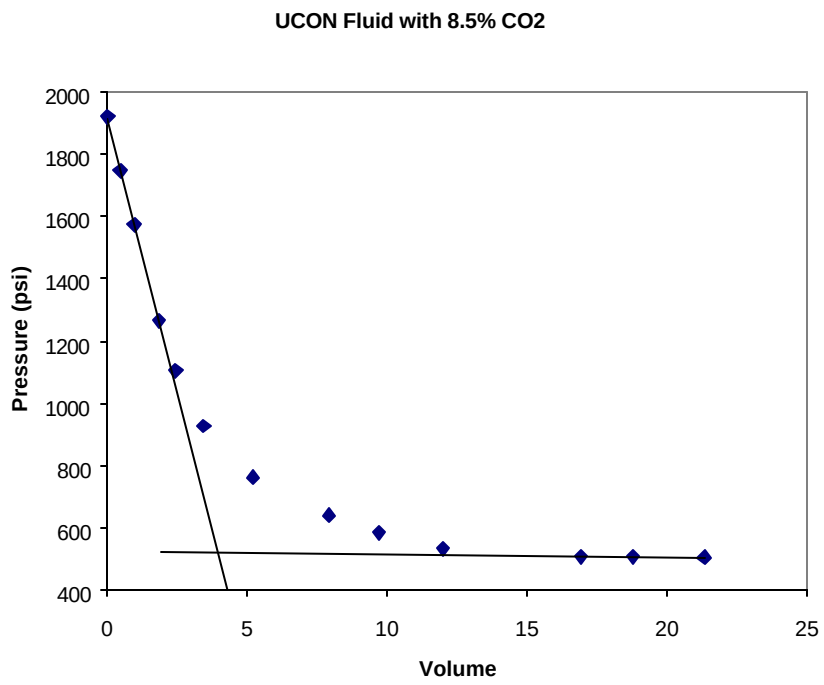

Figure 3.6(a): P-V isotherm at low carbon dioxide concentration

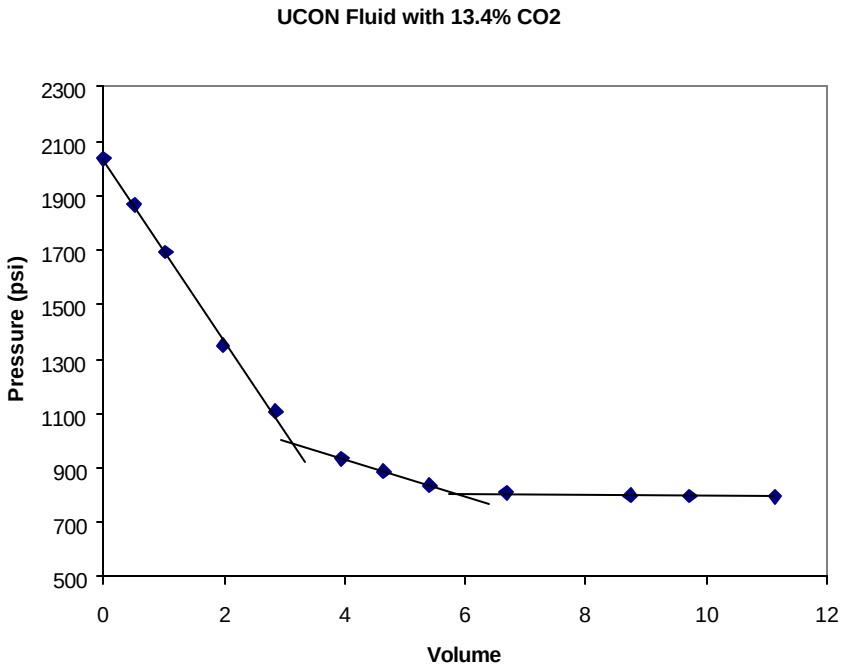

Figure 3.6(b): P-V isotherm at intermediate carbon dioxide concentration

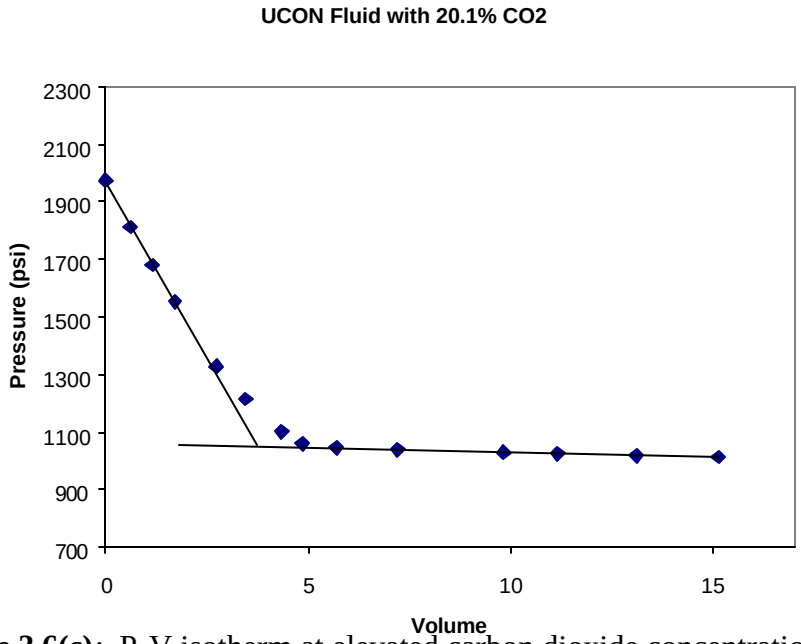

Figure 3.6(c): P-V isotherm at elevated carbon dioxide concentration

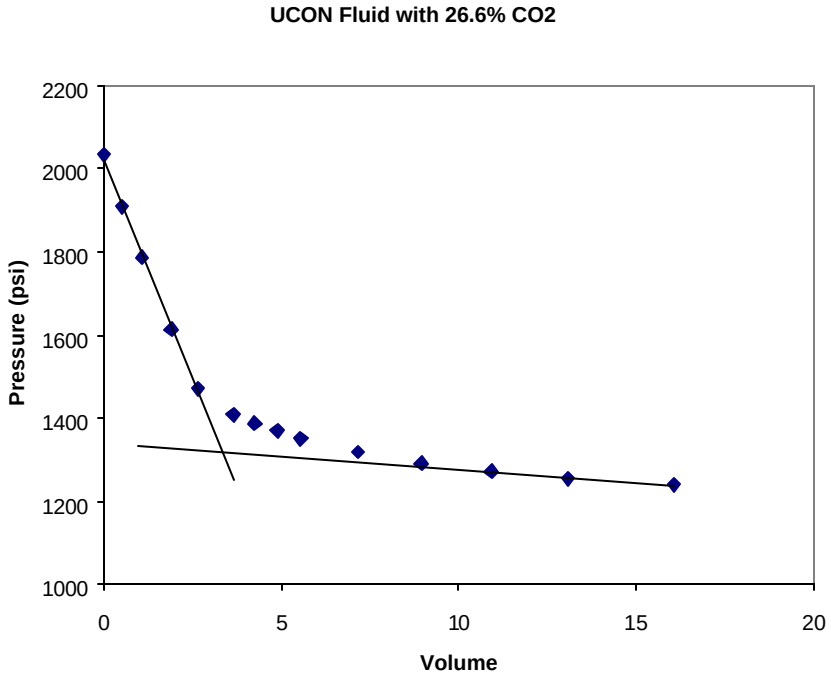

Figure 3.6(d): P-V isotherm at high carbon dioxide concentration

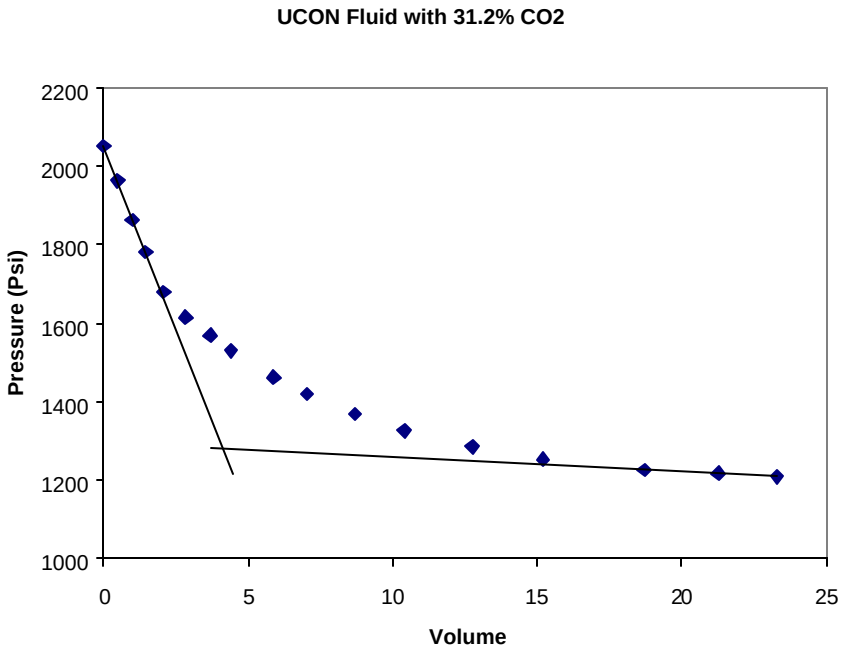

Figure 3.6(e): P-V isotherm very high carbon dioxide concentration

as a straight line, and it deviates from the initial slope as the system undergoes a phase transition. However, the isotherm has a hyperbolic shape and eventually turns into a line with small negative slope instead of changing into a less steep line or a completely flat line. As the carbon dioxide concentration was increased from 20.1% to 31.2%, the hyperbolic shape became more obvious and the final slope of the isotherm increased.

The unusual shape of this P-V isotherm can be explained by first considering the mechanism of the phase transition at high carbon dioxide content. As the mixture undergoes a phase transition, two different phases were formed, a polymer-rich phase and a carbon dioxide-rich phase. The carbon dioxide rich phase contains very little polymer due to the high overall carbon dioxide concentration in the system. As a result, the mixture behaves almost like pure carbon dioxide with the critical point of this phase being close to that of the pure fluid. In the case where a phase transition occurs at

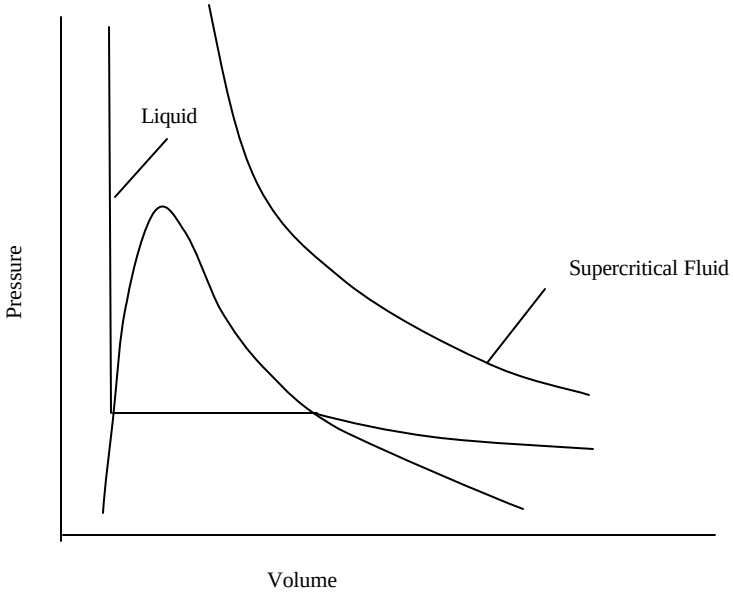

Figure 3.7: P-V isotherm for fluid existing above and below the critical point.

temperature and pressure below the critical point, the newly formed, carbon dioxide-rich phase is a liquid and the phase transition is a liquid to liquid-liquid transition. This type of phase transition is typical in most experiments. However, in the case where the phase transition occurs at temperature and pressure above the critical point, the carbon dioxide-rich phase is a supercritical fluid and the phase transition is a liquid to liquid-fluid (L-LF) transition. Although the L-LF transition is unusual, this is the transition observed in this system at 50 °C since the temperature is above the critical point of carbon dioxide. A correlation of the L-LF transition to the shape of the mixture P-V isotherm can be made by considering the P-V isotherm of a pure fluid. Shown in Figure 3.7 are the P-V isotherms for a pure fluid below and above its critical point, calculated using the van der Waals equation of state. Below the critical point, the isotherm is a steep line, which is similar to the isotherm obtained at 13% carbon dioxide concentration. Such similarity is expected because the newly formed phase during a L-LL transition is a liquid phase. Above the critical point, the isotherm is a hyperbola, and it is similar to the isotherm obtained the mixture at high carbon dioxide concentrations, in which the newly formed phase during a L-LF transition is a supercritical fluid. From this similarity, it can be concluded that the hyperbolic shape of P-V isotherm was indeed due to a L-LF transition that occurs at high carbon dioxide concentration. In addition, the hyperbolic P-V isotherm can be used as a signature for the L-LF transition in the future.

3.4 References

1. Scott, R.L.; van Konynenburg, P.B. *Discuss. Faraday Soc.*, **1970**, *49*, 87.
2. Kirby, C.F.; McHugh, M. A. *Chem. Rev.*, **1999**, *99*, 565-602.
3. Kiamos, A. A. High Pressure Behavior of Polymer-solvent-Supercritical Fluid Mixtures. M.S. Thesis, The Johns Hopkins University, 1992.
4. Schultze, C. Phase Behavior of Mixtures Containing Supercritical Fluid: Equation of State Calculations and Experiments. Ph. D. Dissertation, The Johns Hopkins University, 1998.
5. Folie, B; Radosz, M Ind. Eng. *Chem. Res.* **1995**, *34*, 1501-1516.

4. Results and Discussion: Block Copolymer Adhesives

4.1 Introduction

Block copolymers are polymeric materials made from at least two chemically distinct regions. One example is the styrenic block copolymer, which is a thermoplastic rubber that was developed by Shell Oil Inc. (1). Styrenic block copolymers are formed from anionic polymerization of three monomers: styrene, butadiene, and isoprene. This polymerization reaction is living and usually is carried out in cyclohexane. Like most anionic polymerization reaction products, styrenic block copolymers have a narrow range of molecular weights. The polymerization mechanism is shown below:

$$RI^- + M \rightarrow RMI^- \rightarrow R^+MMMI^-$$

The anion initiates the polymerization by first reacting with the styrene monomer to begin a styrene block chain. Next, either butadiene or isoprene is added to build a second block, forming a styrene-butadiene (S-B) or styrene-isoprene (S-I) diblock copolymer, respectively. The polymerization can be continued by adding styrene again to form a S-B-S or S-I-S triblock, or by adding coupling agent to form coupled structures that are linear, radial, or star. Another type of block copolymer is formed by the hydrogenation of the butadiene or isoprene of the SBS or SIS, which results in a styrene-ethylene butadiene-styrene (S-EB-S) or a styrene-ethylene propylene-styrene (S-EP-S) structure, respectively.

The styrene-rubber-styrene block copolymer has attracted great interest in adhesive applications for its combination of thermoplasticity and strength without vulcanization. This combination of properties is due to the unusual phase separated morphology of the block copolymer. The copolymer tends to phase separate into a rubber phase and a plastic polystyrene domain. In the rubber phase, polyisoprene or polybutadiene gives toughness and rubberiness without vulcanization, while the polystyrene domains are plastic blocks that give solubility and thermoplasticity (1-3). The configuration of the polystyrene domain can be varied from spheroids to cylinders, and eventually to plates as the polystyrene content increases (1). The strength resulting from the phase separated morphology allows thermoplastic rubbers to be used as a strength-bearing adhesive base polymer.

When formulating adhesives, the adhesive properties depend a great deal on the base block copolymer. The choice of rubber midblock type, polystyrene content and block size, diblock content, and polymer molecular weight all can affect the properties of adhesives (4). An isoprene midblock gives the most softness and lowest viscosity, while a hydrogenated midblock results in the least softness and highest viscosity. Polystyrene and diblock content also affect stiffness and viscosity, as well as strength. Increasing polystyrene content increases all three properties, while increasing diblock content decreases all three properties. Furthermore, increasing polystyrene increases viscosity and temperature resistance, while increasing total polymer molecular weight increases viscosity and shear strength. Simpson and Fowler (5) studied the effect of molecular weight and polystyrene content on solution properties and adhesion strength at different temperatures.

Since polymer structure is an important factor in determining adhesive properties, specific types of block copolymers are chosen for different applications. SBS block copolymers generally have high cohesive strength, and therefore are commonly selected for solvent-based contact adhesives. SIS block copolymers generally are easy to tackify and are suited for pressure sensitive adhesives. Hydrogenated block copolymers typically show excellent resistance to oxygen, ozone and UV light due to the saturated backbone structures. Thus, SEBS or SEPS block copolymers are used for applications that require resistance to harsh environments, such sealants and oil gels. Formulations of different types of adhesives based on block copolymers have been described in the literature and patented. Bronstert *et al.* (6) patented a hot-melt contact adhesive formulation based on a hydrogenated styrene-butadiene block copolymer. In addition, the viscoelastic behavior of SBS-based, hot-melt contact adhesive was investigated by Jacob (7). Formulations of solvent-free and solvent-based contact adhesives also have been patented by Schunck (8) and Vitek (9), respectively.

4.2 Experimental Results

Pressure versus volume (P-V) isotherms and visual observations were obtained for each of the six block copolymer systems. Measurements and observations were made at 40, 50, 60, and 70 °C and at various carbon dioxide concentrations. At the pressure of 2000 psi, all six copolymer systems were in the one-phase region at the temperatures and CO_2 concentrations studied. Plots of the P-V isotherms are presented in Appendix A.

4.2.1 System #1— 1:3 SIS Block Copolymer:Toluene

At the conditions of 2000 psi, 40°C, and 11% carbon dioxide, the appearance of the solution was almost transparent, and the stirring bar could be seen. As the temperature increased, the solution became slightly more opaque. A larger increase in opacity was observed when the carbon dioxide concentration was increased. As the carbon dioxide concentration increased from 11% to 34%, the solution transformed from clear to milky white, and the stirring bar was barely visible. The appearance of the solution remained unchanged as the pressure was decreased until the bubble point was reached. At the bubble point, a new vapor phase began to form and started to nucleate into bubbles. The formation of bubbles began near the stirring bar, and propagated outward. The bubbles then rose slowly to the top of the system cell. No formation of a new liquid phase was observed in the range of temperatures and carbon dioxide concentrations studied. The specific pressures at which the bubble points occurred were determined from P-V isotherms. The P-V isotherms obtained for this system are shown in Figures A1-16. All of these data begin as a steep line and then sharply become flat. This type of P-V isotherm was described by Murlidharan and Donohue (10) and in Chapter 3.3 as a signature for a bubble-point phase transition. The bubble point pressure was determined by the intersection of the steep line and the flat line. With the knowledge that there would be no cloud-point phase transition, efforts in this work were made to obtain only enough P-V data to establish trends for the steep line at small volumes, and for the flat line at large volumes. Thus, only a few pressures corresponding to intermediate volumes were recorded. Bubble points were determined from P-V isotherms at various temperatures and carbon dioxide concentrations and plotted in a

pressure versus temperature phase diagram, shown in Figure 4.1. In this phase diagram, the pressure of the bubble point at constant carbon dioxide concentration increased as temperature increased, and established a trend for the vapor pressure curve. As carbon dioxide was added to the system, the vapor pressure curve moved to higher pressures. Because this system was cloudy, but no cloud point transition was found over the range of pressures, temperatures, and compositions studied here, it is not clear whether this system will exhibit a decompressive spray in the UNICARB® process.

4.2.2 System #2— 17:33 SIS Block Copolymer:Toluene

In comparison to the previous system discussed, the polymer content of this system was increased and the initial appearance of the solution was more opaque. An increase in the opaqueness of the solution was again observed as temperature and carbon dioxide concentration were raised. Similar to the results from the previous system, only bubble points were observed as carbon dioxide concentration increased from 9 to 27% wt. The bubble point pressures were determined from P-V isotherms as shown in Figures A17-25. Bubble points were plotted in a P-T phase diagram, and vapor pressure curves were mapped out at each carbon dioxide concentration as shown in Figure 4.2. As the carbon dioxide concentration increased, the vapor pressure curve also moved to higher pressures. Again, because this system was cloudy, but no cloud point transition was found over the range of pressures, temperatures, and compositions studied here, it is not clear whether this system will exhibit a decompressive spray in the UNICARB® process.

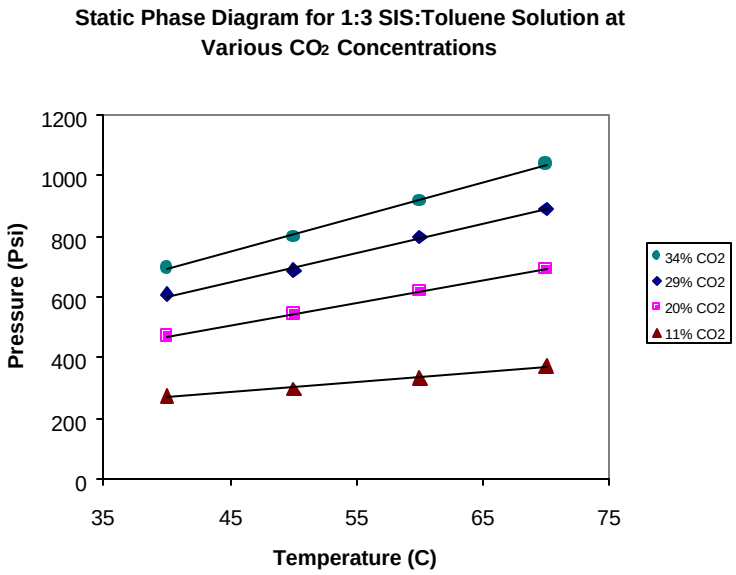

Figure 4.1. Static phase diagram for 1:3 SIS block copolymer:toluene mixture.

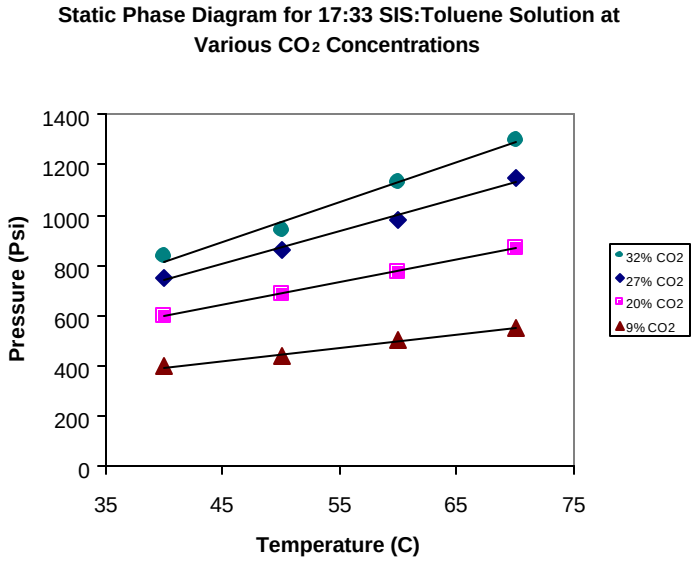

Figure 4.2. Static phase diagram for 17:33 SIS block copolymer:toluene mixture.

4.2.3 System #3— 2:3 SIS Block Copolymer:Toluene

In this system, the polymer content was further increased and the carbon dioxide composition was set to 32 wt. %. Contrary to the previous two systems, only cloud points were observed at various temperatures. The system began as a one-phase opaque solution at 2000 psi, with the stirring bar barely visible. As pressure was decreased to the cloud point, the solution become even more cloudy and dark at the top the cell. Further decreases caused the darkness to propagate downward and fill up the whole cell, making visual observation impossible. The solution turned dark because a new liquid phase began to form. A large number of small liquid particles nucleated, preventing light from passing through. P-V isotherms for this system at four different temperatures were obtained and are shown in Figures A26-29. Contrary to the isotherms of system #1 and #2, data from this system changed slope twice rather just once. The isotherms began as a steep line, then became less steep, and eventually turned completely flat. This type of isotherm was also described by Murlidharran and Donohue (10) and in Chapter 3.3 as an indication for a cloud point phase transition followed by a bubble-point phase transition. The pressure at which the cloud occurred was determined by the intersection of the steep line and the less steep line, and the pressure at which the bubble point occurred was determined by the intersection of the less steep line and the flat line. Shown in Figure 4.3 are the vapor pressure curve mapped out by the bubble points and the lower critical solution temperature (LCST) curve, mapped out by the cloud points. Data in Figure 4.3 show that the slope of the LCST curve is smaller than that of vapor pressure curve, which is just opposite to what is expected. Although this result is surprising, it can happen when the carbon dioxide concentration is high. At high carbon dioxide concentrations,

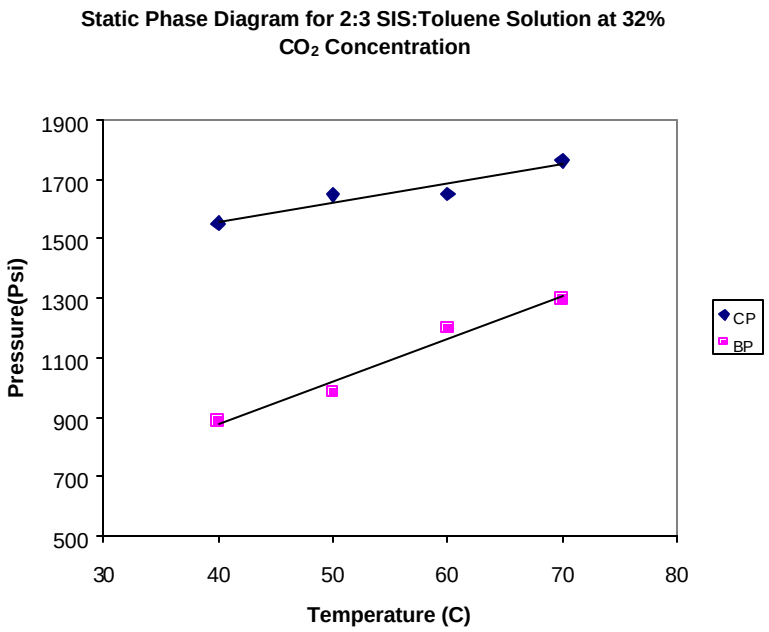

Figure 4.3. Static phase diagram for 2:3 SIS block copolymer:toluene mixture.

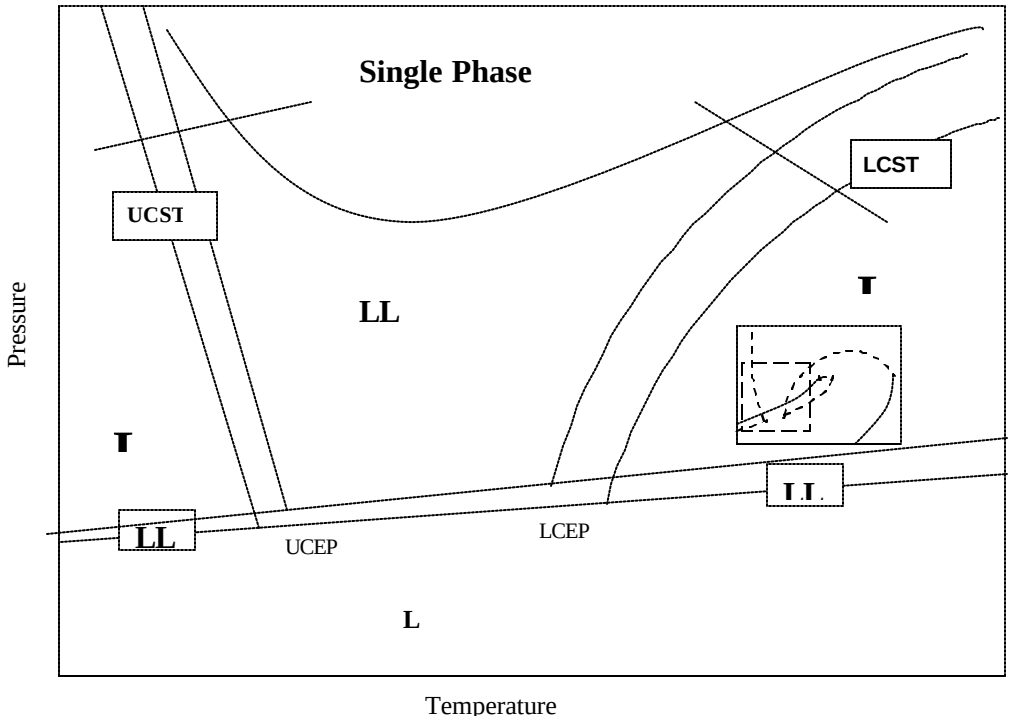

Figure 4.4. Effect of increasing solute concentration.

the upper critical solution temperature curve and lower critical solution temperature curve eventually will merge into one single curve. A P-T phase diagram showing merged critical curves is shown in Figure 4.4. Near the minimum in Figure 4.4, the merged critical curve can be flatter than the vapor pressure curve. Because this system exhibited both cloud point and bubble point in the range of pressures, temperatures, and compositions studied here, it would be a good starting point for future formulations of block copolymer-based contact adhesives for use in the UNICARB® processes.

4.2.4 System #4— 1:3 SEBS Block Copolymer:Toluene

In this system, the SBS block copolymer was replaced by SEBS block copolymer. The polymer content was equal to that in system #1, and the solution appearance was slightly cloudier. Similar to the results for system #1 and #2, only bubble points were observed as carbon dioxide concentration increased from 13 to 32 wt %. The bubble point pressures were determined from P-V isotherms shown in Figures A30-41. Bubble points were plotted in P-T phase diagram, and vapor pressure curves were mapped out at each carbon dioxide concentration as shown in Figure 4.5. As the carbon dioxide concentration increased, the vapor pressure curve also moved to higher pressures. Because this system was cloudy, but no cloud point transition was found over the range of pressures, temperatures, and compositions studied here, it is not clear whether this system will exhibit a decompressive spray in the UNICARB® process.

4.2.5 System #5— 1:2 SEBS Block Copolymer:Toluene

Compared to system #4, the polymer to solvent ratio was raised in this system

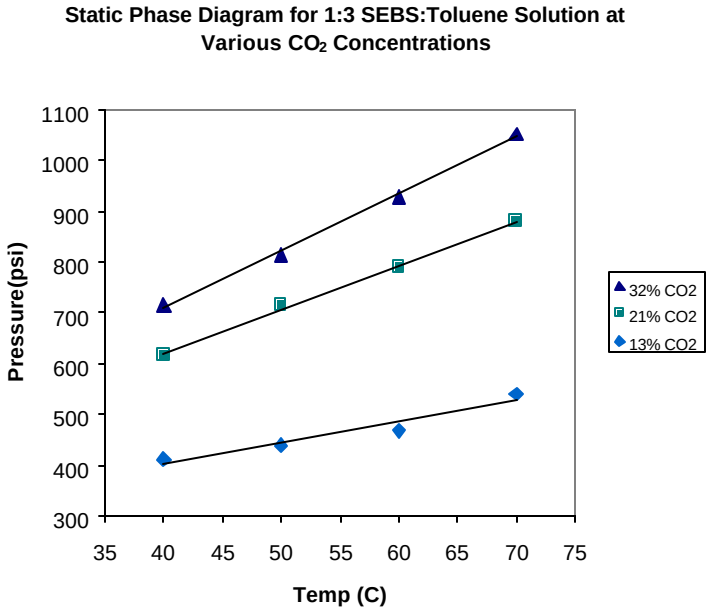

Figure 4.5. Static phase diagram for 1:3 SEBS block copolymer:toluene mixture.

from 1:3 to 1:2. As expected, the solution appeared cloudier, similar to the appearance of system #3. For this system, two phase transition phenomena were visually observed as the carbon dioxide concentration increased from 20 to 38% wt. At first, phase transitions that looked like bubble points were observed at low carbon dioxide concentrations. These phase transitions were indicated by the formation of bubbles as the pressure is lowered during volume expansion. As the carbon dioxide concentration and temperature increased to above 31% and 50 °C, the bubble-point-like phenomena were replaced by phase transitions that looked like cloud points. These phase transitions were characterized by the sudden blackening of the system, which began at the top of the pressure cell and propagated downward. To verify the visually observed phase transitions, P-V isotherms for this system at various conditions were examined. These isotherms are shown in Figures A42-57. Isotherms obtained at low carbon dioxide concentrations began with a steep line, which then flattened, indicating that these phase transitions are indeed bubble points. However, P-V isotherms obtained at higher carbon dioxide concentrations surprisingly also had this same shape. Because these P-V isotherm lacked the less steep line and a second change in slope, it was determined that the corresponding phase transitions were just bubble points that looked like cloud points. The appearance of the bubble point transition was similar to that of cloud point transition because as the system become saturated with carbon dioxide, there were a large number of very fine bubbles that were formed when the pressure is lowered. Just like small liquid droplets, they prevented light from passing through, resulting in the black appearance. Bubble points were plotted in a P-T phase diagram, and vapor pressure curves were mapped out at each carbon dioxide concentration as shown in Figure 4.6. As

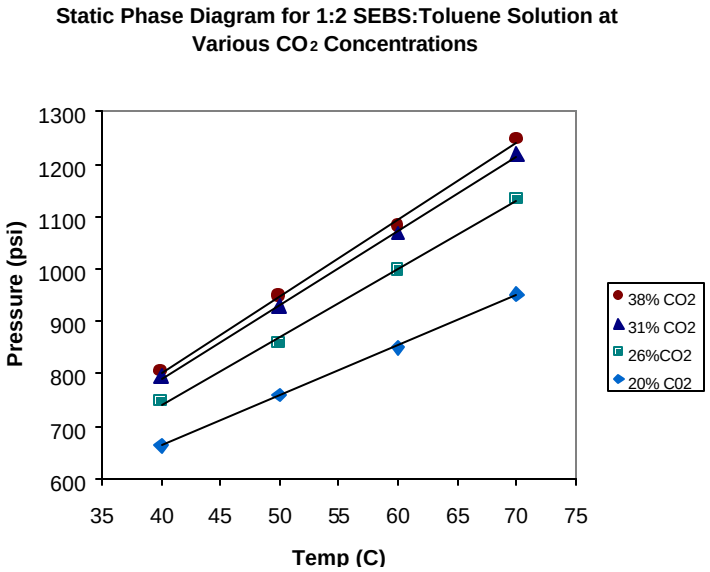

Figure 4.6. Static phase diagram for 1:2 SEBS block copolymer:toluene mixture.

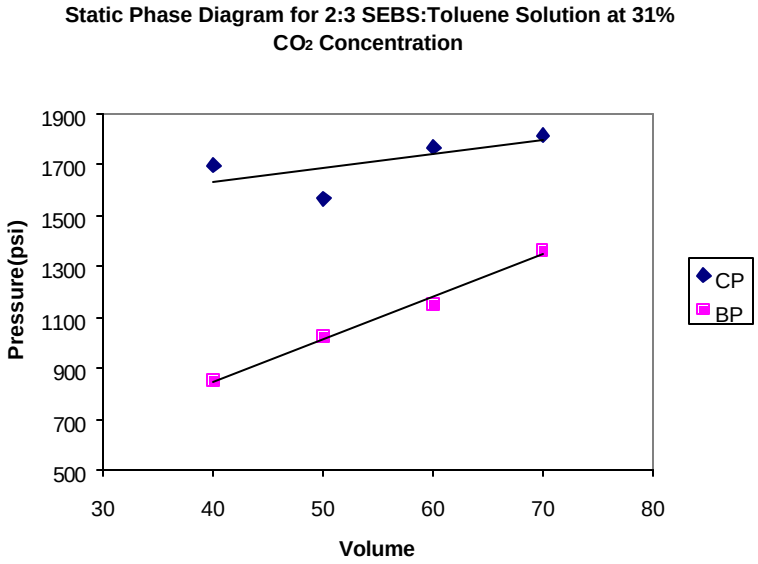

Figure 4.7. Static phase diagram for 2:3 SEBS block copolymer:toluene mixture.

the carbon dioxide concentration increased, the vapor pressure curve also moved to higher pressures. Again, because this system was cloudy, but no cloud point transition was found over the range of pressures, temperatures, and compositions studied here, it is not clear whether this system will exhibit a decompressive spray in the UNICARB® process.

4.2.6 System #6— 2:3 SEBS Block Copolymer:Toluene

In this system, the polymer content was further increased and the carbon dioxide composition was fixed at 31% wt. Similar to system #3, only cloud points were observed at various temperatures. Cloud points and bubbles points were determined from P-V isotherms and are plotted in Figure 4.7. The P-V isotherms obtained at various temperatures are shown in Appendix B. As indicated by Figure 4.7, this system exhibited the same unusual phase behavior found in system #3, in which the slope of the LCST curve was smaller than that of the vapor pressure curve. Because this system exhibited both cloud points and bubble points in the range of pressures, temperatures, and compositions studied here, it would be a good starting point for future formulations of block copolymer-based contact adhesives for use in the UNICARB® processes.

4.3 Dynamic Phase Behavior

In addition to the investigation of the static phase behavior of the block copolymer systems, the dynamic phase behavior of rapidly expanding systems was investigated. The dynamic pressure versus time profiles were obtained for each of the six systems at various temperatures and carbon dioxide compositions. At each temperature

and composition, the experiment was repeated three times to account for errors. All pressure versus time profiles are included in Appendix B. For simple systems, the determination of phase transitions from pressure versus time data is straightforward. Shown in Figure 4.8 is a pressure versus time profile for pure carbon dioxide as it underwent a rapid expansion. As the expansion began, the pressure profile started out as a straight line with negative slope. This part of pressure profile was expected because as time increased, the expansion lasted longer, and pressure became lower. When a phase transition occurred as the system expanded, the slope of pressure profile changed due to the different compressibility of the newly formed phase. The change from steeper to less steep slope resulted in a kink in the pressure profile, and it could be used to determine the pressure at which a phase transition occurred during dynamic expansion. For instance, as carbon dioxide expanded, there was a kink at approximately 1010 psi, which indicated that phase boundary is at 1010 psi. Using this technique to determine dynamic phase transitions, were analyzed to map out the dynamic phase boundaries for each system. Unlike pure carbon dioxide data, the pressure versus time profiles for polymeric solutions were nonlinear, and approximations had to be made. In general, the profile could be broken down into two parts. First, immediately after expansion, the pressure profile took a slightly curved shape. This curvature was approximated by a straight line as demonstrated in Figure B1, thus allowing the establishment of an initial slope. Second, as the phase transition occurred, the pressure profile took on a hyperbolic shape and deviated from the initial slope. By approximating an initial slope and finding the pressure at which the profile deviated from this initial slope, the dynamic phase transition became identifiable.

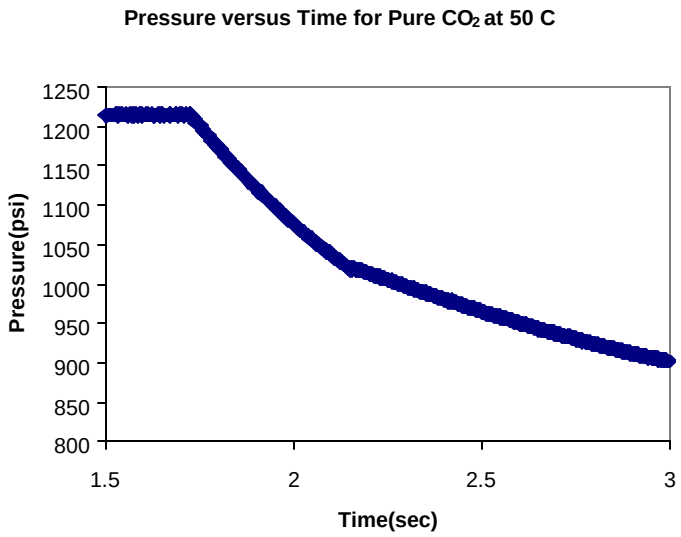

Figure 4.8. Pressure profile for pure carbon dioxide undergoing rapid expansion

Phase boundaries at various temperatures and compositions were determined and dynamic phase diagrams were obtained by plotting the average phase transition pressure versus temperature at various carbon dioxide concentrations. The dynamic phase diagrams are shown in Figures 4.9(a-e). Comparing the five systems, system #4 contained the smallest error and exhibited the clearest trends for dynamic phase boundaries. Best linear fits of the data points for vapor pressure showed a monotonically increasing function as expected, and the vapor pressure curve shifted to higher pressures as carbon dioxide concentration increased. Other dynamic phase diagrams did not show as clear of a trend, and the vapor pressure curve was not a monotonically increasing function. Dynamic phase diagrams also were compared to the corresponding static phase diagrams. For all systems except system #3, the dynamic phase boundaries occurred above the pressure at which corresponding static phase boundaries occurred. For system #3, there was no difference between the two types of phase boundaries. These results suggest that some polymeric systems in rapid expansion undergo a phase transition at a

higher pressure than where it normally would occur. One hypothesis that could explain these results is based on the fact that polymers are large molecules, which cannot rearrange fast enough during rapid expansion. Consequently, the polymers cannot achieve the lowest energy state and therefore may phase separate prematurely. This idea also could be explained by considering the coexistence curves calculated from mean field approximations and Monte Carlo (MC) simulation data. The coexistence curves are shown in Figure 4.10. During a rapid temperature quench, if the system behaved according to the mean field approximation, it would phase separate at temperature below the coexistence curve. However, as the system was allowed to rearrange after the quench, the system would form one phase again if it were above the coexistence curve established by the MC data.

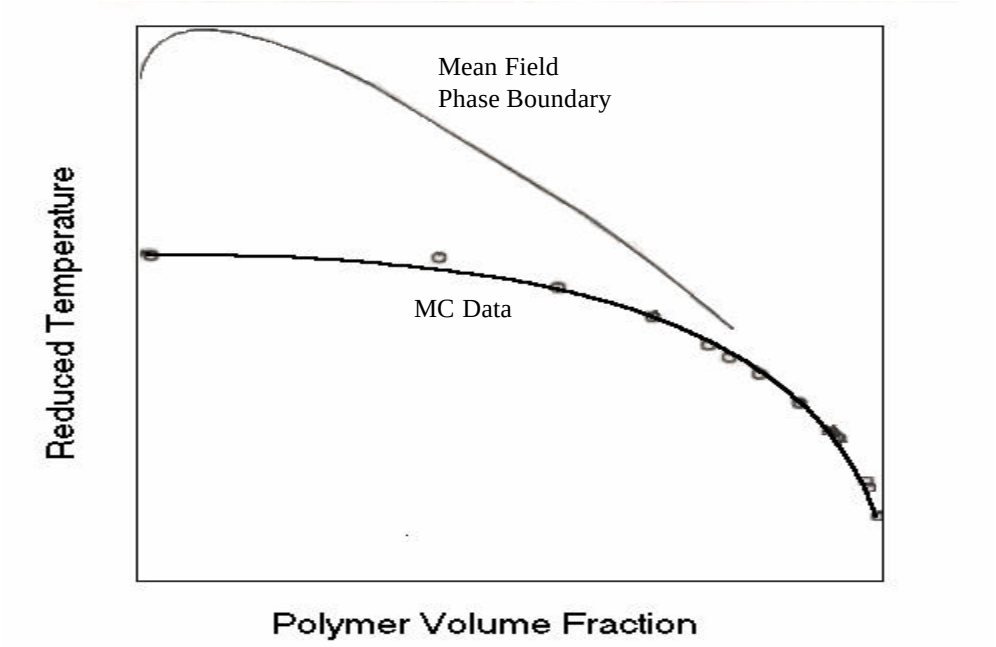

Figure 4.10. Coexistence curve calculated from mean field approximation and Monte Carlo simulation

4.4 References

1. Korcz, B. *Kraton® Rubbers: The Basics*, Kraton® Training Course, Westhoolow Technology Center, May 18, 1999.
2. Landdrock, A.H. Adhesives Technology Handbook, 1985, Noyes Publications.
3. Pocius, A.V. Adhesion and Adhesives Technology, 1997, Hanser Publishers.
4. Salazar, L. *Kraton® Rubber in Adhesive Applications,* Kraton® Training Course, Westhoolow Technology Center, May 18, 1999.
5. Simpson, B.D.; Fowler, P.R. *Adhes. Age* **1974**, *17(9)*, 32-5.
6. Bronster, K.; Druschke, W.; Groh, W.; Ladenberger, V.; Mueller, H. *Ger. Offen. DE 2736952*, 1979.
7. Jacob, L *Adhesion* **1991**, *35(4)*, 16, 18-20, 23.
8. Vitek, R. *Brit. UK Pat. Appl. GB 2020292*, 1979.
9. Schunck, E.; Schmelzer, H.; Sattelmeyer, R *Ger. Offen. DE 2558858,* 1977.
10. Muralidharan, V.; Donohue, M.D. *The Journal of Supercritical Fluids*, **1994**, *7*, 275-281.

5. Results and Discussion: Polyalkylene glycol

5.1 Introduction

Polyalkylene glycol (MW~ 2500 g/mol) from Union Carbide Corporation was analyzed experimentally. Polyalkylene glycol is a clear liquid with low viscosity at room temperature. Solubility data were obtained as described in Chapter 2 over carbon dioxide concentrations ranging from 9 to 19 weight % at 40 °C. Phase transitions at each composition were determined from P-V isotherms. The bubble points were found to occur at 9 wt. % carbon dioxide, in which the shape of P-V isotherm began as a straight line, and then deviated from the initial slope in the form of a curve before turning into a flat line. The curvature in this P-V isotherm can be attributed to the close proximity of the mixture critical point in these measurements. As carbon dioxide concentrations were increased a bubble point was identified. A summary of the Polyalkylene glycol data can be seen in Figure 5.1.1.

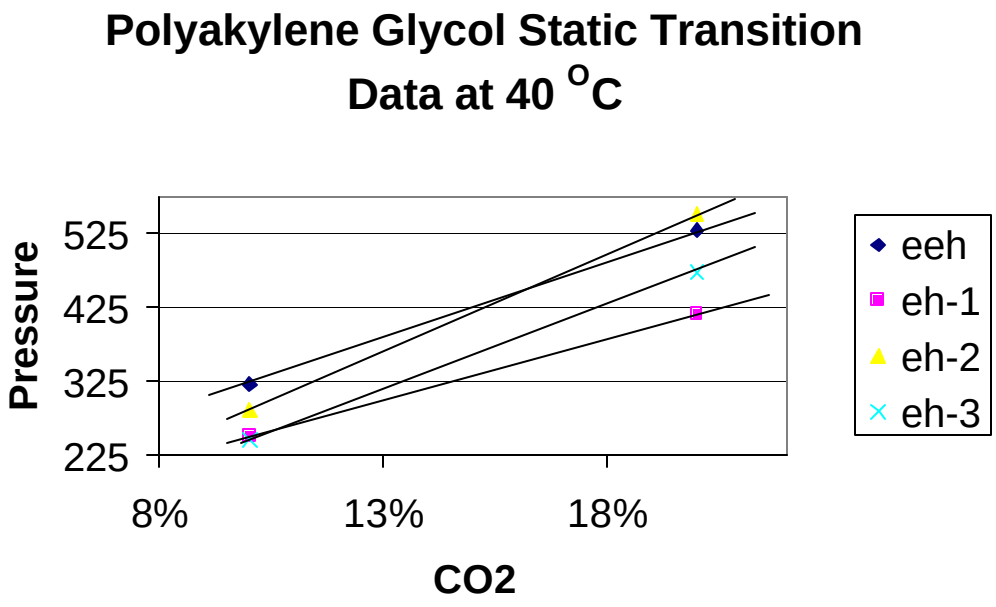

Figure 5.1.1 Summary of static data for polyalkylene glycol samples

5.2.1 System #1— EEH Polyalkylene glycol

Pressure versus volume isotherms were obtained for the EEH sample at both 9% and 19% carbon dioxide concentrations and at a temperature of 40 °C. At the maximum pressure of 2000 psi all of the systems were in the one phase region for the concentrations and temperature studied. The shape of the static isotherms began as a steep straight line, went through a small region of curvature, and eventually flattened to a very small or zero slope. The static transition was determined by the intersections of these two lines, as seen in figure 5.2.1 for EEH.

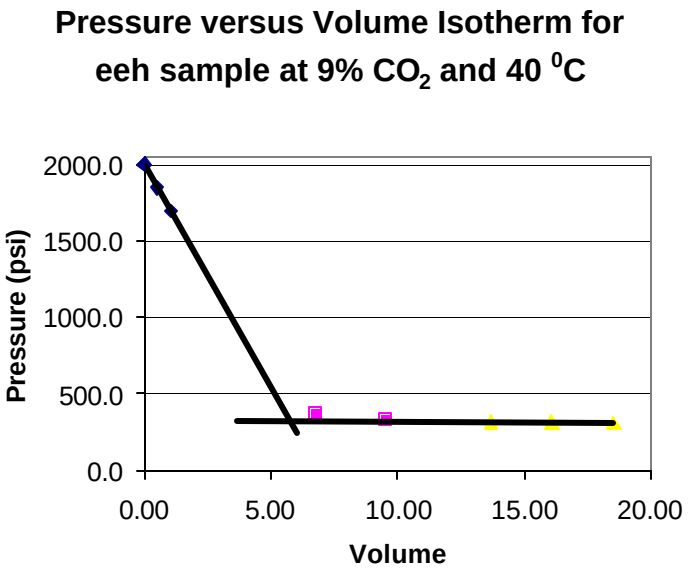

Figure 5.2.1 – P-V Isothermo for low carbon dioxide concentration

5.2.2 System #2— EH-1 Polyalkylene glycol

Pressure versus volume isotherms were obtained for the EH-1 sample at both 9% and 19% carbon dioxide concentrations and at a temperature of 40 °C. At the maximum pressure of 2000 psi all of the systems were in the one phase region for the concentrations and temperature studied. The shape of the static isotherms began as a steep straight line, went through a moderate region of curvature, and eventually flattened to a very small or zero slope. The static transition was determined by the intersections of these two lines, as seen in figure 5.2.2 for EH-1. Additionally, this system's phase transitions were seen at lower pressures than the previous EEH sample.

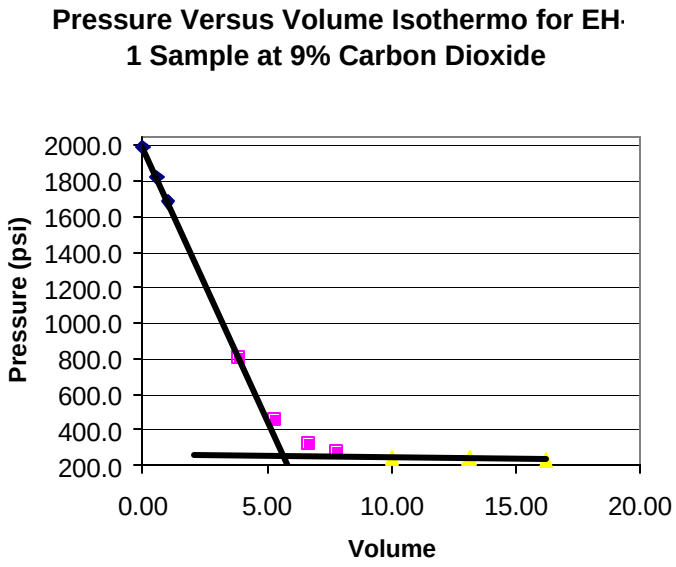

Figure 5.2.2 P-V diagram showing moderate curvature

5.2.3 System #3— EH-2 Polyalkylene glycol

Pressure versus volume isotherms were obtained for the EH-2 sample at both 9% and 19% carbon dioxide concentrations and at a temperature of 40 °C. At the maximum pressure of 2000 psi all of the systems were in the one phase region for the concentrations and temperature studied. The shape of the static isotherms began as a steep straight line, went through a small region of curvature, and eventually flattened to a very small or zero slope. The static transition was determined by the intersections of these two lines, as seen in figure 5.2.3 for EH-2. This sample has phase transitions at pressures between those of EEH and EH-1.

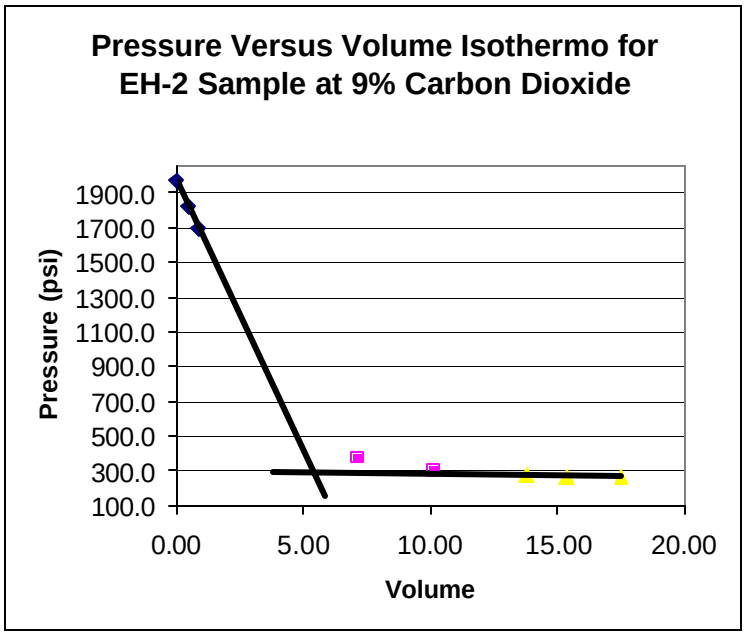

Figure 5.2.3 P-V Diagram for EH-2 at 40 ºC

5.2.4 System #4— EH-3 Polyalkylene glycol

Pressure versus volume isotherms were obtained for the EH-3 sample at both 9% and 19% carbon dioxide concentrations and at a temperature of 40 °C. At the maximum pressure of 2000 psi all of the systems were in the one phase region for the concentrations and temperature studied. The shape of the static isotherms began as a steep straight line, went through a very small region of curvature, and flattened to a very small or zero slope. The static transition was determined by the intersections of these two lines, as seen in figure 5.2.4 for EH-3.

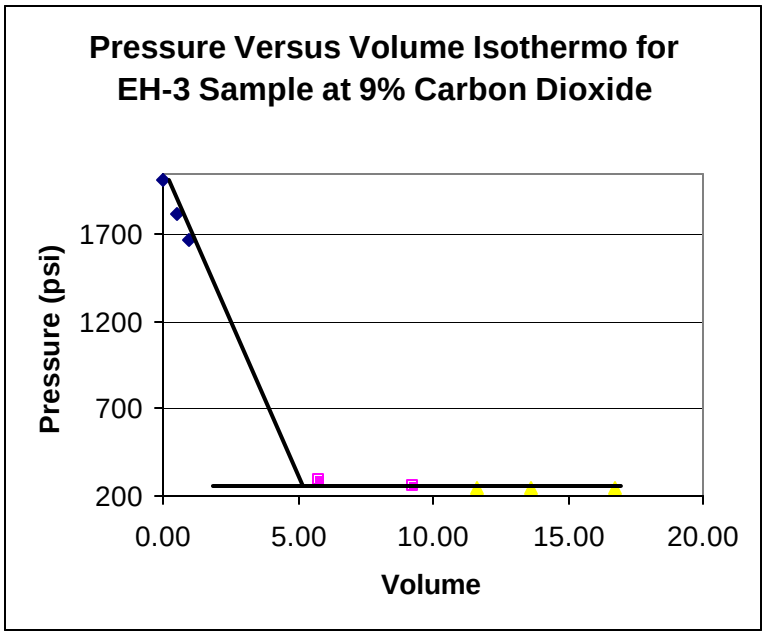

Figure 5.2.4 P-V diagram for EH-3

5.3 Dynamic Phase Behavior

The dynamic phase behavior of all of the polyakylene glycol systems were investigated along with the static behavior. The dynamic pressure versus time profiles were obtained for all four of the systems and analyzed using the procedure from Chapter 4. All of these were simple single phase transition systems in which the phase transition could be determined by finding the transition from steep to less steep slope or the kink. A summary of this data for all four systems is illustrated in Figure 5.3.1. It should also be noted that in the case of these systems that dynamic phase transitions occur at much higher pressure. The transition pressures are approximately one thousand psi higher under dynamic versus static conditions.

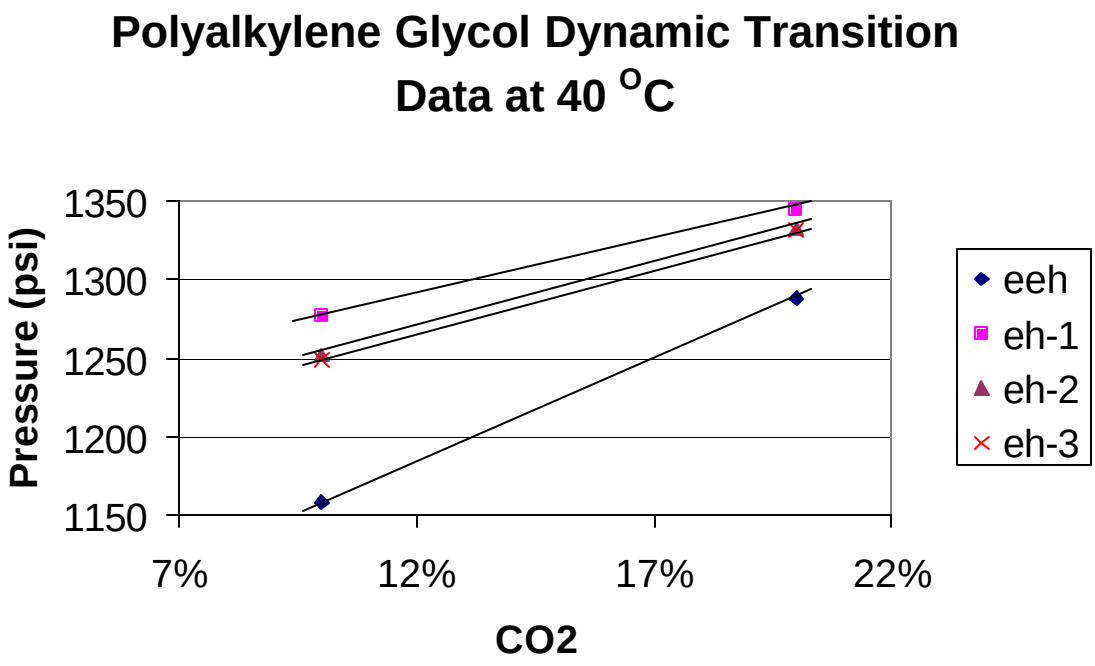

Figure 5.3.1 Trend lines for dynamic phase transition data

6. Results and Discussion: Polyethylene glycol

6.1 Introduction

Two systems of polyethylene glycols (PEG) were studied, molecular weight 4600 and 8000. These systems were studied at carbon dioxide concentrations between 5 and 32 weight percent and at a temperature of 70 °C. Phase transitions were observed in both systems with lower transition pressures in PEG 4600 at low carbon dioxide concentrations. While at high concentrations of carbon dioxide this trend is reversed, with PEG 8000 transitioning at lower pressures.

6.2 Experimental Results

Pressure volume isotherms were obtained for each PEG system. Measurements and observations were made at over a wide range of carbon dioxide concentrations. This information is illustrated and summarized in Figure 6.2.1 and 6.2.2. As well a bubble and cloud point can be seen at high carbon dioxide concentration in PEG 4600.

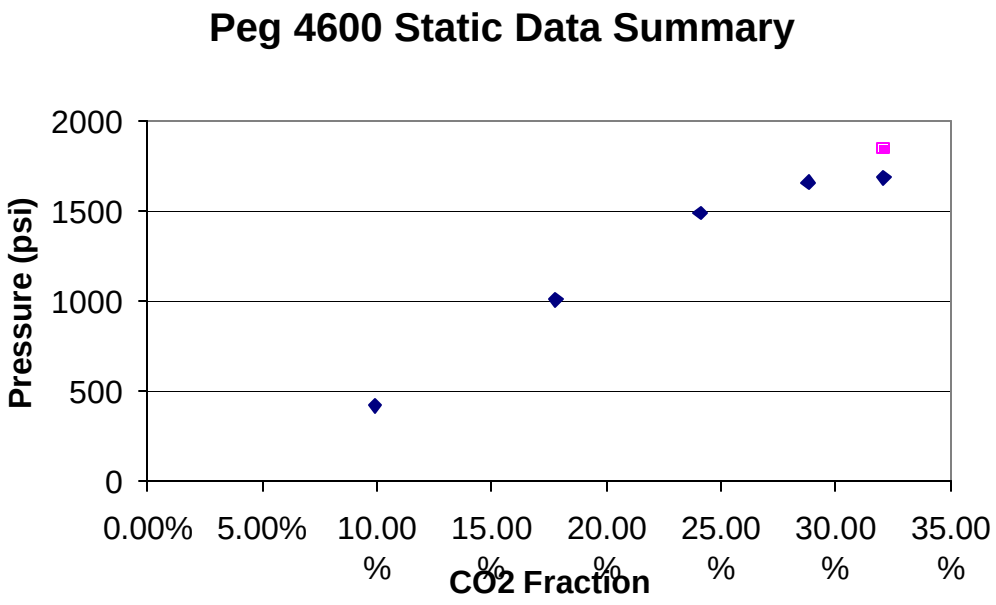

Figure 6.2.1 Phase boundary diagram for PEG 4600

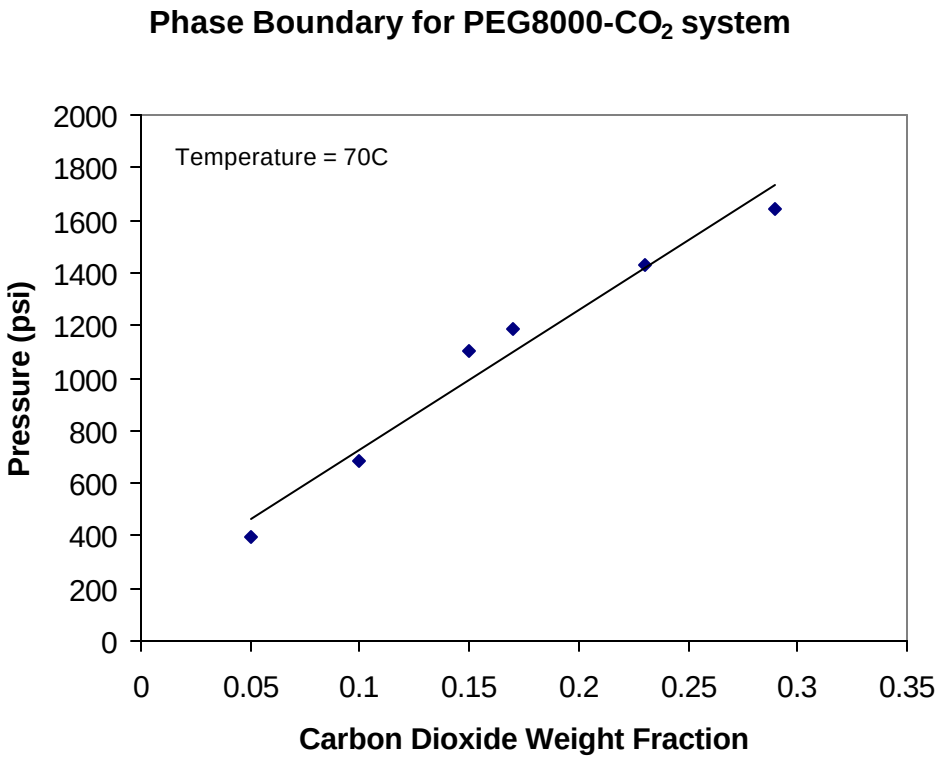

Figure 6.2.2 Phase boundary diagram for PEG 8000

6.3.1 System #1—Polyethylene glycol MW 4600

Pressure versus volume isotherms were obtained for the Poly ethylene glycol 4600 system at 10%,18%, 24%, 29% and 32% carbon dioxide concentrations and at a temperature of 70 °C. At the maximum pressure of 2000 psi all of the systems were in the one phase region for the concentrations and temperature studied. Static transition data was taken under these conditions. Using the process detailed in Chapter 3 a phase transition pressure was determined for each data set. This an example of this information can be seen for 10 weight % carbon dioxide in Figure 6.3.1a as well an example of a static isotherm with two transitions is seen in Figure 6.3.1b.

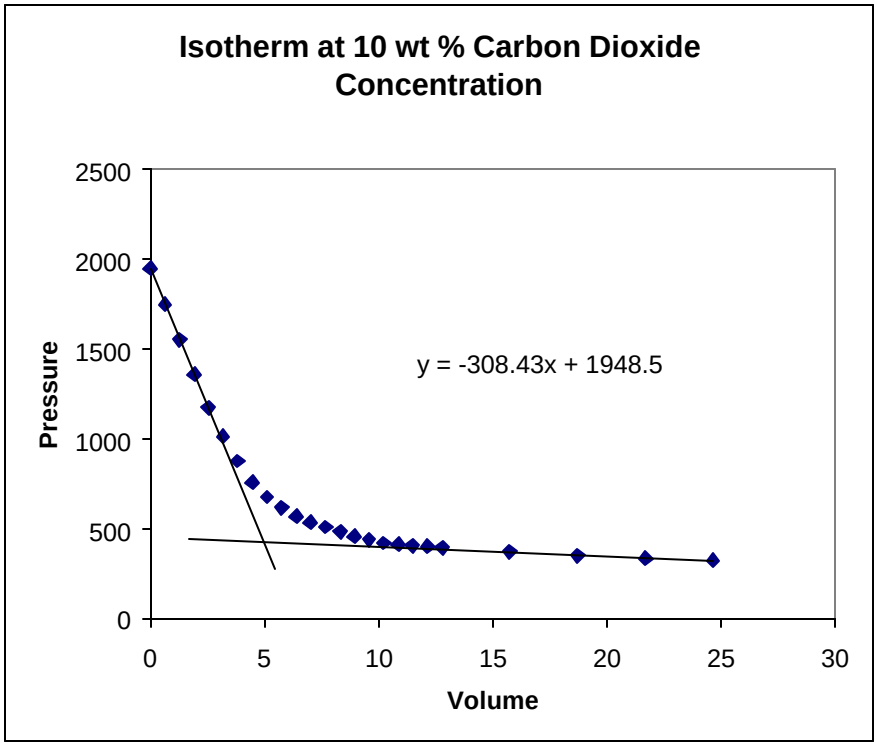

Figure 6.3.1a Pressure volume isothermo for PEG 4600

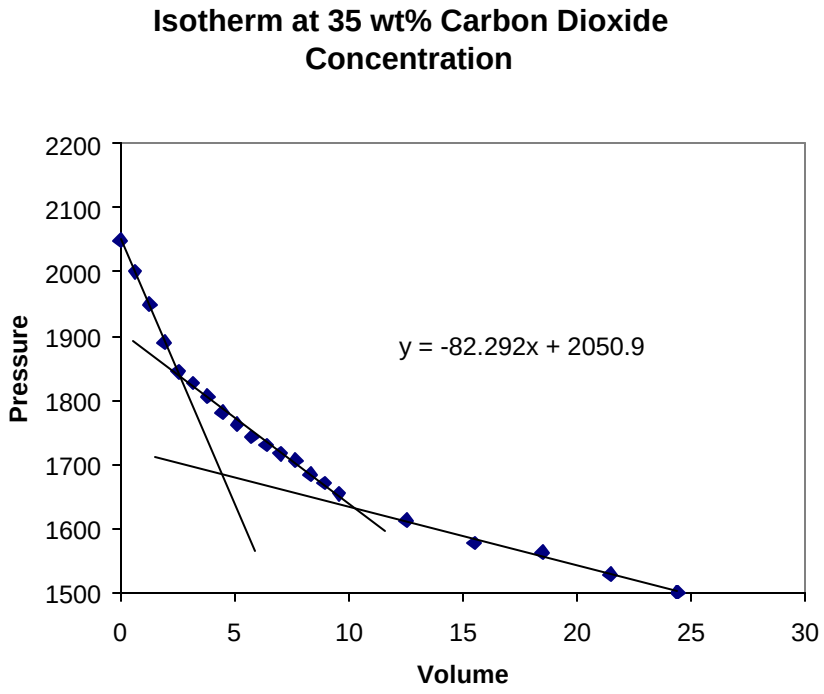

Figure 6.3.1b Pressure volume isothermo for PEG 4600 with two phase transitions

6.3.2 System #2—Polyethylene glycol MW 8000

Pressure versus volume isotherms were obtained for the Poly Etylene Glycol 8000 fluid at 5%, 10%, 15%, 17%, 23% and 29% carbon dioxide concentrations and at a temperature of 70 °C. At the maximum pressure of 2000 psi all of this system was in the single phase region for the concentrations and temperature studied. Static transition data was taken under these conditions. Using the process detailed in Chapter 3 a phase transition pressure was determined for each data set. This information can be seen in Figure 6.3.2

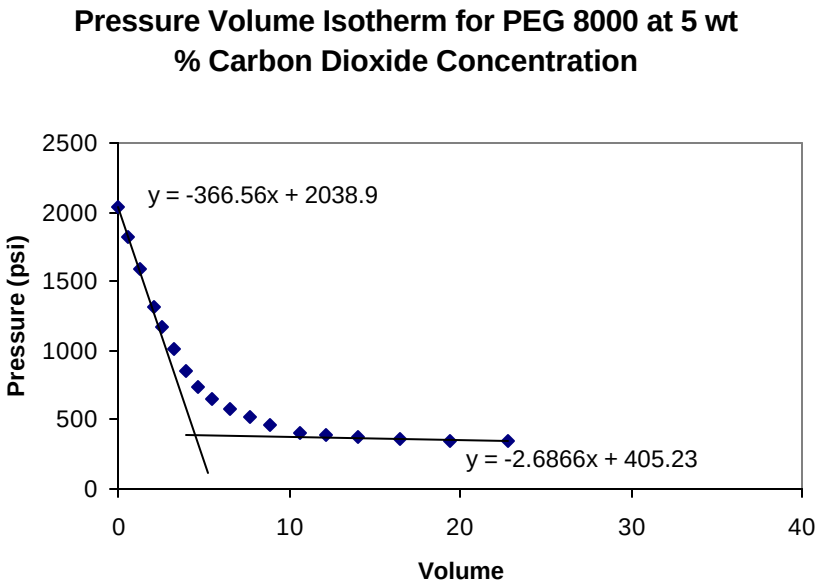

Figure 6.3.2 Pressure volume isothermo for PEG 8000

7. Results and Discussion: Urethane Systems

7.1 Introduction

Three urethane systems were studied: Desmocoll 540-Acetone, Desmomelt-Acetone, and Desmomelt-Toluene. All three of these systems had static phase transitions evident at the temperatures and carbon dioxide concentrations observed. While two of the systems were studied dynamically for further phase transitions. Only Desmocoll 540 and Desmomelt-Toluene had both bubble and cloud points observed in their static data.

7.2.1 System #1—Desmomelt 540-Acetone

Pressure versus volume isotherms were obtained for a Desmocoll 540- Acetone mixture at both 15% and 20% carbon dioxide concentrations and at a temperatures of 50, 60, and 70 °C for 15% carbon dioxide and additionally 40 °C for 20% carbon dioxide. At the maximum pressure of 2000 psi all of the systems were in the one phase region for the concentrations and temperature studied. Both static and dynamic transition data was taken under these conditions. The dynamic transitions were seen at similar pressures as those of the static transitions. The shape of the static isotherms began as a steep straight line, went through a region of curvature, and eventually flattened to a very small or zero slope. The curvature of the line displayed two dramatic changes in slope. This indicates both a bubble and a cloud point are present in the dynamic data. The trends of the static data can be seen clearly in Figure 7.2.1a.

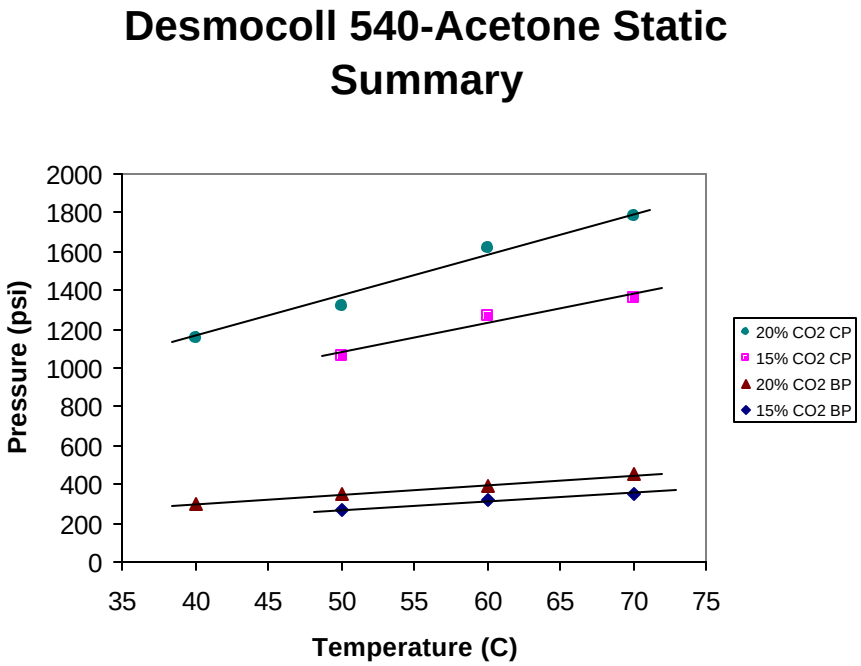

Figure 7.2.1a Pressure volume isotherm with cloud and bubble points

In the dynamic data only one phase transition is evident and this transition occurs near the static cloud transition. This data was collected and analyzed using the procedures outlined in Chapter 4. The summary of dynamic transition data is illustrated in Figure 7.2.1b.

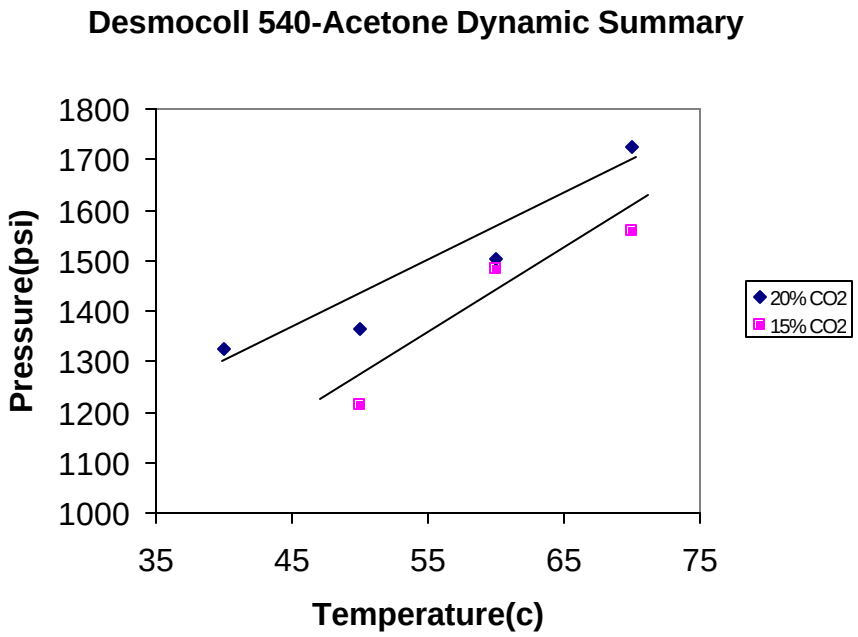

Figure 7.2.1b Pressure volume isotherm for dynamic data

7.2.2 System #2—Desmomelt-Acetone

Pressure versus volume isotherms were obtained for a Desmomelt- Acetone mixture at 5%, 9% and 14% carbon dioxide concentrations and at temperatures of 40, 50, 60, and 70 °C. At the maximum pressure of 2000 psi all of the systems were in the one phase region for the concentrations and temperature studied. Both static and dynamic transition data was taken under these conditions. The dynamic transitions were seen at similar pressures as those of the static transitions. The shape of the static isotherms began as a steep straight line, went through a small region of curvature, and eventually flattened to a very small or zero slope. The trends of the static data can be seen clearly in Figure 7.2.2a.

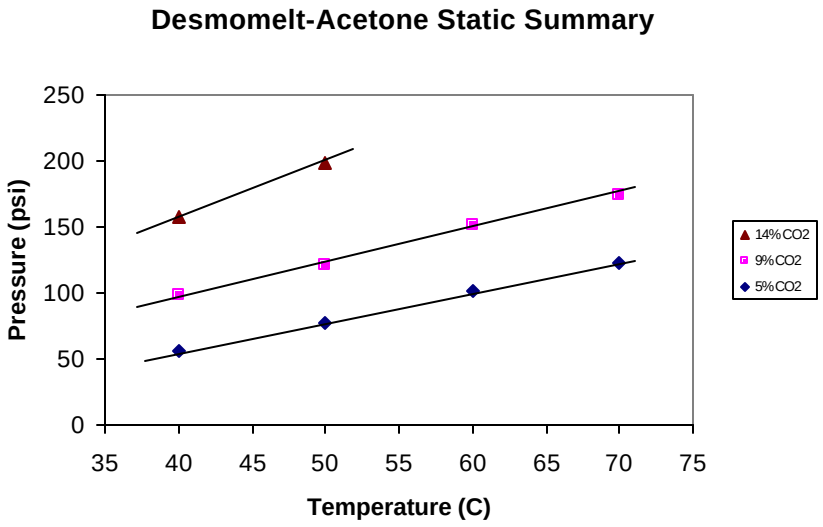

Figure 7.2.2a Desmomelt-Acetone Static Summary

In the dynamic data only one phase transition is evident and this transition occurs at slightly higher pressure than the static cloud transition. This data was collected and analyzed using the procedures outlined in Chapter 4. The summary of dynamic transition data is illustrated in Figure 7.2.2b.

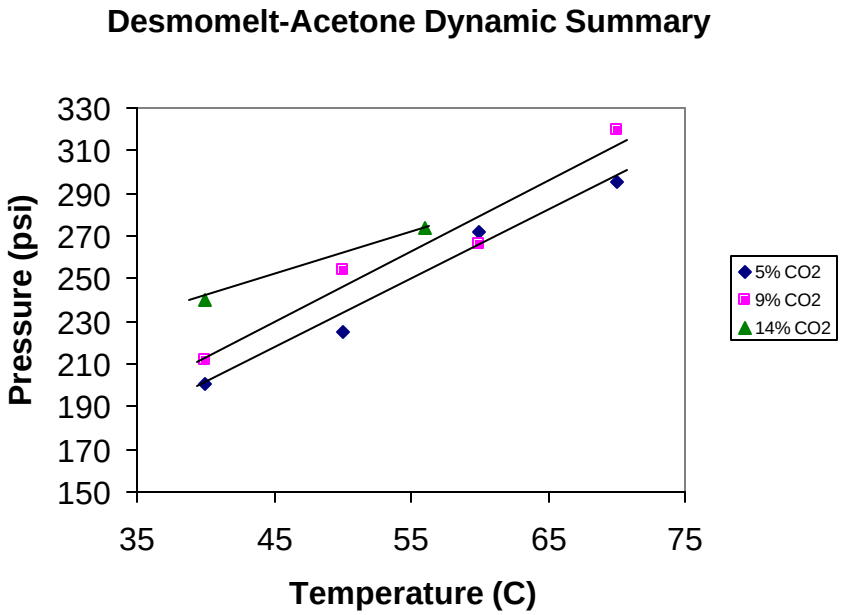

Figure 7.2.2b Desmomelt-acetone dynamic data summary

7.2.3 System #3— Desmomelt-Toluene

Pressure versus volume isotherms were obtained for a Desmomelt- Acetone mixture at 5%, 10%, 18% and 24% carbon dioxide concentrations and at various temperatures. At the maximum pressure of 2000 psi all of the systems were in the one phase region for the concentrations and temperature studied. The shape of the static isotherms began as a steep straight line, went through a small region of curvature, and eventually flattened to a very small or zero slope as can be seen in Figure 7.2.3a.

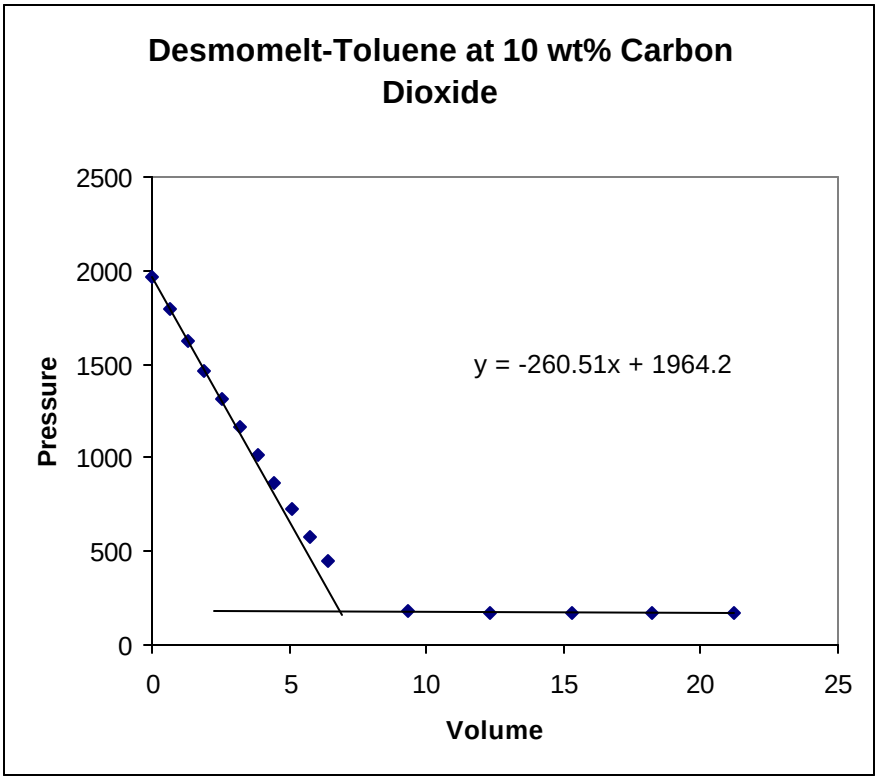

Figure 7.2.3a Pressure volume isotherm for 10 weight % Carbon Dioxide

The trends of the static data can be seen clearly in Figure 7.2.3b. It is also interesting to note that at higher carbon dioxide concentrations, 18% and 24%, and temperatures two phase transitions occur in the system.

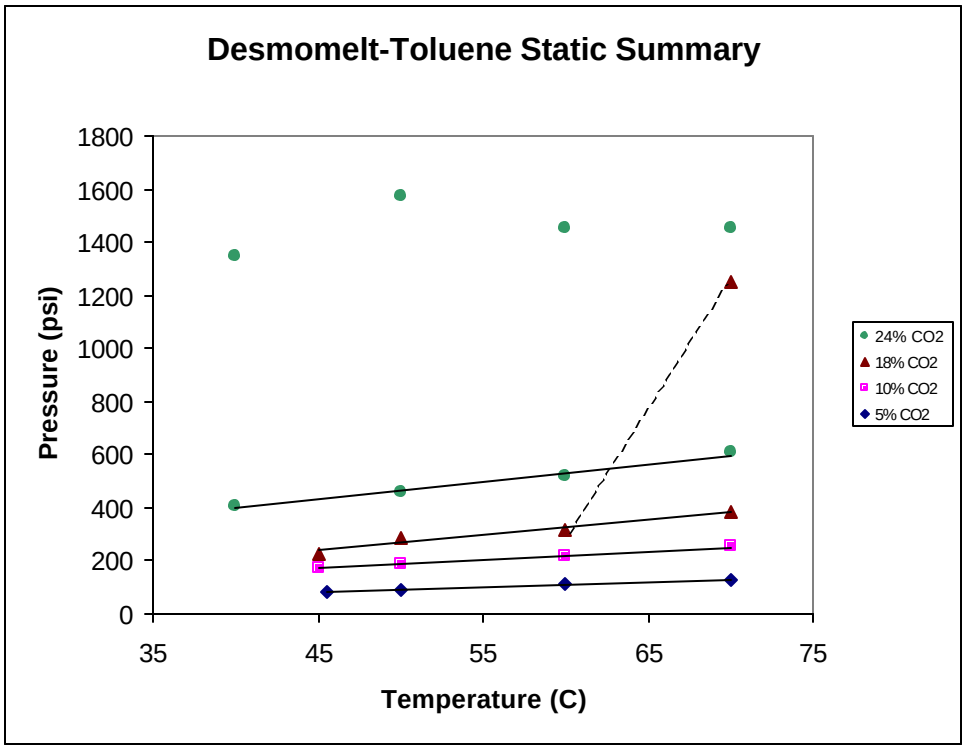

Figure 7.2.3b Static data summary for desmolmelt-toluene

8. Results and Discussion: Polychloroprene Adhesives

8.1 Introduction

Polychloroprene was developed in the 1920s by Father Nieuwland of the University of Notre Dame in collaboration with E.I. duPont de Nemours and Company (1). It was first commercialized in 1932, and, because it had many properties of natural rubber, it became widely used when there was a short supply of natural rubber during World War II. Today, one of the most common uses of polychloroprene is as base polymer for contact adhesives. A contact adhesive is an adhesive that is applied to two surfaces and allowed to dry before assembly. It differs from structural adhesives in that it must have sufficient bond strength to allow handling shortly after assembly, before full cure is obtained. This strength is called the green strength. Polychloroprene has several attractive properties in contact adhesive applications. It has high green strength and ultimate strength, excellent aging properties and temperature resistance, and is resistant to light, weather, mild acids and oils (1,2). As a result, contact adhesives formulated with polychloroprene have been used in a variety of applications. In the furniture industry, polychloroprene adhesives have been used to bond foam to foam, fabric to foam, foam to wood, as well as substrates such as metal, fiberglass, and plastics (1). In the automobile industry, polychloroprene adhesives have been used for sponge insulation strips, vinyl landau top and padding, vehicle sidewalls, and trim bonding applications (1). In addition,

countertop construction, panel fabrication, leather goods manufacturing, and laminating operations all have used polychloroprene contact adhesives extensively (1).

There are many different grades of polychloroprene and they offer different properties due to different chemical structures. Polychloroprene usually is prepared by emulsion polymerization of 2-chloro-1,3-butadiene. The synthesized polymers can have different cis-trans content as the temperature of polymerization is varied (3). Cis-trans content in polychloroprene is important because it determines the rate of crystallization, which in turn affects the rate of strength build up and the ultimate strength. At low temperatures, more polymers with trans content can be obtained, which have higher crystallization rate, and faster strength development (1,3). In addition to varying cis-trans structures, the backbone of polychloroprene also can have different degree of linearity. Polychloroprene with high linearity is chosen for most solvent-based adhesive formulations. For applications in latex-based adhesive formulation, polychloroprene usually has varying degrees of gel structure and is marginally solvent-soluble (3). Latex polychloroprene often is stabilized with rosin acid-based emulsifiers, which are anionic stabilizers (3). Another factor that differentiates grades of polychloroprene is molecular weight. Lower molecular weight polychloroprene easily can be dissolved by stirring in solvent. High molecular materials sometimes have to be broken down in a mill before being dissolved in solvent.

Formulating a contact adhesive requires one to take into account factors such as adhesion strength, resistance to elements of environment, and open time. By adding additives such as cross-linkers or resins, strength of polychloroprene adhesives can be increased. For example, the strength of polychloroprene adhesives formulated with

phenolic resins are higher, and these adhesives are used to bond substrates such as aluminum, magnesium, stainless steel, glass, and ceramics (2). Phenolics are known to provide heat resistance, which needs to be sufficient to prevent excess adhesive softening or releasing due to temperature variation. Polychloroprene contact adhesives also can be formulated with different solvents to provide different open times, ranging anywhere from very short to 24 hours (1).

8.2 Experimental Results

Pressure versus volume (P-V) isotherms and visual observations were obtained for two polychloroprene:toluene systems, and for the formulated contact adhesive described in Chapter 2. Measurements and observations were made at 40, 50, 60, and 70 °C, and at various carbon dioxide concentrations. The polymer content in the systems studied was limited to a maximum of 25 wt. % in toluene due to the high viscosity of the solution. Solutions with high viscosity could not be loaded into the high-pressure cell because highly viscous fluids do not flow easily through the narrow feed port. Phase transitions were determined by plots of the P-V isotherms, which are shown in the Appendix.

8.2.1 System #1— 9: 41 Polychloroprene:Toluene

At the conditions of 2000 psi, 45 °C, and 10% carbon dioxide, the appearance of the solution was cloudy white, and the stirring bar barely was visible. As the temperature and carbon dioxide concentration increased, the solution became increasingly more opaque. During volume expansion, the appearance of the solution remained unchanged

as the pressure of the system was decreased until the bubble point was reached. At the bubble point, a new vapor phase began to form. The formation of bubbles began near the stirring bar well, and propagated outward. The bubbles then rose slowly to the top of the cell. No formation of a new liquid phase was observed in the range of temperatures and carbon dioxide concentrations studied. The specific pressures at which the bubble points occurred were determined from P-V isotherms. The P-V isotherms obtained for this system are shown in Appendix B. The shape of the isotherms generally began as a steep line, went through a region of small curvature, and eventually turned into a flatter line with negative slope. Although it was not typical for the isotherm to have a curved region before turning flat in a liquid to liquid-vapor phase transition, such behavior has been observed for systems that were close to the solution critical point as discussed in Chapter 3.3. Large polydisperity in the polymer may cause the isotherm to be non-linear. Thus, the type of isotherm observed for this system was determined to be a variation of the typical P-V isotherm for a bubble point. An argument could be made that this type of P-V isotherm is similar to those described in Chapter 3.3 for a liquid to liquid-fluid (L-LF) transition. However, by examining the isotherms at various carbon dioxide concentrations, two trends that differed from those of L-LF transition were found. For this system, the curvature became less obvious and the slope of the flat line became less negative as carbon dioxide concentration increased. These two trends contradicted the phase behavior observed in L-LF transitions. Moreover, a liquid to liquid-fluid transition is a rare phase transition that occurs at pressures higher than the critical pressure of carbon dioxide, which is approximately 1060 psi. With the exceptions of experiments at above 30% carbon dioxide and 60 °C, the isotherms obtained under

most experimental conditions were at pressures well below the critical pressure. The bubble point pressure was determined by the intersection of the initial steep line and the flat line. Bubble points were determined from P-V isotherms at various temperatures and carbon dioxide concentrations and plotted in pressure versus temperature phase diagram. In this phase diagram, the bubble point pressure at constant carbon dioxide concentration increased as temperature increased, and established a trend for the monotonically increasing vapor pressure curve. As carbon dioxide was added to the system, the vapor pressure curve moved to higher pressures. Because this system was cloudy, but no cloud point transition was found over the range of pressures, temperatures, and compositions studied here, it is not clear whether this system will exhibit a decompressive spray in the UNICARB® process.

8.2.2 System #2— 1:3 Polychloroprene:Toluene

In comparison to the previous system discussed, the polymer content of this system was higher and the appearance of the mixture was milky white.

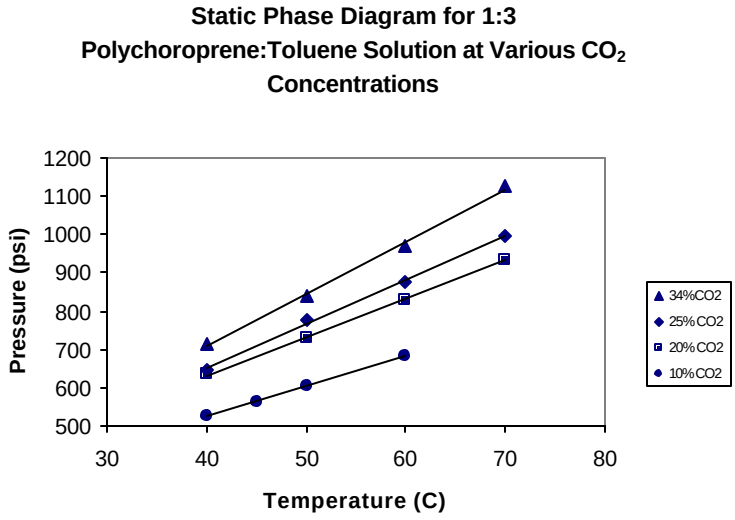

Figure 8.1. Effect of increasing solute concentration for system #1

The stirring bar was no longer visible and visual observations of the solution could not be made. P-V isotherms were obtained at temperatures ranging from 40 to 70 °C and carbon dioxide concentrations ranging from 10 – 34 wt. %. Plots of P-V isotherms are shown in Appendix B. The shapes of the P-V isotherms were similar to those observed in system #1, although the slopes of the flat lines were smaller in this system. The similarity in the shape of the isotherm indicated that only bubble points occurred in this system. The bubble point pressures were determined from P-V isotherms and were plotted in a P-T phase diagram. Vapor pressure curves were mapped out at each carbon

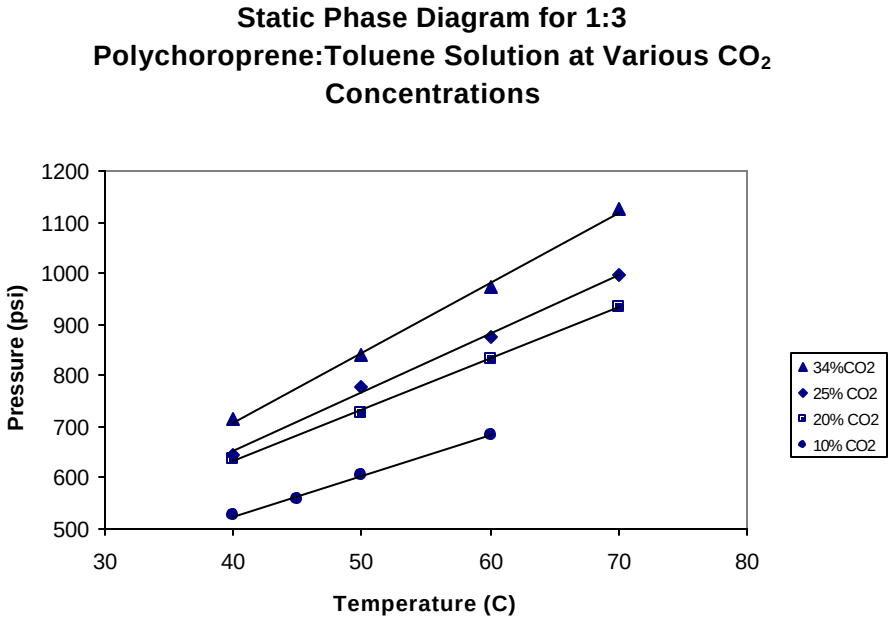

Figure 8.2. Effect of increasing solute concentration for system #2

dioxide concentration as shown in Figure 8.2. As the carbon dioxide concentration increased, the vapor pressure curve also moved to higher pressures. Again, because this system was cloudy, but no cloud point transition was found over the range of pressures, temperatures, and compositions studied here, it is not clear whether this system will exhibit a decompressive spray in the UNICARB® process.

8.2.3 System #3— Polychloroprene-based Contact Adhesive

A polychloroprene-based contact adhesive was formulated with phenolic resins and other additives. The contact adhesive had a thick yellowish appearance and was opaque. As a result, it was not possible to make visual observations of the phase behavior in the high-pressure cell. P-V isotherms were obtained at temperatures ranging from 40 to 70 °C and carbon dioxide concentrations ranging from 18 – 31 wt. %. Plots of P-V isotherms are shown in Appendix B. The shape of the P-V isotherms had almost no deviation from the initial steep line or the eventual flat line, and was not similar to those observed in systems #1 and #2. Rather, this result was the expected shape of a typical isotherm in the liquid to liquid-vapor transition. The bubble point pressures were determined from P-V isotherms and were plotted in a P-T phase diagram. Vapor pressure curves were mapped out at each carbon dioxide concentration as shown in Figure 8.3. As the carbon dioxide concentration increased, the vapor pressure curve also moved to higher pressures. Again, because this system was cloudy, but no cloud point transition was found over the range of pressures, temperatures, and compositions studied here, it is not clear whether this system will exhibit a decompressive spray in the UNICARB® process.

8.3 Dynamic Phase Behavior

Dynamic phase behavior for each of the systems discussed previously was determined by analyzing pressure versus time profiles using the technique described in Chapter 4. Pressure profiles were obtained at each temperature and composition, and the experiment was repeated three times to account for errors. These pressure profiles are plotted in Appendix D. For the formulated polychloroprene adhesive system, there was a

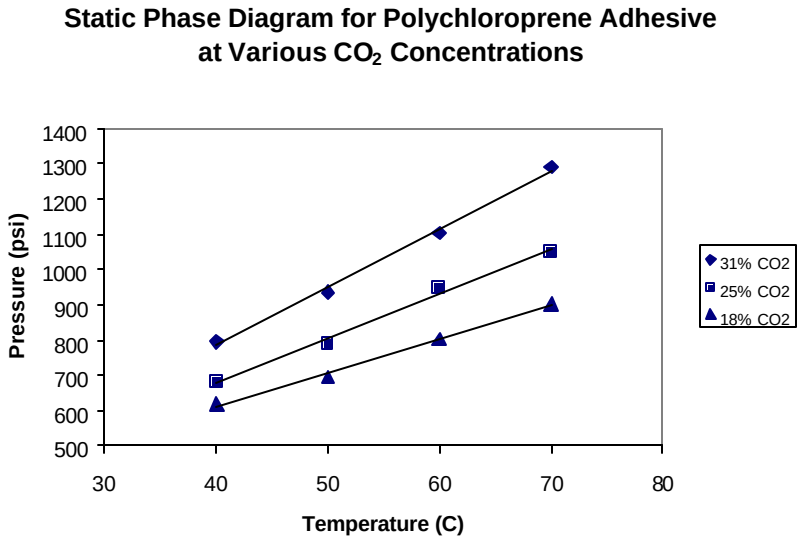

Figure 8.3. Effect of increasing solute concentration for system #3

kink within the first five data points after depressurization in most of the pressure profiles. An example is shown in Figure 8.4, in which the pressure profile initially began as a steep line after depressurization, and then became less steep at the kink, and eventually deviates from a line to become a curve this indicates two possible phase transitions. The pressure at which the pressure profile became curved already was determined to be a bubble point in Chapter 4. Additionally, the initial kink could be a cloud point, but no conclusion has been reached yet since the data showed puzzling and

inconsistent trends. Figure 8.5 shows a plot of kink pressure versus temperature at various carbon dioxide concentrations. The pressures at which the kinks were found did not show any clear dependence on temperature and composition, which cloud point pressures would be expected to show. Table 8.1 also shows variations among the repeated trials. During the first trials, the kink generally was not found. However, kinks were found in all but one case during the third trials. Although there is no clear explanation for the randomness in the P-T plot and the variation in the repeated trials, an unevenly mixed system was identified as a possible cause. An unevenly mixed system could cause a part of the system to undergo phase transition prematurely. Since the degree of uneven mixing did

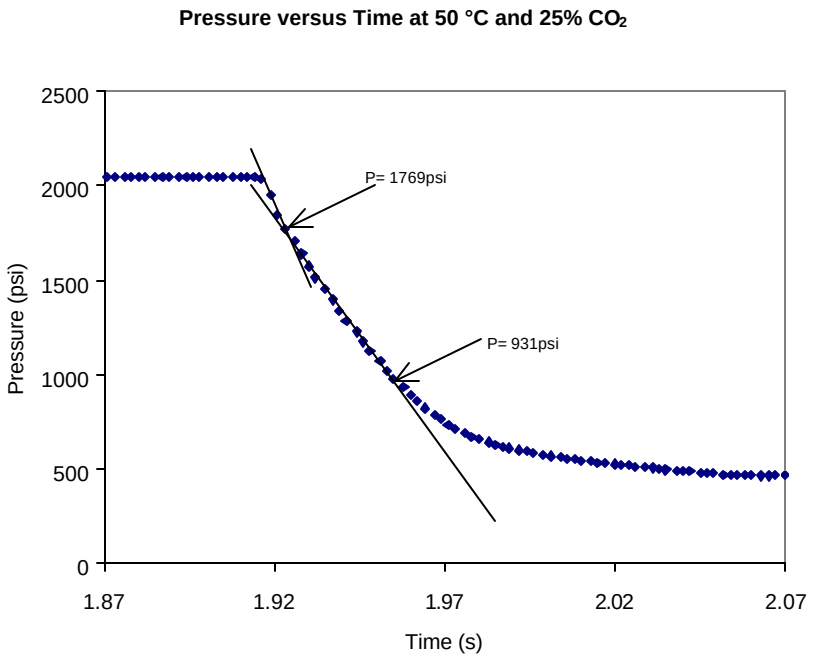

Figure 8.4. Pressure versus time profile showing a kink at high pressure.

CONCENTRATION (WT. %)	TEMPERATURE (C)	TRANSITION PRESSURE - TRIAL 1 (PSI)	TRANSITION PRESSURE - TRIAL 2 (PSI)	TRANSITION PRESSURE - TRIAL 3 (PSI)	AVERAGE
17%	40	-	-	1704	1704
	50	1555	1521	1713	1596
	60	-	-	1700	1700
	70	-	-	-	-
25%	40	-	1748	1640	1694
	50	1769	1727	1773	1756
	60	-	-	1881	1881
	70	-	1796	1783	1790
31%	40	1622	1617	1597	1612
	50	1885	1718	1802	1802
	60	-	1848	1885	1867
	70	1947	1812	1923	1894

not depend strongly on temperature and composition, and varied from trial to trial, it thus could cause both the randomness in the P-T plot and the variation among repeated trials. Similar kinks in pressure versus time profile due to unevenly mixing also were reported

Table 8.1: Comparison of transition pressures for repeated trials.

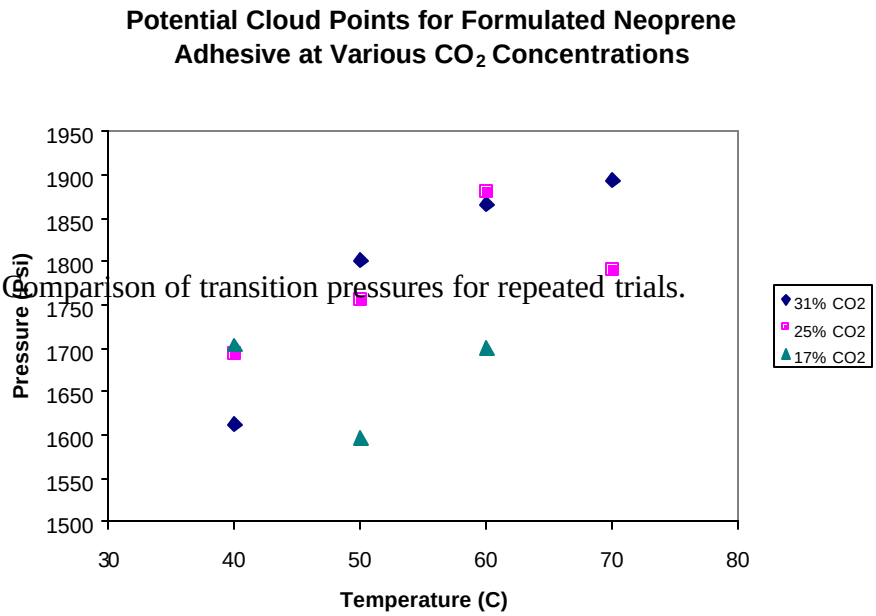

Figure 8.5. P-T plot of potential cloud points showing no clear trend.

by Schultze (4). Despite that uneven mixing was identified as a possible cause for the kink, whether a phase transition or uneven mixing was the real cause remained undetermined. Thus, dynamic behavior only can be discussed basing on the analysis of data points obtained after this first kink. Figure 8.6(a-c) shows the dynamic phase diagrams constructed from the analysis of pressure versus time profiles. Unlike most of the block copolymer systems, each polychloroprene system showed clear trends for the dynamic phase boundaries. The best linear fits of the data points for the vapor pressure showed a monotonically increasing function as expected, and the vapor pressure curve shifted to higher pressures as carbon dioxide concentration increased. When the dynamic phase diagrams were compared to the corresponding static phase diagrams, it was found

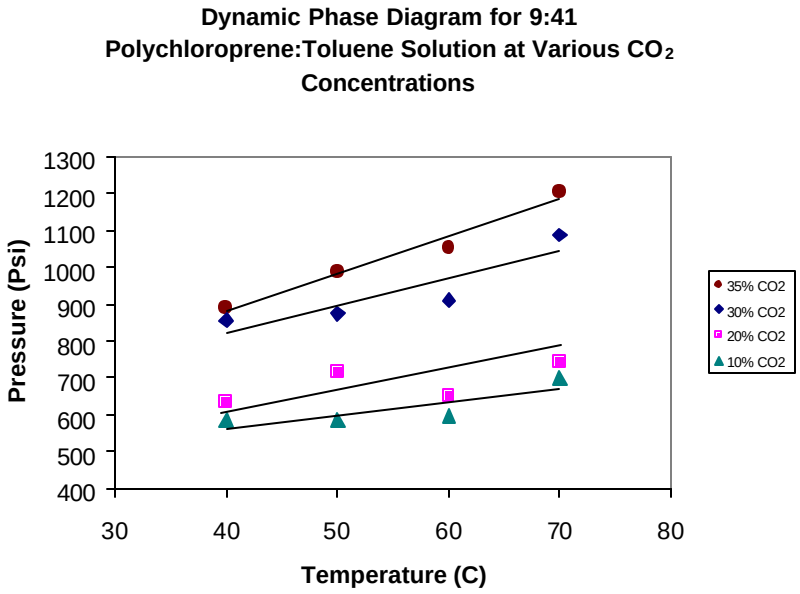

Figure 8.6 (a). Effect of increasing solute concentration for system #1

that dynamic phase boundaries always occurred at slightly higher pressures. These results suggested that during rapid expansion, these three polymeric systems undergo phase transitions at higher pressures than where it would normally occur during gradual expansion.

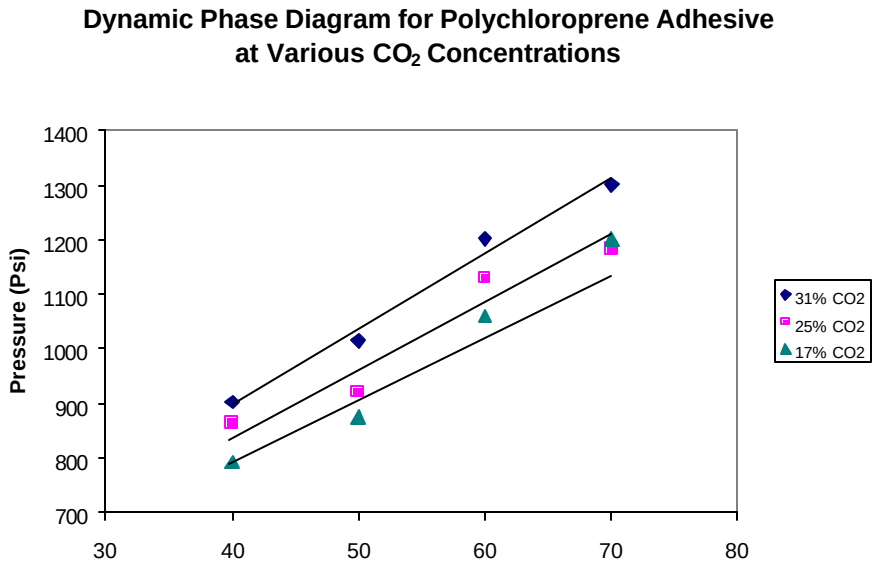

Figure 8.6(c). Effect of increasing solute concentration for system #3

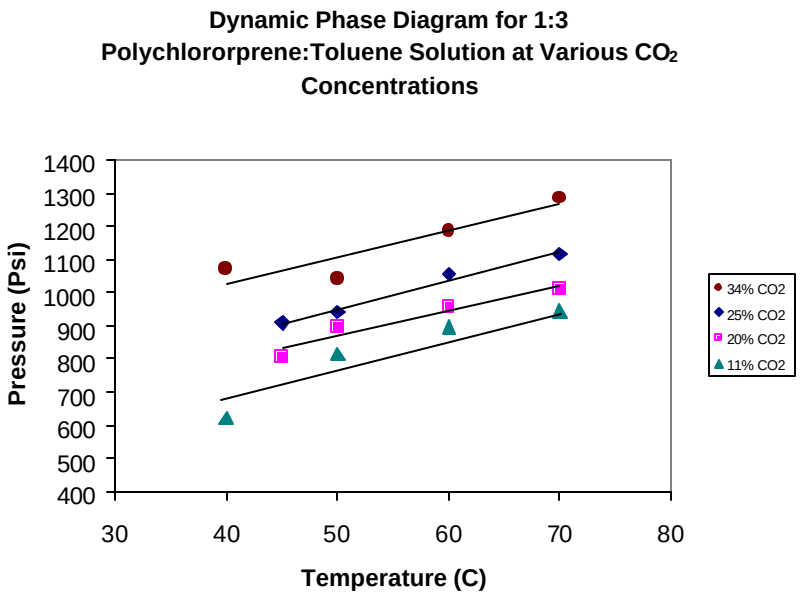

Figure 8.6(b). Effect of increasing solute concentration for system #2

8.4 References

1. Brinson, H.F. Adhesives and Sealants, 1990, Engineering Materials Handbook Vol. 3.
2. Landdrock, A.H. Adhesives Technology Handbook, 1985, Noyes Publications.
3. Pocius, A.V. Adhesion and Adhesives Technology, 1997, Hanser Publishers.
4. Schultze, C. Phase Behavior of Mixtures Containing Supercritical Fluid: Equation of State Calculations and Experiments. Ph. D. Dissertation, The Johns Hopkins University, 1998.

9. Results and Discussion: Solvent-Based Acrylic Adhesives

9.1 Introduction

There are many types of adhesives that are based on acrylates, including anaerobic, cyanoacrylate, curable acrylic, and acrylic solution adhesives. These adhesives differ significantly in chemistry, curing mechanism, and formulation. This discussion will focus on solvent-based acrylic adhesives, which have been used in many non-structural applications. Base polymers or copolymers for solvent-based acrylic are usually polymerized by free radical polymerization. Some of the most common acrylic monomers include ethyl acrylate, methyl acrylate, acrylic acid, acrylamide, and acrylonitrile (2). Polyacrylates have several attractive properties for non-structural adhesive applications. These polymers are resistant to UV and oxidative degradation due to their saturated chemical structure (1). Furthermore, polyacrylates allow good adhesion to many substrates, such as glass, plastic, metal, and paper, and have the capability to adhere to wet, oily, and dusty surfaces (1). Solvent-based acrylic adhesives cure by solvent release, and they can be formulated to perform a range of different tasks, from those of a pressure-sensitive adhesive (PSA) to those of a contact adhesive. For PSA applications, formulations consist of copolymers of acrylates with a low degree of cross-linking and solvents. The desired performance of acrylic PSA can be achieved by choosing the right combination of various monomers at specific ratios (3). For contact adhesive applications, highly cross-linked acrylics are used to improve strength.

Polyacrylates are cross-linked by using multifunctional monomers to carry reactive groups into the polymer chains. Applications of acrylic adhesives include bonding cloth, plastics, leather (2), tapes, labels, decals, trims and moldings (1). Phase behaviors of acrylic systems have been investigated in the past for paint coating applications with the UNICARB® process (4,5). In this work, the phase behavior of acrylic-based adhesive systems are investigated to determine the potential application in the UNICARB® process.

9.2 Experimental Results

Pressure versus volume (P-V) isotherms and visual observations were obtained for the two acrylic systems. Measurements and observations were made at 40, 50, 60, and 70 °C, and at various carbon dioxide concentrations. Observed visually in both systems, the solution always remained in one phase at 2000 psi for the range of temperatures and carbon dioxide concentrations studied. Plots of the P-V isotherms are shown in Appendix B.

9.2.1 System #1— Undiluted Morstik® Adhesive

At the conditions of 2000 psi, 45 °C, and 11.7 wt. % carbon dioxide, the appearance of the solution was almost clear, and the stirring bar was visible clearly. As the temperature and carbon dioxide concentration increased, the solution became increasingly more opaque. The appearance of the solution remained unchanged during volume expansion until a phase transition occurred. At the bubble point, a new vapor phase began to form and started to nucleate into bubbles. The formation of bubbles

began near the stirring bar well, and propagated outward. The bubbles then rose slowly to the top of the system cell. At 70 °C and 42.2 wt. % carbon dioxide, formation of a new liquid phase was observed. At the cloud point, the solution began to turn dark near the top of the high-pressure cell, and the dark shadow propagated down. Eventually, the stirring bar could no longer be seen as the whole system turned completely dark. The specific pressures at which the bubble points occurred were determined from P-V isotherms. The isotherms began as a steep line and then sharply turned into a completely flat line. This type of P-V isotherm was described by Murlidharan *et al.* (6) and in Chapter 3.2 as signature for a bubble-point phase transition. The bubble point pressures were determined by the intersections of the steep lines and the flat lines of the P-V isotherms, and a pressure versus temperature phase diagram was constructed as shown in Figure 9.1. Nevertheless, a P-V isotherm showing a cloud point could not be obtained and used for finding the phase boundary at 70°C and 42.2 wt. % carbon dioxide. At this experimental condition, the system reached its maximum volume shortly after the cloud point had occurred, and could not be further expanded to establish a complete P-V isotherm that would show a change in its slope. Thus, the pressure at which the cloud point occurred had to be determined visually. Using a technique described by Kiamos (5), cloud point pressure was determined to be the pressure at which it was impossible to see the stirring bar, and it is shown in Figure 9.1. In this phase diagram, the pressure of bubble point at constant carbon dioxide concentration increased as temperature increased, and established a trend for the monotonically increasing vapor pressure curve. As carbon dioxide was added to the system, the vapor pressure curve moved to higher pressures.

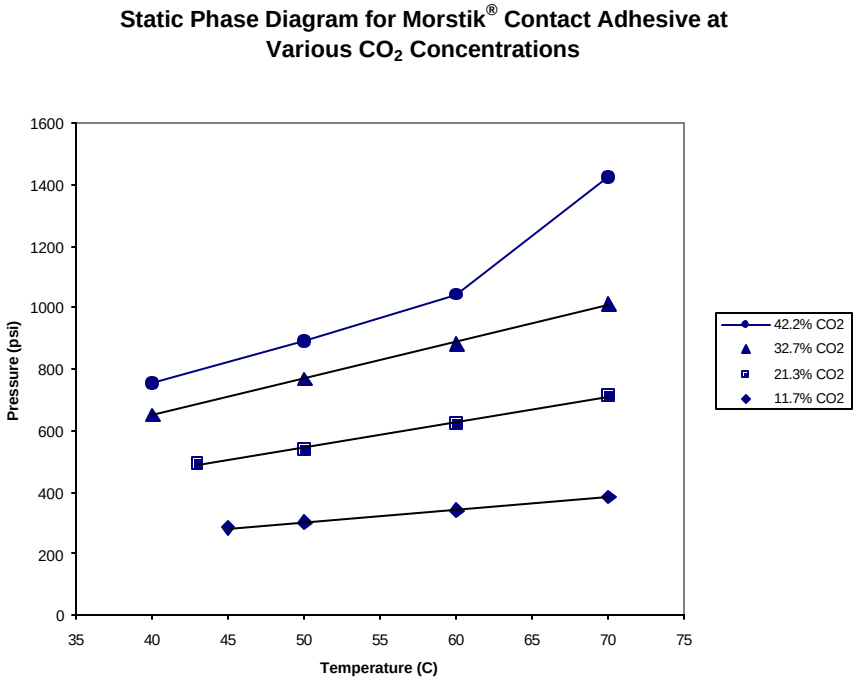

Figure 9.1: Effect of increasing solute concentration in system #1

Because this system exhibited both a cloud point and a bubble point in the range of pressures, temperatures, and compositions studied here, it would be a good starting point for future formulations of acrylic-based contact adhesives for use in the UNICARB® process.

9.2.2 System #2— 8:1 Morstik®:Toluene Solution

The diluted adhesive system had an appearance that was similar to the undiluted system described previously. However, only one type of phase transition, the bubble point, was observed in this system. P-V isotherms were obtained at temperatures ranging from 40 to 70 °C and carbon dioxide concentrations ranging from 11.7 – 41.8 wt. %. The shape of the P-V isotherms were similar to those observed in system #1, which confirmed that only bubble points occurred in this system. The bubble point pressures were determined from P-V isotherms and were plotted in a P-T phase diagram. Vapor pressure curves were mapped out at each carbon dioxide concentration as shown in Figure 9.2. As the carbon dioxide concentration increased, the vapor pressure curve moved to higher pressures. Because this system was cloudy, but no cloud point transition was found over the range of pressures, temperatures, and compositions studied here, it is not clear whether this system will exhibit a decompressive spray in the UNICARB® process.

9.3 Dynamic Phase Behavior

Pressure profiles as functions of time were obtained and plotted in Appendix B.

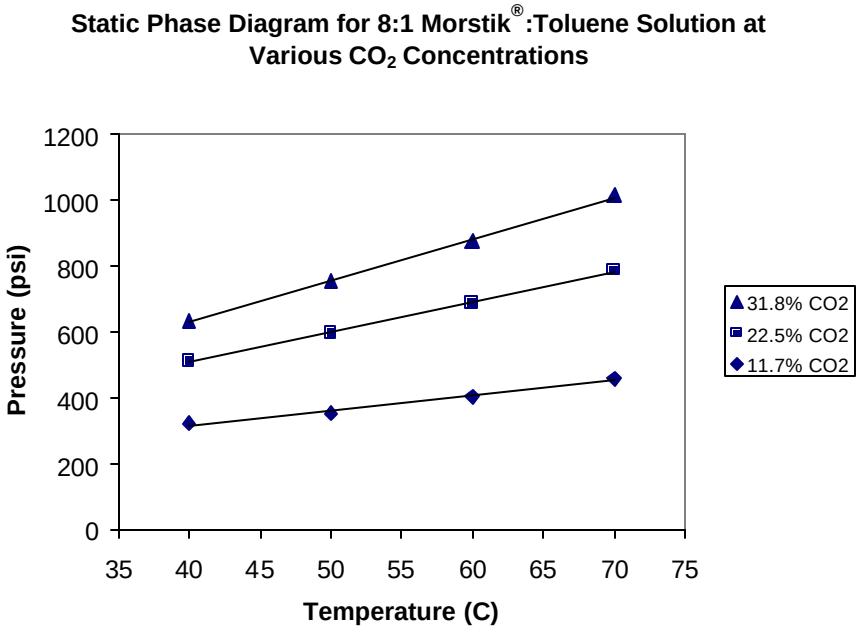

Figure 9.2: Effect of increasing solute concentration in system #2

Dynamic phase diagrams for each system discussed previously were determined by analyzing the pressure versus time profiles at various temperatures and compositions. At each temperature and composition, rapid expansion experiments were repeated three times, and the phase transition pressures were determined from the pressure versus time profiles. In a few trials, pressure versus time profiles did not have an obvious transition from a straight line into a curve. As a result, the dynamic phase boundary was undeterminable for these trials. Shown in Table 9.1 is a summary of experimental results for system #1. A summary of experimental results for system #2 is shown in Table 9.2. For each system, averages of the phase transition pressures of the repeated trials were calculated for all experimental conditions, and were used to construct dynamic phase diagrams shown in Figures 9.3(a) and 9.3(b). The phase boundaries from these diagrams

CO_2 wt.%	Temp (C)	Trial 1 (psi)	Trial 2 (psi)	Trial 3 (psi)	AVG
12%	45	798	819	835	817
	50	938	1041	978	986
	60	1028	1036	1031	1032
	70	1132	1193	1269	1198
21%	43	787	850	868	835
	50	903	936	1024	954
	60	undeterminable	859	1060	960
	70	undeterminable	1059	1103	1081
33%	40	821	923	992	912
	50	1012	1024	undeterminable	1024
	60	undeterminable	1032	1115	1074
	70	1418	1327	1392	1360
42%	40	953	1028	985	989
	50	1016	1052	1167	1078
	60	1312	undeterminable	1322	1317
	70	1292	1327	1410	1343

Table 9.1 Summary of experimental results for undiluted Morstik® adhesive

CO_2 wt.%	Temp (C)	Trial 1 (psi)	Trial 2 (psi)	Trial 3 (psi)	AVG
12%	40	713	808	806	776
	50	867	649	876	797
	60	828	766	684	759
	70	-	1007	939	973
23%	40	1003	806	631	813
	50	1189	1129	996	1105
	60	1142	1170	1058	1123
	70	1117	1102	1115	1111
32%	40	1167	998	701	955
	50	997	1101	830	966
	60	933	971	910	941
	70	1361	1239	1194	1217
42%	40	1156	1190	839	1062
	50	-	-	-	-
	60	-	-	-	-
	70	-	-	-	-

Table 9.2 Summary of experimental results for 8:1 Morstik®:toluene dilution

did not show trends that were expected. For system #1, the vapor pressure curve was monotonically increasing, but the vapor pressure curve did not shift to higher pressures as carbon dioxide concentration increased. For system #2, the vapor pressure curve was not monotonically increasing and it did not shift to higher pressures as carbon dioxide concentration was increased. These trends did not make sense because vapor pressure curves were expected to be monotonically increasing, and the static phase behaviors suggested that the phase boundaries should move to higher pressures as carbon dioxide concentration was increased. The lack of clear and logical trends in either system was due to the large variations among trials at the same experimental conditions. For example, at 23% carbon dioxide and 40 °C, the phase transition pressure for trial #1 was 1003 psi while the pressure for trial #3 was 631 psi. Large variations from trial to trial raise the possibility that the final averages that used to construct the dynamic phase diagrams could be inaccurate, and could be showing the wrong trends. The cause of this variation

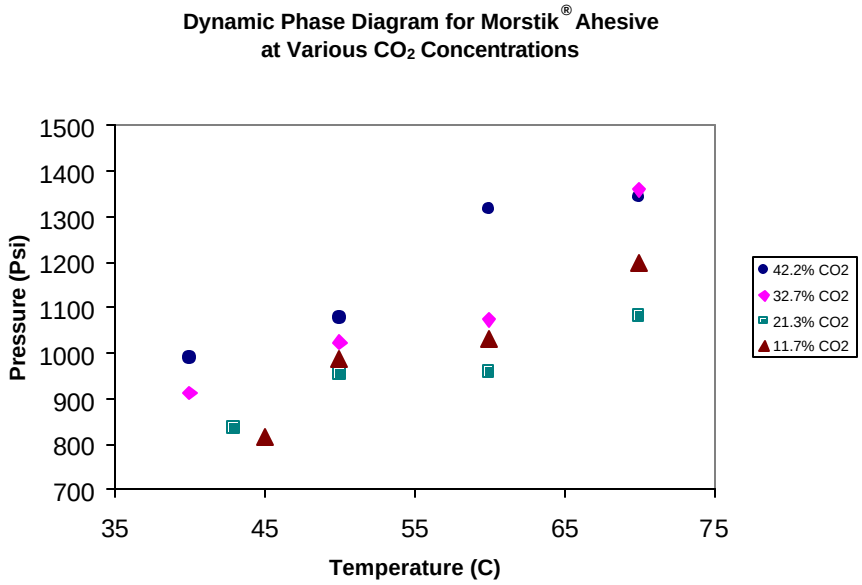

Figure 9.3(a): Dynamic phase behavior of undiluted acrylic adhesive

stemmed from the variations in the pressure versus time profiles. The pressure versus time profile usually began as a straight line. However, these profiles were seen to transform into various shapes immediately after the pressure at which a phase transition

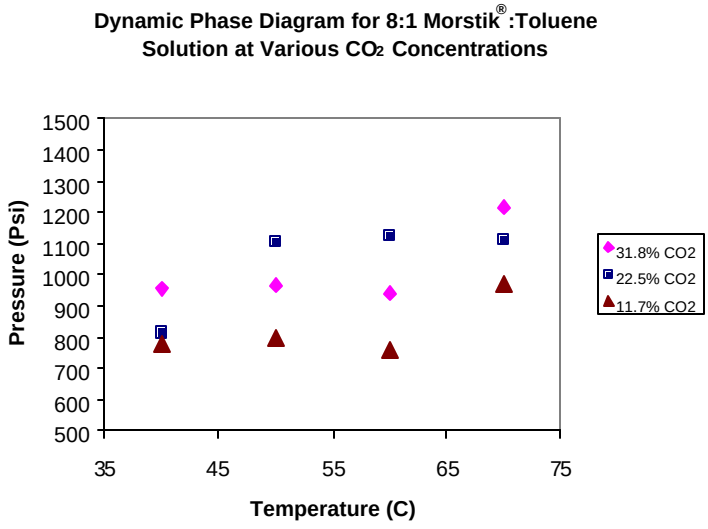

Figure 9.3(b): Dynamic phase behavior for diluted acrylic adhesive

behavior seemed to occur. In the supporting data, the shape of the pressure profile turned into a less steep line, whereas in later experiments, it turned into a curve with different degrees of curvature. Variations such as these examples also existed for other sets of pressure profiles. The cause for variations in the pressure versus time profile remains unclear, but it could be due to a number of causes: unevenly mixed solution, temperature gradient in the system, noise in the pressure detection device, and varying resistance met by the piston as the system expanded.

9.4 References

1. Brinson, H.F. Adhesives and Sealants, 1990, Engineering Materials Handbook Vol. 3.
2. Landdrock, A.H. Adhesives Technology Handbook, 1985, Noyes Publications.
3. Pocius, A.V. Adhesion and Adhesives Technology, 1997, Hanser Publishers.
4. Schultze, C. Phase Behavior of Mixtures Containing Supercritical Fluid: Equation of State Calculations and Experiments. Ph. D. Dissertation, The Johns Hopkins University, 1998.
5. Kiamos, A. A. High Pressure Behavior of Polymer-solvent-Supercritical Fluid Mixtures. M.S. Thesis, The Johns Hopkins University, 1992.
6. Muralidharan, V.; Donohue, M.D. *The Journal of Supercritical Fluids*, **1994**, *7*, 275-281.

10. Basics of Adhesives and Adhesion

10.1 Introduction

In contrast to traditional joining methods such as riveting & screwing, adhesive bonding has no adverse effect on the material characteristics of the surfaces to be bonded; e.g.: damaging and weakening them by drilling holes in them.

In manufacturing and repair environments, adhesive bonding technology permits characteristic material properties to be utilized to the utmost. Below is a summary of advantages of adhesive bonding technology:

- Separation of surfaces
- Easy integration into automated production processes
- Bonding of different materials
- Prevention of crevice corrosion
- Bonding of heat-sensitive materials
- Weight-saving
- Bonding of materials over large areas
- Uniform distribution of tension in bonded areas
- High vibration damping
- Low-heat joining processes
- Enabling of recycling of primary materials

10.2 Basics of adhesion

The mechanism of adhesion has been investigated for years; many theories have been proposed in an attempt to provide an explanation for adhesion phenomena. However, no single theory explains adhesion in a general, comprehensive way.

The bonding of an adhesive to an object or a surface is the sum of a number of mechanical, physical, and chemical forces that overlap and influence one another. As it is not possible to separate these forces from one another, we distinguish between mechanical interlocking , caused by the mechanical anchoring of the adhesive in the pores and the uneven parts of the surface, electrostatic forces, the differences in electonegativities of adhering materials, and the other adhesio n mechanisms dealing with intermolecular and chemical bonding forces that occur at the interfaces of heterogeneous systems.

This chemical adhesion mechanism is explained in the case of the intermolecular forces by the adsorption theory, and in the case of chemical interactions by the chemisorption theory. The processes that play a role in the bonding of similar types of thermoplastic high-polymer materials, e.g. homogeneous systems, can be determined with the diffusion theory.

10.2.1 Adsorption

The adsorption theory states that adhesion results from intimate intermolecular contact between two materials, and involves surface forces between the atoms in the two surfaces.

This theory is the most important mechanism in achieving adhesion (1). The most common surface forces that form at the adhesive-adherend interface are van der Waals

forces. In addition, acid-base interactions and hydrogen bonds, generally considered a type of acid-base interaction, may also contribute to intrinsic adhesion forces. Research has experimentally demonstrated that the mechanism of adhesion in many adhesive joints only involves interfacial secondary forces. The calculated attractive forces between two surfaces are considerably higher than the experimentally measured strength of adhesive joints; this discrepancy between theoretical and experimental strength values has been attributed to voids, defects or other geometric irregularities which may cause stress concentrations during loading (2).

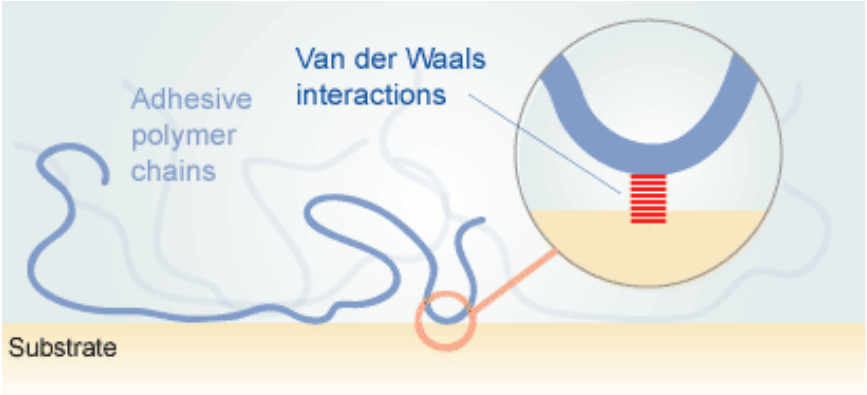

Figure 10.1 – Van der Waals Interactions for Bonding (1)

To obtain good adsorption, intimate contact must be reached such that van der Waals interaction or the acid-base interaction or both take place; hence good wetting is essential. According to Young's equation, the surface tensions (liquid/vapor: γ_{LV}, solid/liquid: γ_{SL} and solid/vapor: γ_{SV}) at the three phase contacts are related to the equilibrium contact angle σ through:

$$\gamma_{SV} = \gamma_{SL} + \gamma_{LV} . \cos \sigma$$

The one important factor that influences the adhesive joint strength is the ability of the adhesive to spread spontaneously on the substrate when the joint is initially formed. For spontaneous wetting to occur:

$$\gamma_{SV} >= \gamma_{SL} + \gamma_{LV}$$

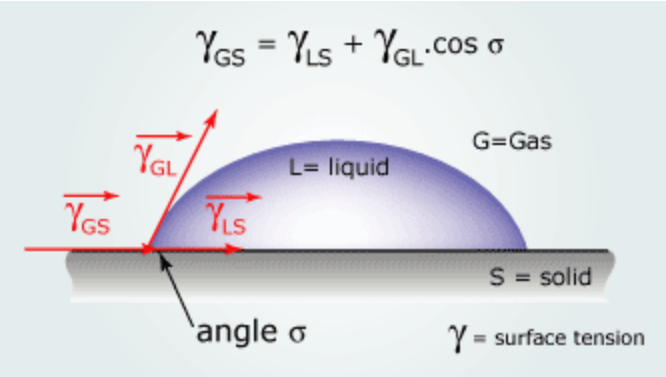

Figure 10.2 - Angle of contact of a drop of liquid with the surface of a solid object. (1)

We can say that for good wetting: $\gamma_{SV} < \gamma_{LV}$

Generally speaking, the liquid surface tension of the adhesive should be less than the critical wetting tension of the solid surface of the substrate.

10.2.2 Chemisorption

The chemical bonding mechanism suggests that primary chemical bonds may form across the interface. Chemical bonds are strong and make a significant contribution to the intrinsic adhesion in some cases.

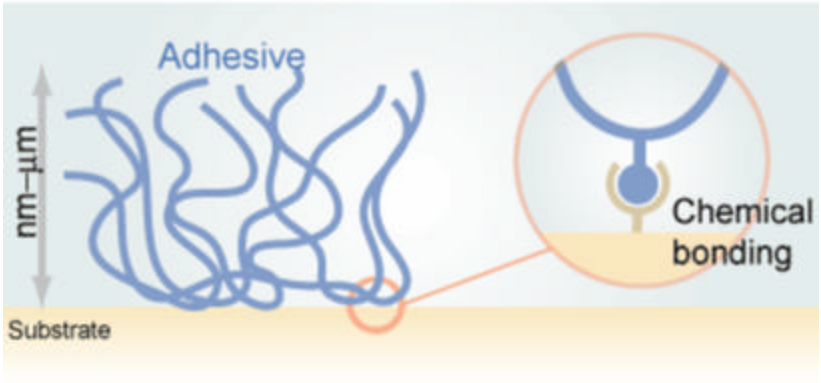

Figure 10.3 – Chemical Bonding for Adhesion (1)

For example, primary chemical forces have energies ranging between 60-1100 kJ/mol, which are considerably higher than the bond energies secondary forces have $(0.08\text{-}5\ kJ/mol)^2$. We should also mention the coupling agents and adhesion promoters that are used to help in fixing the adhesive at the surface by chemical reaction. (3)

10.2.3 Mechanical Interlocking

The mechanical interlocking theory of adhesion states that good adhesion occurs only when an adhesive penetrates into the pores, holes and crevices and other irregularities of the adhered surface of a substrate, and locks mechanically to the substrate. The adhesive must not only wet the substrate, but also have the right rheological properties to penetrate pores and openings in a reasonable time.

This theory explains a few examples of adhesion such as rubber bonding to textiles and paper. Since good adhesion can occur between smooth adherend surfaces as well, it is clear that interlocking may help promote adhesion.

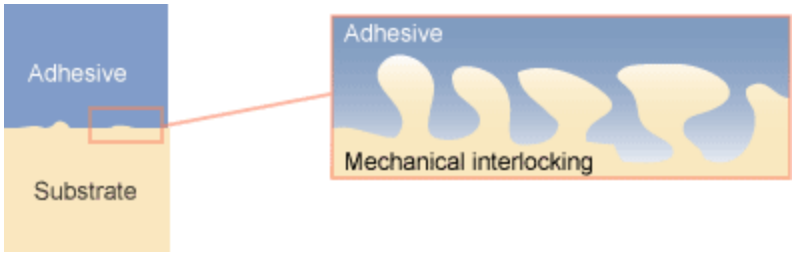

Figure 10.4 – Mechanical Interlocking (1)

Pretreatment methods applied on surfaces enhance adhesion (3). These pretreatments (especially plastic surface treatments) result in roughness on the adherend surface, which can improve bond strength and durability by providing mechanical interlocking. Beyond mechanical interlocking, the enhancement of the adhesive joint strength due to the roughing of the adherend surface may also result from other factors such as formation of a larger surface, improved kinetics of wetting and increased plastic deformation of the adhesive.

10.2.4 Diffusion

The diffusion theory attributes the adhesion of polymeric materials to the inter-penetration of chains at the interface. The major driving force for polymer autohesion and heterohesion is due to mutual diffusion of polymer molecules across the interface (3). This theory requires that both the adhesive and adherend are polymers, which are capable of movement and are mutually compatible and miscible (other materials may be bonded by similar phenomena). To describe the self-diffusion phenomenon of polymers, several theories have been proposed: entanglement coupling (3), cooperativity (4), and reptation (5). The reptation model has been applied to study tack, green strength, healing, and welding of polymers.

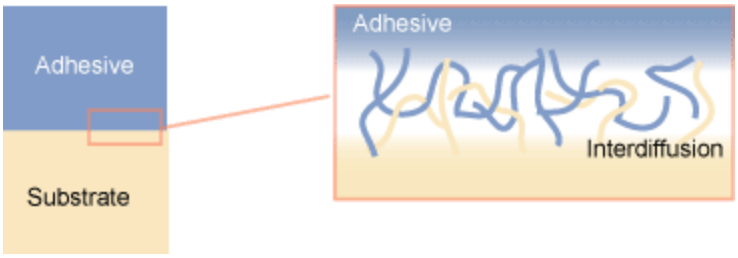

Figure 10.5 – Interdiffusion (1)

Parameters affecting the diffusion process are: contact time, temperature, molecular weight of polymers and physical form (liquid, solid). Polarity generally increases adhesion.

Some evidence has demonstrated that the interdiffusion phenomenon exists in mobile and compatible polymers and may promote the intrinsic adhesion. The diffusion theory, however, has found limited application where the polymer and adherend are not soluble or the chain movement of the polymer is constrained by its highly crosslinked, crystalline structure, or when it is below its glass transition temperature.

10.2.5 Electrostatic

The basis of the electrostatic theory of adhesion is the difference in electonegativities of adhesing materials. Adhesion is attributed to the transfer of electrons across the interface creating positive and negative charges that attract one another. For example, when an organic polymer is brought into contact with metal, electrons are transferred from metal into the polymer, creating an attracting electrical double layer (EDL). The electrostatic theory (3) tell us that these electrostatic forces at the interface (i.e. in the EDL), account for resistance to separation of the adhesive and the substrate.

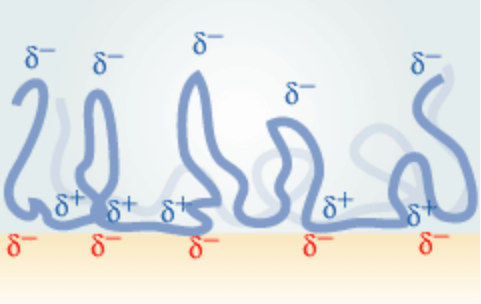

Figure 10.6 – Electrical Double Layer (1)

Some controversies have arisen surrounding the electrostatic theory owing to the fact that the EDL could not be identified without separating the adhesive bond. Additionally the effect of the electrical double layer on the adhesive bond strength was exaggerated, as argued by many researchers (3).

10.3 Factors that influence the adhesion

The stronger adhesion of bonds between mechanically or chemically roughened surfaces is based on the enlargement of the effective surface (contact surface between the adhesive and the substrate), and an increase in the number of active centers, e. g. edges, corners, and faulty parts which, as in the heterogeneous catalysis, increase the interactive forces in the interface adhesive/surface.

The following factors have a predominant importance in the adhesion process:

- Wetting of the surface
- Surface treatment
- Structure of the materials to be bonded (incl. Adhesives and substrates)
- Design of the joint (incl. stresses applied on the bonded materials)

10.3.1 Wetting of the surface

To enable the adhesive bonds between the adhesive and the surface, the adhesive must first wet the surface; in other words, it must be applied in the liquid form (as a solution, dispersion, or hot-melt).

A measure for the wettability of a surface is the angle of contact that forms between a drop of liquid and a smooth, plain surface.

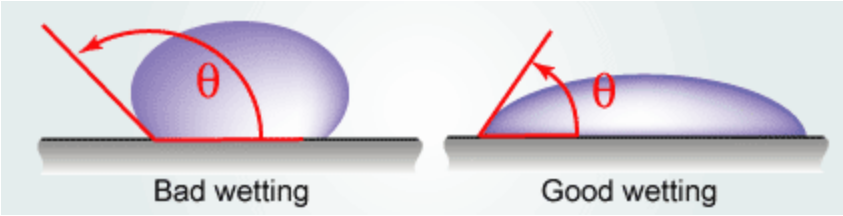

Figure 10.7 – Wetting Angles (1)

A good wetting occurs when the angle of contact (θ) between the adhesive and the substrate is less than 90. Complete wetting occurs when the molecular attraction between the liquid and solid molecules is greater than that between similar liquid molecules. Whether or not a given liquid will wet a solid depends on the surface tension of both substances.

The contact surface formed during wetting depends on the surface tension and the viscosity of the adhesive, and also on the structure (shape and size of the pores) of the surface. The size of the effective surface is generally smaller than the true surface of the substrate, because the pores and uneven parts of the surface are not completely filled by the adhesive.

Pressure may also help enhance the adhesion. Generally, bonds that have been set under pressure have higher adhesive strength. Pressure imparts better wetting due to flow and consequently, more complete interfacial contact.

The viscosity of the adhesive is critical to wetting, e.g.: the lower the viscosity, the more easily it will wet the substrate. Therefore, rheological properties of the adhesive must be adapted to the application conditions (substrate's surface, curing time, pressure, temperature).

10.3.2 Surface treatment

All surfaces exposed to the normal atmosphere undergo gas and water adsorption in the molecular range; the surface condition can be also changed by oxidation processes. To ensure good adhesion to metals it is sometimes necessary to carry out mechanical and/or chemical pre-treatment (e.g. sandblasting and pickling). On the other hand, inert (too little reactive) plastics surfaces are activated by subjecting them to specific surface treatment for plastics (eg flame treatment, corona discharge). In principle, these processes serve to form active centers and polar, reactive groups, which favor the wettability and the chemisorption of suitably pretreated surfaces.

The quality of the parts being joined is paramount for the quality of the bonded joint and, in particular, its resistance to aging. The surface must be treated before the adhesive is applied. Wide-ranging methods of surface pretreatment exist. In every case, contaminants such as oil, grease, drawing and releasing agents, plasticizers, etc. must be removed with suitable cleaning agents.

Cleaning & degreasing	Mechanical treatment	Chemical & physical treatment
Removal of dust, oxides, remnants of paints and dirt	Processing with hard and powered brushes of varying types (after degreasing)	Picking of aluminium, hardened and stainless steel and hard metals
Surface priming	Use of abrasive belts,disks, emery paper (120 to 180grain) etc. after degreasing	Pickling of plastics which are difficult to bond, e.g. PTFE, POM and PP
Removal of unwanted contaminating films by degreasing/cleaning agents.	Blasting treatments of all types (dry or wet) using a fine-grain sharp sand or shot	Flame treatment, corona pretreatment, plasma treatment of plastics which are difficult to bond, e.g. PE, PA, PP...

Table 10.1 – Surface Treatment methods (5)

In this connection, we should also mention coupling agents or adhesion promoters. These are in most cases bifunctional, low-molecular substances, e.g. titanates, chlorosilanes, and chromium complexes of unsaturated carboxylic acids, which fix the adhesive on the surface by chemical reactions. The mode of action of these adhesion promoters is based on their bifunctionality. One group reacts with reactive groups of the adherends, while the second group reacts with the adhesive. It is advisable, therefore, to use adhesion promoters whose groups react differently or according to different types of reaction, e.g. by substitution or radical reaction.

10.3.3 Structure of the materials to be bonded

Besides the surface condition, the structure of the materials to be bonded is of decisive importance. Porous materials (e. g. wood, paper, and textiles) absorb low viscosity adhesives. The result of this adhesive's penetration are thin, uneven ("starved") joints which often impair the strength of the bond. On the other hand, the capillaries absorb the more volatile, low molecular substances, e.g. solvents, preferably. This process results in a rapid adhesion, but it can have a negative influence on the distribution of the polymer in the bond line owing to the simultaneous separation of oligomers. In addition, the solvent molecules compete with the adhesive molecules in regard to the adsorption. The adhesive molecules are first adsorbed out of the adhesive solution through contact points separated by loops. With progressing evaporation of the solvent, the adhesive molecules or segments are then adsorbed mainly at the surface.

The molecular structure of the adhesive is decisive for the cohesion, i.e. the state in which the particles of a single substance are held together, and in connection with the surface condition described above, for the adhesion. The principal molecular influencing factors are: the molecular weight or the distribution of the molecular weight, the number and size of the side-groups, and the polarity:

The macromolecules acting as an adhesive are either produced by a preceding polyreaction and then applied in the liquid form (solution, dispersion, or hot-melt) to the adherend, or they are produced by polyreactions of reactive low-molecular compounds in the bond line direct. For contact adhesives, the first is the case. In the case of adhesives produced by preceeding polyreaction, the molecular weight must not be infinitely high (viscosity and solubility depend on the molecular weight).

With adhesives produced by polyreaction of reactive low-molecular compounds, it is frequently a desired objective to achieve a high molecular weight, which is often obtained by crosslinking reactions. The higher the molecular weight, the higher the tensile strength of linear polymers, which is a measure for the cohesion, as shown below.

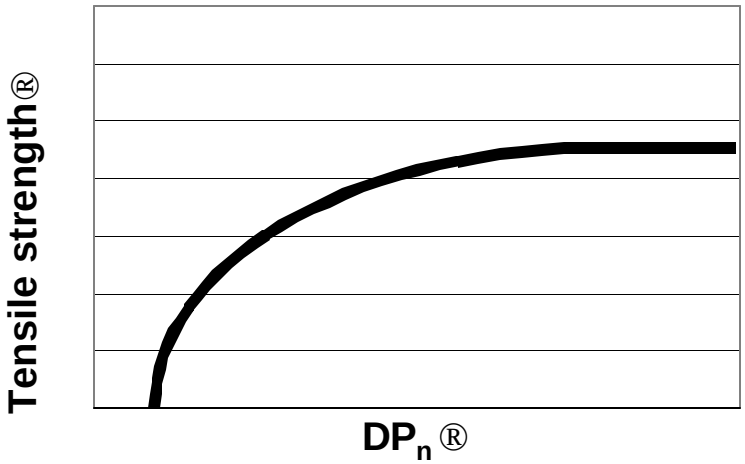

Figure 10.7 – Tensile Strength versus Degree of Polymerization

Tensile strength (TS) of a polymer as a function of the degree of polymerization DP(n)

$$TS = TS_{\infty} - \frac{C}{DP_n}$$

TS = Tensile strength at the degree of polymerization DP(n)

TS ∞ = Tensile strength at infinitely high degree of polymerization

C = Polymer constant

DP(n) = Numerically average degree of polymerization

The influence exerted by the side-groups of some polymers is also important. When increasing the size of the side-groups, owing a change of crystallinity within the

polymer structure, the strength increase as well. The incorporation of large side-groups "loosens" the polymer structure. Some of the molecular regions become more volatile. This permits orientation of the polar adhesive groups to the surface.

Generally speaking, with increasing content of polar groups in the adhesive, the strength of the adhesion is improved.

10.3.4 Structure of the joint

An important prerequisite for the successful use of bonding technology is that the respective parts be suitably designed for bonding, as distinct from welding, for example.

Care must be taken to provide a sufficiently large bonded area, such as a large area of overlap of the mating parts. The ideal bonded joint is one that under all practical loading conditions the adhesives is stressed in the direction in which it most resists failure. Favorable stress can be applied to the bond by using proper joint design. Bonded joints are particularly vulnerable to peeling stress and therefore should be designed in such a way that the applied forces do not give rise to stress of this type.

However, some joint designs may be impractical, expensive to make, or hard to align. The design engineer will often have to weigh these factors against optimum adhesive performance.

10.3.5 Adhesives for rubber & thermoset substrates(1)

Adhesives	Substrates						
	NR	CR	NBR	PU	Si	UP	Ep
Acrylic							
Acrylic anaerobic						★★	★★
Butyl Rubber						★	★
Cyanoacrylate	★★★	★★★	★★★	★★		★★★	★★★
Epoxy	★★	★★	★★			★★★	★★★
Inorganic						★	★
Melamine Formaldehyde							
Polychloroprene	★★★	★★★	★	★★		★★	★★
Nitrile Rubber	★★★		★★★	★★★		★★★	★★★
Phenol Formaldehyde							
Polyamide							
Saturated Polyester						★	★
Unsaturated Polyester						★★★	★★★
Polysulfide						★	★
Polyurethane	★★			★★★		★★	★★
Polyvinyl Acetate							
Resorcinol						★★	★★
Silicone					★★★	★	★
Styrene Butadiene Rubber						★	★
Urea Formaldehyde							

★★★very good
★★good
★suitable

10.3.6 Adhesives for themoplastic substrates (1)

Adhesives	Thermoplastic Substrates									
	Acrylic	PA	PC	SP	PE	PP	PS	PTFE	PVC flexible	PVC rigid
Acrylic	★★★	★	★★★					★★		★★
Acrylic anaerobic		★★								
Butyl Rubber										★
Cyanoacrylate	★★★	★★	★★★	★★	★	★	★★★	★★	★★	★★★
Epoxy	★	★★	★★	★★			★			★
Inorganic										
Melamine Formaldehyde										
Polychloroprene	★			★				★	★	★★
Nitrile Rubber	★★	★★		★★★	★★★	★★★	★	★★★	★★★	★★
Phenol Formaldehyde										
Polyamide		★★								
Saturated Polyester				★★★						★
Unsaturated Polyester							★★			★
Polysulfide			★★			★★★	★	★★		★★★
Polyurethane		★★	★★★	★					★★★	★★★
Polyvinyl Acetate										
Resorcinol		★★★								
Silicone					★			★		
Styrene Butadiene Rubber										★★
Urea Formaldehyde										

★★★very good
★★good
★suitable

10.3.7 Adhesives for glass, metal, wood & foam substrates (1)

Adhesives	Substrates					
	PS foam	PU foam	PVC foam	Glass	Metal	Wood
Acrylic		★		★★	★★	★
Acrylic anaerobic				★★★	★★★	★★
Butyl Rubber		★	★★★			★★
Cyanoacrylate		★	★		★★★	★
Epoxy	★	★	★	★★	★★★	★★★
Inorganic				★★		★★
Melamine Formaldehyde						★★★
Polychloroprene	★	★★	★★★		★★	★★
Nitrile Rubber	★★★	★★	★★★	★	★★	★★
Phenol Formaldehyde					★	★★★
Polyamide				★	★	★★
Saturated Polyester		★	★	★	★	★
Unsaturated Polyester		★★	★	★★★	★★★	★★
Polysulfide				★★	★★	★★
Polyurethane	★	★★	★	★★	★★	★
Polyvinyl Acetate	★★					★★★
Resorcinol	★					★★★
Silicone				★	★★	★
Styrene Butadiene Rubber		★	★★★		★★	★
Urea Formaldehyde	★★					★★★

★★★very good
★★good
★suitable

10.4 References

1. L. H. Lee, *Adhesive Bonding*, Plenum Press, New York, 1991.
2. D. L Allara, et al., Bonding and Adhesion of Polymer Interfaces, *Materials Science and Engineering*, **1986**, *83*, 213-226.
3. A.J. Kinloch, Interfacial Fracture Mechanical Aspects of Adhesive Bonded Joints – A Review, *J. Adhesion*, **1979**, *10*, 193-219.
4. A.J. Kinloch, The Science of Adhesion 1: Surface and Interfacial Aspects, *J. Materials Science*, **1980**, *15*, 216-266.
5. A.J. Kinloch, *Adhesion and Adhesives: Science and Technology*, Chapman and Hall, New York, 1987.
6. E.P. Plueddemann, Adhesion Through Silane Coupling Agents in *Fundamentals of Adhesion* (L.H. Lee, ed.), Plenum Press, New York, 1991.
7. W. Jennings, Surface Roughness and Bond Strength of Adhesives, *J. Adhesion*, **1972**, *4*, 25-40.
8. S.S. Voyutskii, *Autohesion and Adhesion of High Polymers*, Interscience, New York, 1963.
9. J. Klein, The Self-Diffusion of Polymers, *Contemporary Physics*, **1979**, *26(6*), 611-629.
10. S.F. Edwards and J.W.V. Grant, The Effect of Entanglements on the Viscosity of a Polymer Melt, *J. Phys*, **1973**, *6*, 1186-1195.
11. F. Brochard and P.G. DeGennes, Polymer-Polymer Interdiffusion, Europhysics Letters, **1986**, 1, 221-224.
12. B.V. Deryagin, Research, **1913**, *8*, 70.
13. W. Possart, Experimental and Theoretical Description of the Electrostatic Component of Adhesion at Polymer Metal Contacts, *Int. J. Adhesion*, **1988**, *8*, 77-83.

11. Antioxidants

In order to properly introduce the formulation of adhesives, a discussion of additives is necessary. The two additives most important to the formulator of contact adhesives are antioxidants and tackifiers. Antioxidants increase the stability of both the product prior to application and the finished bond joint. A brief discussion of each of the relevant systems follows. Tackifiers are short chain molecules that improve the tack of a material. A more extensive discussion of tackifiers follows.

11.1 Primary Antioxidants

Primary or free radical scavenging antioxidants inhibit oxidation via chain terminating reactions. They have reactive OH or NH groups. (Hindered phenols and Secondary aromatic amines) Inhibition occurs via a transfer of a proton to the free radical species. The resulting radical is stable and does not abstract a proton from the polymer chain (1).

11.1.1 Hindered Phenols

Phenolic stabilizers are primary antioxidants that act as hydrogen donors. They react with peroxy radicals to form hydroperoxides and prevent the abstraction of hydrogen from the polymer backbone. Often used in combination with secondary antioxidants, phenolic stabilizers are offered in an extensive range of molecular weights, product forms, and functionalities.

Sterically hindered phenols are the most widely used stabilizers of this type and were used in this program. They are effective during both processing and long term thermal aging and many have FDA approvals.

11.1.2 Secondary Aromatic Amines

Secondary aromatic amines act as primary antioxidants and are excellent hydrogen donors (3).

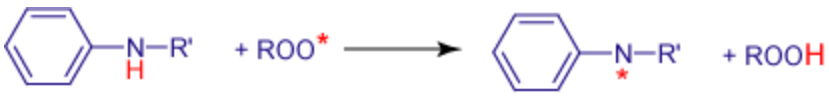

Secondary Aromatic Amines - Mechanism

Also available in an extensive range of molecular weights and product forms, aromatic amines are often more active than hindered phenols, because of less steric hinderance. Aromatic amines, however, are more discoloring than hindered phenols, especially on exposure to light or combustion gases (gas fade) and have limited FDA approvals.

11.2 Secondary Antioxidants

Secondary antioxidants, frequently referred to as hydroperoxide decomposers, decompose hydroperoxides into non-radical, non-reactive, and thermally stable products. They are often used in combination with primary antioxidants to yield synergistic stabilization effects.

Hydroperoxide decomposers prevent the split of hydroperoxides into extremely reactive alkoxy and hydroxy radicals. Organophosphorus compounds and Thiosynergists are widely used hydroperoxide decomposers (1).

11.2.1 Organophosphorus Compounds

Organophosphorus compounds are secondary antioxidants that decompose peroxides and hydroperoxides into stable, non-radical products. They are extremely effective stabilizers during processing and are normally used in combination with a primary antioxidant.

Trivalent phosphorus compounds are excellent hydroperoxide decomposers. Generally, phosphites (or phosphonites) are used and react according to the following general reaction, generating phosphates.

$$(RO)_3 - P + ROOH \longrightarrow (RO)_3 - P = O + ROH$$

Some of these compounds are sensitive to water and can hydrolyze, leading to formation of acidic species. While the addition of an acid scavenger can minimize the effect, the industry has generally converted to hydrolysis-resistant compounds. Commercially available phosphites differ by the nature of the aryl groups. Some typical structures are shown below.

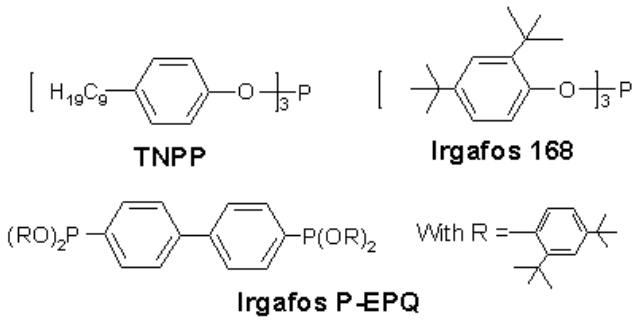

(Structures courtesy Ciba Specialty Chemicals)

11.2.2 Thiosynergists

Among sulfur-based hydroperoxide decomposers, esters of 3,3-thiodipropionic acid play an important role. Thiosynergists react according to the following general reaction, generating sulfoxides and sulfones (1).

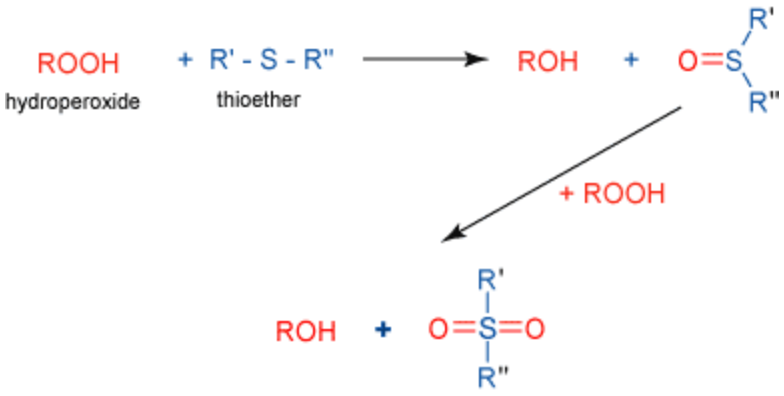

Although thiosynergists do not improve the melt stability of polymers during polymer processing, they are very efficient for long-term thermal aging applications. Sulfur based hydroperoxide decomposers are mainly used in combination with hindered phenol antioxidants. The most common commercially available thiosynergists are based on either lauric or stearic acid.

11.3 Multi-functional antioxidants

Multi-functional antioxidants have recently become available. Due to their special molecular design, they optimally combine primary and secondary antioxidant functions in one compound (3). Having several stabilizing functions combined in the same molecule, multi-functional antioxidants eliminate the need for co-stabilizers, such as phosphites and thioethers. This not only simplifies the formulation, but it also simplifies the storage, handling, and use of the stabilizer.

Hydroxylamines may act as both primary and secondary antioxidants, providing processing stability, comparable to phenol/phosphite systems. In addition, they provide excellent light stability when used in combination with hindered amines and are resistant to gas-fade discoloration.

11.4 Radical scavengers

Radical scavengers are antioxidants capable of trapping radicals. Scavenging of alkyl radicals would immediately inhibit the autoxidation cycle. Under oxygen deficient conditions alkyl radical scavengers contribute significantly to the stabilization of the polymer. Scavenging the extremely reactive alkoxy and hydroxy radicals is practically not possible (3).

Carbon centered radical scavengers, such as lactones and acrylated bis-phenols, are extremely effective in oxygen deficient environments.

Lactones (Benzofuranone derivatives) are powerful radical scavengers. Even when added in small amounts, they help control melt stability during polymer processing. Substituted benzofuranone are excellent radical scavengers. They are mainly used in combination with phenolic compounds and phosphite to provide materials excellent performance even at low concentrations. Acting as traditional hindered phenols, acrylate functionalized hindered phenols are efficient C-radical scavengers. They are very effective in preventing styrene copolymers from cross linking or degrading during processing, particularly under oxygen deficient conditions. They are usually used in conjunction with other stabilization chemistries.

11.5 Benefits of Antioxidants

During their life cycle, adhesives or adhesives components can undergo degradation as shown in the table below. Any one of the factors in the life cycle leads to an undesirable change in physical properties of the unstabilized adhesives, creating manufacturing problems, poor product appearance and reduction of adhesive strength. The role of antioxidants is to prevent or retard all these undesirable changes.

Typical Adhesives Life Cycle	Typical Reasons for Degradation	Benefits of antioxidants
1. Raw material manufacturing	. High temperature treatment . Catalyst residues . Stripping process	Color stability
2. Raw material storage and shipment	. Prolonged exposure to oxygen at ambient temperatures	
3. Adhesives manufacturing	. High temperature treatment . Shear . Oxygen exposure	Viscosity stability
4. Application of adhesives to substrate	. High temperature treatment . Oxygen exposure	Retention of adhesive properties
5. Final stages of the adhesion bond	. Prolonged exposure to oxygen at ambient or elevated service temperatures	
	. Exposure to light	

Figure 11.15 – Antioxidant Benefits (courtesy Ciba Specialty Chemicals)

Main benefits of antioxidants like color stabilization, viscosity stabilization,or retention of adhesive properties will preserve quality an performance of adhesive formulations during all its life cycle, as illustrated in the figure above.

12. Tackifiers

12.1 Introduction

Tackifier resins are added to base polymers/elastomers in adhesives to improve the tack (ability to stick). This is achieved mostly by better wetting out onto a surface and improved specific adhesion. All of these properties can be summarized in one definition; a tackifier resin is used to modify the rheological properties of the final adhesive system, pressure sensitive or non-pressure sensitive. In simple terms one can visualize a tackifier resin reducing viscosity. More specifically, the resin ultimately determines the viscoelastic behavior of the final adhesive. As an example, one can take a suitable styrenic block copolymer (that does not have tack and cannot wet out) and mix it with a suitable concentration of compatible resin making it sticky[1].

Resins are low molecular weight amorphous polymers. Their main applications are in adhesives, inks, and chewing gum. In adhesives, resins are used to generate tack and specific adhesion. Mostly they are used together with larger polymers, which form the backbone of the adhesive and thus generate cohesion. Formulators use resins to create the best balance between adhesion and cohesion. There are many different resins available to the marketplace.

Tackifying resins can be divided into three groups: hydrocarbon resins, rosin resins and terpene resins. Hydrocarbon resins are based on a petroleum feedstock, i.e., a synthetic source, rosin resins are based on a natural feedstock: gained from pine trees and terpene resins are generated from a natural source, wood turpentine or from the kraft sulphate pulping processes.

12.2 Rosin resins

Rosin is one of the oldest raw materials for the adhesives industry, either as such or converted to rosin ester. Three types of rosin are used for resin manufacture, gum rosin, wood rosin and tall oil rosin. All are generated from the pine tree.

Gum rosin was once the only commercial source of rosin. It is the oleoresin (pine gum) of the living pine tree. The harvesting of the oleoresin is simple, involving periodic wounding of the tree and collecting of the exudates or sap.

Wood rosin. After harvesting pine trees the stump is allowed to remain in the ground for about ten years so that its bark and sapwood may decay and slough off to leave the heartwood rich in resin. Resinous material is extracted from the stump.

Tall oil rosin is obtained by distillation of crude tall oil (CTO), a by-product of the kraft sulphate pulping process. CTO contains 70-90% acidic material, which is composed essentially of fatty acid and tall oil rosin (3). Tall oil rosin (TOR) has a tendency to crystallize and usually contains 200-600 ppm sulfur. Highly distilled TOR can produce esters that are similar to gum and wood rosin derivatives.

12.2.1 Rosin Chemistry

Rosin resins, unlike hydrocarbon resins, are not polymers. In fact, they are a blend of different molecules. Rosin molecules have poor stability caused by unsaturation. Stability can be improved by various methods such as disproportionation and hydrogenation. Rearrangement of the double bonds by disproportionation leads to improved stability. Another method to improve stability is to hydrogenate the rosin.

The carboxylic acid can be converted to an ester using various alcohols. The molecular weight of the alcohol determines the softening point of the subsequent ester. Glycerol and pentaerythritol are the most commonly used alcohols. Methanol and tri-ethylene-glycol are used to produce lower softening point esters.

Rosin resins have a wide span of compatibility with almost all polymers. They are well known for their peel and tack contribution to the adhesive, but generally decrease cohesive strength.

12.2.2 Terpene resins

Terpene resins are based on three feedstreams: a-pinene, b-pinene, d-limonene. These resins are formed by a cationic polymerization reaction using a Lewis acid catalyst. These resins have excellent initial color and have a broad range of softening points and have been produced for many years. Alpha-pinene and beta-pinene are derived primarily from two processes: stump extraction leading to the isolation of steam distilled wood turpentine and the kraft sulfate pulping process leading to the isolation of sulfate turpentine. The individual terpene compounds are isolated by distillation from these two streams. d-Limonene is obtained from citrus sources and a similar compound, dipentene,

is obtained by distillation from petroleum sources. The main difference for the formulator between these resins is that the d-limonene (and dipentene based) resins are not compatible with SBR polymers (4).

There are other resins based on these terpene feedstocks:

- Styrenated terpenes - mixed aliphatic/aromatic resin
- Terpene phenolics - polar resins with excellent adhesion and broad compatibility with polar polymers
- Hydrogenated terpenes - improved color by hydrogenation

12.2.3 Hydrocarbon resins

There are three major types of hydrocarbon resins:

- C5 aliphatic resins
- C9 aromatic resins
- DCPD cycloaliphatic resins (dicyclopentadiene)

A sub-category, hydrogenated hydrocarbon resins, based on the above major types will also be discussed. The feedstocks to produce C5 and C9 hydrocarbon resins are fractions from a naphtha cracker. The feed streams to produce hydrocarbon resins can be divided into two groups: C5 piperylene feedstock and C9 resin oil.

12.2.4 C5 Aliphatic Hydrocarbon

C5 piperylene contains various monomers species including: trans-1, 3-pentadiene, cis-1, 3-pentadiene, 2-methyl-2-butene, dicyclopentadiene, cyclopentadiene, cyclopentene.

The liquid C5 feedstock can be polymerized to a hard resin using a Lewis acid catalyst and carefully selecting temperature and pressure to obtain the desired softening point and molecular weight (5).

C5 resins are in essence aliphatic materials. They are available in a wide range of softening points and molecular weights.

12.2.5 C9 Aromatic Hydrocarbon Resins

C9 resin oil contains various monomers such as: vinyltoluenes, dicyclopentadiene, indene, methylstyrene, styrene, methylindenes. A cationic polymerization reaction converts the liquid feed to a hard resin (4). C9 resins are aromatic molecules. They are also available in a wide variety of softening points and molecular weights.

C5 and C9 resins can be modified by mixing the two feed streams together. The mix ratio determines the aliphatic/aromatic balance of the resin. A useful method to characterize the aliphatic/aromatic balance of a resin will be later. The aliphatic C5 feed can be replaced with a terpene feedstock and modified with styrene to form styrenated terpenes which have excellent color and stability and are very good tackifiers for SBS block copolymers (3).

12.2.6 Dicyclopentadiene Hydrocarbon Resins

Dicyclopentadiene (DCPD) feedstock contains various structures such:dicyclopentadiene, cyclopentadiene, and cyclopentene; but is primarily made up of dicyclopentadiene. The feedstock contains co-dimers with dienes such as isoprene, butadiene and methylcyclopentadiene. At elevated temperature (170-190C), dicyclopentadiene will crack into cyclopentadiene.

Although the exact structure of DCPD resins is not known, early steps of the thermal polymerization most likely involve the addition of cyclopentadiene to the norbornene olefin followed by continued additions of this type by additional cyclopentadiene to propagate the growing chain.

Dicyclopentadiene is polymerized either thermally or with a catalyst to form dark and unstable resins with a characteristic odor. They are normally used for construction adhesives and inks. They are more commonly used as a base resin for subsequent hydrogenation to form water white resins with excellent stability and low odor and will be discussed below (5).

12.2.7 Hydrogenated Hydrocarbon Resins

Hydrogenating the hydrocarbon resins described above produces another class of hydrocarbon resins. Hydrogenation is primarily used to improve color and stability of the resin by removing vulnerable double bonds. Partial and selective hydrogenation are methods used to produce resins with broad compatibility and good stability.

The most common base resins used for hydrogenation are C9, C5 resins, DCPD, and modified DCPD resins. These resins are ideal for tackifying SIS and SEBS block copolymers (3).

12.2.8 Hydrogenated C9 Hydrocarbon Resins

C9 resins contain double bonds, which are relatively unstable. A useful way to stabilize these resins is to hydrogenate them. C9 resins have predominantly aromatic ring structures with an overall aromaticity around 40%, measured by proton NMR. Resins are hydrogenated in solution with very specific operating parameters: temperature, pressure, hydrogen concentration and catalyst level. Changing any one of these operating parameters will bring a change in the degree of hydrogenation of the final resin. During hydrogenation, the aromatic ring structures gradually lose their aromatic nature and become cyclo-aliphatic.

When the process is allowed to go to completion, the result is a fully hydrogenated hydrocarbon resin with full aliphatic character. The process can also be adjusted so that partially hydrogenated resins are the end result.[1] This is necessary in order to prepare resins for wide use in adhesive formulations and is achieved through sequential, but not total hydrogenation of the rings. This means that partially hydrogenated resins still have some aromatic rings. The ability to be hydrogenated to varying degrees, resulting in various aliphatic/aromatic balances, gives these resins their unique properties. In theory any degree of hydrogenation can be manufactured. Resins carry a range of hydrogenation levels, varying from 50% to 100%.

12.3 Selective Hydrogenation of Mixed Feedstocks

To obtain resins with comparable compatibility to partially hydrogenated C9 resins, aromatic modification of DCPD (and other cycloaliphatic structures) and C5 resins is necessary. This is usually achieved by the addition of styrene-based monomers to the aliphatic monomers and subsequently polymerization. Then selective hydrogenation needs to be performed in order to reduce unsaturation and improve color of the cycloaliphatic and aliphatic structures without significantly affecting the aromatic content (6).

There are various physical and chemical parameters that are important to characterize tackifier resins. For hydrocarbon tackifier resins the aromatic/aliphatic balance of the resin is of special interest to adhesive formulators since it largely determines compatibility and ultimately, adhesive performance (7). The following criteria may be used to characterize resins:

- Color, Gardner and Hunter Lab scales
- Softening point, Ring & Ball
- Molecular Weight
- Melt Viscosity
- Thermal Stability
- Compatibility and Polarity, Cloud Points

12.4 Compatibility

The molecular weight and the aromatic/aliphatic balance of a resin are critical to allow for the correct compatibility. Hydrocarbon resins can be designed with a specific molecular weight distribution and proper aliphatic/aromatic balance to impart the correct compatibility with the mid-block for tackification and with the styrenic end-block for melt viscosity optimization and cohesive strength properties in SBS polymers (3).

12.5 Cloud Points and their Applications

The performance characteristics of a resin in a polymer system, such as an adhesive or rubber compound, are directly related to the compatibility of the resin with the polymer. Compatibility can be defined as the ability of the resin to "dissolve" a polymer. Knowing the compatibility of a resin with a polymer is essential to the formulator. The addition of a compatible resin to a polymer results in significant changes to bulk polymer properties including modulus and glass transition temperature (Tg) (9). An incompatible resin does not influence the polymer properties but acts like a thermoplastic filler.

The fine-tuning of adhesive systems is often accomplished by the addition of a resin having limited compatibility, thus producing a lower tack level with higher cohesive strength characteristics. This is the delicate, adhesion/cohesion balance that makes the difference between a good adhesive and an excellent, successful adhesive.

Softening point and resin concentration are familiar concepts to formulators but these alone will not determine all the effects that the resin has on the performance of the

formulated compound. Compatibility data is also required for a more complete understanding of resin performance.

A convenient method to characterize resin compatibility is by determination of cloud points in suitable solvent systems. From the cloud point values obtained, the resin may be characterized as being aliphatic, aromatic, or a combination of both. This characterization can then be used to determine the suitability of the resin for any specific polymer. Additionally, polarity of resins, also an important formulating parameter, can be determined by cloud point methods.

Cloud point determination is easy to do and involves weighing a standard amount of resin that is dissolved in the solvent at high temperature. When homogeneous it is allowed to cool, with mixing. The temperature at which the resin begins to form a separate phase is defined as the cloud point.

12.5.1 Cloud Points, Resin Compatibility and Polarity

An explanation of how these cloud points are related to compatibility follows below.

Mixed methylcyclohexane aniline point (MMAP), being an aromatic solvent system, is a measurement of aromatic solubility and determines the aliphatic/aromatic character of the resin. The lower the MMAP value, the less aliphatic and the more aromatic nature of the resin and vice versa.

The diacetone alcohol cloud point (DACP) method determines the polarity of the resin. Due to the polar nature of the solvent mixture, polar resins will dissolve better. As a general "rule-of-thumb," specific adhesion of an adhesive is related to the polarity of

the resin. The lower the DACP value, the higher the resin polarity and the better the specific adhesion. Measuring more polar resins, such as aromatic hydrocarbon resins and rosin resins, results in DACP cloud points lower than -50°C. Working at these very low temperatures is not without problems. At about -20°C, the DACP solvent reaches its own cloud point, thereby obscuring the cloud point of the resin.

12.6 Resin Properties

Resin molecular weight distribution, ring & ball softening point, MMAP and DACP/EMDA are the main characteristics useful by a formulator. With these parameters in hand, formulators can easily choose their resin of choice to give optimum adhesive performance with a selected polymer (10).

12.7 Conclusion

Resins are low molecular weight amorphous additives useful in many applications. They enhance tack and peel in adhesives. They offer a versatile chemistry with a wide range of properties and can be synthetic, based on hydrocarbons, or generated from natural sources.

In order for the systems analyzed in this project to be extended to use it is necessary for the adhesive formulators to become knowledgeable in the chemistry of resins since this is key for their use in adhesive formulations. It is essential to understand thoroughly the properties of tackifier resins. In this way, resins provide formulators the ability to formulate and optimize their adhesives. The information presented here does

not discuss the role of high pressures or the presence of carbon dioxide on the tackifier resins. These were beyond the scope of the project.

12.8 References

1. J.T. Harlan and L.A. Petershagan, Thermoplastic Rubber (ABA) Block Copolymers) in Adhesives, *Handbook of Adhesives*, 2nd Edition (I. Skeist, ed.), Van Nostrand, New York, 1977.
2. J. Shields, *Adhesives Handbook*, 3rd Edition, Buttersworth, London, 1984.
3. C.A. Rayner, Synthetic Organic Adhesives in *Adhesion and Adhesives*, 2nd Edition, Vol. 1-Adhesives, (R. Houwink and G. Salomon, eds.), 1970.
4. N.J. DeLollis, *Adhesives, Adherends, Adhesion*, Krieger Publishing, New York, 1980.
5. W.C. Wake, *Adhesion and Formulation of Adhesives*, 2nd Edition, Applied Science Publishers, London, 1982.
6. L. H. Lee, *Adhesive Bonding*, Plenum Press, New York, 1991.
7. D. L Allara, et al., Bonding and Adhesion of Polymer Interfaces, *Materials Science and Engineering*, **1986**, *83*, 213-226.
8. A.J. Kinloch, The Science of Adhesion 1: Surface and Interfacial Aspects, *J. Materials Science*, **1980**, *15*, 216-266.
9. A.J. Kinloch, *Adhesion and Adhesives: Science and Technology*, Chapman and Hall, New York, 1987.

13. Environmental Impacts

13.1 Introduction

Since the adhesive industry has followed the paint industry in most areas due to the reduced volume of product applied and the diminished value of the resulting coatings, it is not surprising that the environmental guidelines regarding adhesives follow those for paint closely. As DoD has continued to more closely approximate EPA standards for emissions, it has become of increasing importance to follow developments in the EPA. As a result, the environmental impact section of this report will begin with a general discussion of surface coating before focusing on adhesive systems.

Surface coating operations involve applying a thin layer of coating (e.g., paint, lacquer, enamel, varnish, adhesive, etc.) to an object for decorative, protective, or adhesive purposes. The surface coating products include a liquid carrier that evaporates in the drying or curing process. In 1989, approximately 3.8 billion pounds of organic solvents, roughly one-third of all solvents purchased that year, were used in surface coating operations. These solvents were used both as carriers for coatings and to clean up coating equipment (1).

The use of surface coatings by manufacturing industries and other sectors of the economy is pervasive. Applications include: 1) coatings that are applied during the manufacture of a wide variety of products by Original Equipment Manufacturers (OEMs) including furniture, cans, automobiles, other transportation equipment, machinery, appliances, metal coils, flat wood, wire, and other miscellaneous products, 2) architectural coatings, and 3) special purpose coatings used for applications such as

maintenance operations at industrial and other facilities, auto refinishing, traffic paints, marine finishes, aerosol sprays, and adhesives.

Since the use of surface coatings by manufacturing industries is so widespread, it is extremely difficult to identify all of the industries in which coating materials are consumed. This makes the job of compiling a complete and accurate source inventory for this category a difficult one. The following tables, compiled by EPA, list Standard Industrial Classification (SIC) codes that are likely to be associated with industrial surface coating operations. Table 8.1 lists the SIC codes for which national level data are available to estimate the quantities of coatings consumed. The largest of these industries are shown in Table 8.2, which lists those industries accounting for 90 percent of reported OEM coating consumption on a dollar value basis for 1992. Finally, Table 8.3 lists other manufacturing SICs known to consume surface coatings, but for which no reliable national data are available to estimate the volume used. All of the SICs listed in Tables 8.1 and 8.3 may be thought of as possible industries to be considered for inclusion in an area source industrial surface coating inventory. Many of these sources have equivalents within DoD. However, there is no assurance that this list is totally inclusive, nor can it be stated that these SICs always represent categories that include area source industrial surface coating operations.

13.2 Processes and emissions

Surface coating is the process by which paints, inks, varnishes, adhesives, or other decorative or functional coatings are applied to a substrate (e.g., paper, metal, plastic) for decoration and/or protection. This can be accomplished by brushing, rolling, spraying,

dipping, flow coating, electrocoating, or specialized combinations or variations of these methods. The process by which the coating is applied is determined in part by the product's intended end use, the substrate to which the coating is applied, and the composition of the coating itself.

After the coating has been applied, it is cured or dried either by conventional curing or radiation curing processes. Conventional curing may be accomplished through the use of thermal ovens or air drying. The heat causes the solvents trapped in the coating to be driven off into the atmosphere. Emissions result from the evaporation of the paint solvent and any additional solvent used to thin the coating. Emissions also result from the use of solvents in cleaning the surface prior to coating and in cleaning coating equipment after use. Since this program reduced the weight percent of solvent used in each of the systems studied, it would be expected that a reduction in emissions will be found.

VOC emissions from small industrial surface coating operations, such as depots and repair facilities within DoD are influenced by several factors. Emissions from surface preparation and coating applications are a function of the VOC content of the product used. Emissions also are a function of the coating process used, including the transfer efficiency of the spray equipment. Transfer efficiency is the percentage of coating solids sprayed that actually adhere to the surface being coated.

TABLE 13.1 (1)

PRINCIPAL INDUSTRIAL SURFACE COATING SIC

SIC Code SIC Description

2451 Mobile Homes

2452 Prefabricated Wood Buildings and Components

2493 Reconstituted Wood Products

2499 Wood Products, Not Elsewhere Classified

2511 Wood Household Furniture, Except Upholstered

2512 Wood Household Furniture, Upholstered

2514 Metal Household Furniture

2517 Wood Television, Radio, Phonograph, and Sewing Machine Cabinets

2519 Household Furniture, Not Elsewhere Classified

2521 Wood Office Furniture

2522 Office Furniture, Except Wood

2531 Public Building and Related Furniture

2541 Wood Office and Store Fixtures, Partitions, Shelving, and Lockers

2542 Office and Store Fixtures, Partitions, Shelving, and Lockers, Except Wood

2599 Furniture and Fixtures, Not Elsewhere Classified

3411 Metal Cans

3412 Metal Shipping Barrels, Drums, Kegs, and Pails

3441 Fabricated Structural Metal

3443 Fabricated Plate Work (Boiler Shops)

3444 Sheet Metal Work

3446 Architectural and Ornamental Metal Work

3448 Prefabricated Metal Buildings and Components

3449 Miscellaneous Structural Metal Work

3465 Automotive Stampings

3466 Crowns and Closures

3469 Metal Stampings, Not Elsewhere Classified

3471 Electroplating, Plating, Polishing, Anodizing, and Coloring

3479 Coating, Engraving, and Allied Services, Not Elsewhere Classified

3523 Farm Machinery and Equipment

3524 Lawn and Garden Tractors and Home Lawn and Garden Equipment

3531 Construction Machinery and Equipment

3532 Mining Machinery and Equipment, Except Oil and Gas Field Machinery and Equipment

3536 Overhead Traveling Cranes, Hoists, and Monorail Systems

3561 Pumps and Pumping Equipment

3563 Air and Gas Compressors

3581 Automatic Vending Machines

3585 Air Conditioning and Warm Air Heating Equipment

3586 Measuring and Dispensing Pumps

3593 Fluid Power Cylinders and Actuators

3594 Fluid Power Pumps and Motors

3612 Power, Distribution, and Specialty Transformers

3613 Switchgear and Switchboard Apparatus

3621 Motors and Generators

3631 Household Cooking Equipment

3632 Household Refrigerators and Home and Farm Freezers

3633 Household Laundry Equipment

3634 Electric Housewares and Fans

3635 Household Vacuum Cleaners

3639 Household Appliances, Not Elsewhere Classified

3711 Motor Vehicles and Passenger Car Bodies

3713 Truck and Bus Bodies

3714 Motor Vehicle Parts and Accessories

3715 Truck Trailers

3716 Motor Homes

3721 Aircraft

3724 Aircraft Engines and Parts

3728 Aircraft Parts and Auxiliary Equipment, Not Elsewhere Classified

3731 Ship Building and Repairing

3732 Boat Building and Repairing

3792 Travel Trailers and Campers

3799 Transportation Equipment, Not Elsewhere Classified

3931 Musical Instruments

3949 Sporting and Athletic Goods, Not Elsewhere Classified

3951 Pens, Mechanical Pencils, and Parts

3952 Lead Pencils, Crayons, and Artists' Materials

3953 Marking Devices

3993 Signs and Advertising Specialties

3995 Burial Caskets

TABLE 13.2 (1)

1992 MANUFACTURING INDUSTRY SURFACE COATING CONSUMPTION

SIC Code Description (Million $)

Cost of Coatings Consumed

371 Motor Vehicles and Equipment 1770.1

341 Metal Cans and Shipping Containers 328.2

347 Metal Services, Not Elsewhere Classified 321.7

289 Misc. Chemical Products (Printing Ink) 318.2 b

344 Fabricated Structural Metal Products 218.1

251 Household Furniture 173.3

363 Household Appliances 142.3

254 Partitions and Fixtures 87.7

373 Ship and Boat Building and Repairing 87.7

346 Metal Forgings and Stampings 86.9

352 Farm and Garden Machinery 85.6

249 Miscellaneous Wood Products 82.8

252 Office Furniture 80.2

TABLE 13.3 (1)

OTHER INDUSTRIES THAT MAY CONSUME SURFACE COATINGS

SIC Code	SIC Description
2436	Softwood Veneer and Plywood
262	Paper Mills
263	Paperboard Mills
265	Paperboard Containers and Boxes
3069	Fabricated Rubber Products, Not Elsewhere Classified
308	Miscellaneous Plastic Products, Not Elsewhere Classified
331	Blast Furnace and Basic Steel Products
3433	Heating Equipment, Except Electric
3494	Valves and Pipe Fittings, Not Elsewhere Classified
3452	Bolts, Nuts, Rivets, and Washers
364	Electric Lighting and Wiring Equipment
366	Communications Equipment
367	Electronic Components and Accessories
3812	Search and Navigation Equipment
382	Measuring and Controlling Devices
384	Medical Instruments and Supplies
3861	Photographic Equipment and Supplies
3942	Dolls and Stuffed Toys
3944	Games, Toys, and Children's Vehicles

13.3 VOC Reduction Methods

The main approaches for reducing VOC emissions from small industrial surface coating operations are (1) use of lower-VOC coatings, (2) use of enclosed cleaning devices, and (3)increased transfer efficiency. Other housekeeping activities can also be used to reduce emissions from small industrial surface coating operations. These activities include using tight-fitting containers, reducing spills, mixing paint to need, providing operator training, maintaining rigid control of inventory, using proper cleanup methods, etc.

Regulations designed to reduce VOC emissions have led to the development of high-solids and powder coatings, as well as increased use of water-based coatings. Although these coatings may reduce the VOC content they often do not perform as well as traditional formulations and have inferior transfer efficiencies.

13.4 Estimating Emissions

There are several methodologies available for calculating emissions from small industrial surface coating operations. The selection of a method to use depends on the degree of accuracy required in the estimate, the available data, and the available resources. This section discusses the methods available for estimating emissions from small industrial surface coating operations and identifies a preferred method.

Methods available for estimating emissions from small industrial surface coating operations include the following: (1) using SIC-specific, inventory area-specific per employee emission factors; (2) using national default per employee emission factors; and (3) using per capita emission factors. These methods are summarized in Table 13.4. Each

of these requires extending the SIC codes to comparable DoD functions and defining appropriate inventory areas. Because of the potentially large number of coating operations within an inventory area and the difficulty in identifying candidate applications to be surveyed, conducting surveys to collect activity, product use, and product-specific VOC content data to develop product-specific, site-specific detailed emissions estimates is generally not possible. It was impossible to determine the adhesive families used by DoD, much less the specific products.

The recommended method for estimating emissions from small industrial surface coating operations, according to EPA, involves developing and applying SIC-specific, inventory area-specific per employee emission factors based on reported point source emissions. Other methods for estimating emissions from this category include using national default per employee and per capita emission factors.

TABLE 13.4 (2)

PREFERRED AND ALTERNATIVE METHODS FOR ESTIMATING EMISSIONS FROM SMALL INDUSTRIAL SURFACE COATING OPERATIONS

Methods Description

Preferred Method:

Divide total reported point source emissions (by SIC) for SIC-Specific, Area-Specific Per Employee inventory area by total point source employment (by SIC) Factor for inventory area to develop SIC-specific, inventory area-specific per employee emissions factor.

Subtract total point source employment from total employment within the SIC to develop total area source SIC employment.

Multiply area source employment by SIC-specific, inventory area-specific employee factor.

Alternative Method 1:

Use national default per employee emission factors and National Default Per Employee Factor number of employees in SIC to estimate emissions.

Alternative Method 2:

Use per capita emission factor and population in inventory Per Capita Factor area to estimate emissions.

13.5 Hazardous Air Pollutants

HAP emissions from this source are determined by the same methods discussed above for VOC emissions. Again, conducting a survey to gather specific HAP information may be too resource-intensive for the inventorying agency to undertake. Using the preferred method described above assumes that the coatings and HAP contents used in small facilities are similar to those used and reported by large facilities. The agency may want to verify this assumption with local industry experts.

13.6 Extension to Current Project

Since it was beyond the scope of this project to extend each of the SICs to DoD equivalent activities, an in depth analysis of systemic VOC and HAP reduction was not possible. Instead, an analysis of individual formulation VOC content by weight percent was undertaken. This is a great simplification of actual VOC release but will enable a discussion of relative reduction in VOC emissions by the use of supercritical carbon dioxide for solvent replacement.

On a weight percentage basis, the addition of carbon dioxide to existing adhesive formulations reduces the overall VOC content. As a result, every one of the systems investigated resulted in a reduction in VOC versus a fully loaded solvent system. This is only the first step to reducing the content of VOCs in adhesives since the UNICARB system also enables the reduction of VOCs by increasing transfer efficiency and reducing materials expenditure. Since this is application specific, only generalizations as to VOC reduction from this source are shown.

Solvent choice is another important variable in determining VOC emissions since low vapor pressure solvents tend to become trapped in the adhesive layer and are not emitted. Therefore, significant work was done to identify the correct mix of high and low vapor pressure solvents to reduce VOC emissions and enhance performance. These efforts are ongoing and will be elucidated in the recommendation section.

Table 13.1 shows each system and the resulting reduction in VOC content from both the addition of carbon dioxide and the resulting reformulation.

System	Polymer wt %	Solvent wt %	CO2 wt %	VOC wt %
SIS:Toluene	25	75	0	75
			11	67
			20	60
			29	53
			34	50
	34	66	0	66
			9	60
			20	53
			27	48
			32	45
	40	60	0	60
			32	41
System	**Polymer wt %**	**Solvent wt %**	**CO2 wt %**	**VOC wt %**
SEBS:Toluene	25	75	0	75
			13	65
			21	59
			32	51
	33	67	0	67
			20	54
			26	50
			31	46
			38	42
	40	60	0	60
			31	41

System	Polymer wt %	Solvent wt %	CO2 wt %	VOC wt %
Polychloroprene:Toluene	18	82	0	82
			10	74
			20	66
			30	57
			35	53
	25	75	0	75
			10	68
			20	60
			25	56
			34	50
Polychloroprene Adhesive (Low VOC Formulation)	27	62	0	62
			18	51
			25	47
			31	43

System	Polymer wt %	Solvent wt %	CO2 wt %	VOC wt %
Morstik	43	27	0	27
			12	24
			21	21
			33	18
			42	16
	65	35	0	35
			12	31
			23	27
			32	24
			42	20

System	Polymer wt %	Solvent wt %	CO2 wt %	VOC wt %
Polyurethane (Desmocoll)	25	75	0	75
			15	64
			20	60

System	Polymer wt %	Solvent wt %	CO2 wt %	VOC wt %
Polyurethane (Desmomelt):acetone:ethyl acetate:toulene	22	34/34/10	0	80
			5	74
			10	70
			18	64
			24	59

System	Polymer wt %	Solvent wt %	CO2 wt %	VOC wt %
UCON Fluid	100	0	9	0
			13	0
			20	0
			27	0
			31	0
System	**Polymer wt %**	**Solvent wt %**	**CO2 wt %**	**VOC wt %**
PEG 4600	100	0	10	0
			18	0
			24	0
			29	0
			32	0
System	**Polymer wt %**	**Solvent wt %**	**CO2 wt %**	**VOC wt %**
PEG 8000	100	0	5	0
			10	0
			15	0
			17	0
			23	0
			29	0

Table 13.1 – VOC Reduction

Each system has a reduction in VOC except those systems without VOC initially. The reductions range up to 29 percent by weight and show the advantage of using carbon dioxide in every system tested. For the systems without initial VOCs, the supercritical carbon dioxide made it possible to spray these systems, something that had not been done previously.

13.5 Conclusions

Therefore, it is possible to greatly reduce the VOC emissions of adhesives by use of supercritical carbon dioxide in solvent bourne adhesives and it is possible to utilize nonVOC adhesives that are not otherwise sprayable by using the UNICARB system.

13.4 References

1. Procedures for the Preparation of Emission Inventories for Carbon Monoxide and Precursors of Ozone, Volume 1 (EPA, 1991) and AP-42 (EPA, 1995)
2. *1992 Census of Manufactures, Geographic Area Series,* U.S. Department of Commerce, Bureau of the Census, Washington, DC.

14. Sprayer Design and Execution

The UNICARB® process was developed as a continuously operating process requiring a single phase polymer/solvent/supercritical fluid to start the process. While adhesives can be reformulated to this process, we have miniaturized this technology and made it portable. The device was developed in collaboration with Thar Designs and Dow Chemical. The first prototype is shown in Figure 14.4. In principle it can be envisioned as a seltzer-bottle, but for pressure rated for 1000 - 2000 psi. The body and the lid were made from stainless steel with a volume of approximately 250 cubic centimeters. The lid was screwed to the body. A quick-connect port on the vessel allows filling the device with supercritical carbon dioxide gas cylinder where the volume loading (or pressure) was monitored. The devise was designed so that it is easily cleaned and refillable.

This portable system operates in the following manner. The vessel is filled with approximately 140 cubic centimeters of concentrated adhesive (i.e., polymer and "slow" solvent). After securing the lid, supercritical carbon dioxide is loaded until the can is pressurized to approximately 2000 psi (the exact pressure were determined for each adhesive during the course of the research project). A substantial amount of the carbon dioxide will dissolve in the polymeric material. This is in contrast to traditional hand-held spray cans where the gas's function is a propellant to force material out of the canister (usually butane or nitrogen) and does not dissolve appreciably in the adhesive (or paint). Essentially, this miniature UNICARB® system starts with a two phase system (i.e., carbon dioxide-rich and polymer-rich phase), and in this case, it is crucial to know, how much of the carbon dioxide dissolves in the polymer phase and how much of the usually heavy (slow) solvent of the adhesive concentrate is extracted into the carbon dioxide phase. To gain a better understanding for this type of mixture behavior, and to find proper operating conditions for the devise proposed, ternary mixture (polymer-solvent-carbon dioxide) diagrams were measured and mapped.

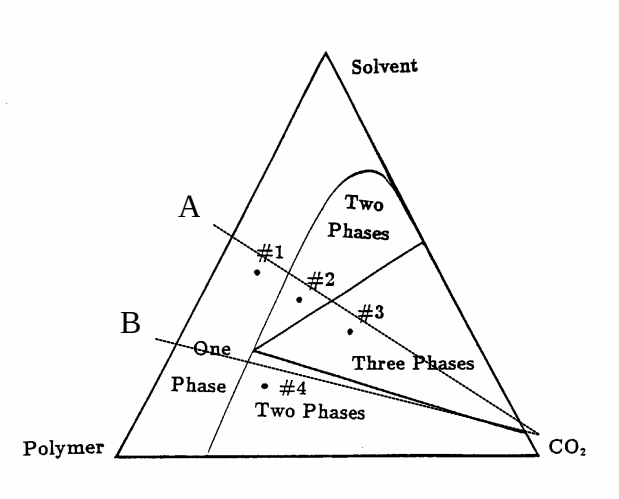

Figure 14.1 Ternary phase diagram.

Figure 14.1 shows a ternary diagram for a polymer-solvent-supercritical fluid mixture at constant temperature and pressure containing one-, two- and three-phase regions. It is bounded on the left by a curve that detaches very close to the high solvent concentration and then moves almost parallel to the polymer-solvent axis until it intersects with the polymer-supercritical fluid axis. Note that for the self-contained miniaturized UNICARB® system, the concentrations of the chemical species in the vessel change as the volume of the adhesive left in the can changes with spraying. This results in a dynamic shift in the phase boundaries and miscibilities of the species as the process continues. As such an extended operating window needs to be delineated respective to the phase diagrams for this process.

Starting with a low to medium concentrated polymer/solvent binary (Point A), the mixture exists in the single phase region for low supercritical fluid concentrations (Point #1). An increase in the SCF concentration (i.e. one moves on a straight line drawn through the lower left hand corner) brings the system into the two phase region (solvent-rich and polymer-rich phase, LL or LF, Point #2). At SCF concentrations typically above 90%, a predominantly carbon dioxide vapor phase is formed, that is, three phases coexist (LLV or LLF, Point #3). Starting with a highly concentrated polymer/solvent binary (Point B), adding SCF brings the system into the two phase region (LV, Point #4). As temperature or pressure increases, the lines in the ternary diagram shift.

Figure 14.2 shows a model ternary phase diagram as it applies to the proposed process. Tie-lines are drawn to relate the liquid mixture composition to the gas phase composition which essentially is a pure gas. Starting out with a high concentrated polymer concentration (Point A), the addition of a substantial amount of supercritical fluid leads to point B in the diagram, which

means that the gas phase is essentially pure SCF and the liquid phase leaving the spray can has a composition indicated by C. Using up adhesive concentrate, the composition will change and from point B one would move to point D. However, since the tie lines are essentially flat, the composition of the liquid adhesive concentrate leaving the can is still very much like the one before, as indicated by point E. The slope of the tie-lines and the ternary diagram itself very much depend on the polymer system and solvent used, that is, it is possible to have tie-lines with the opposite slope. Therefore, it is important for the hand-held device to work within the boundaries of the tie-lines to maintain the same concentration and quality of material over the duration of the spraying procedure.

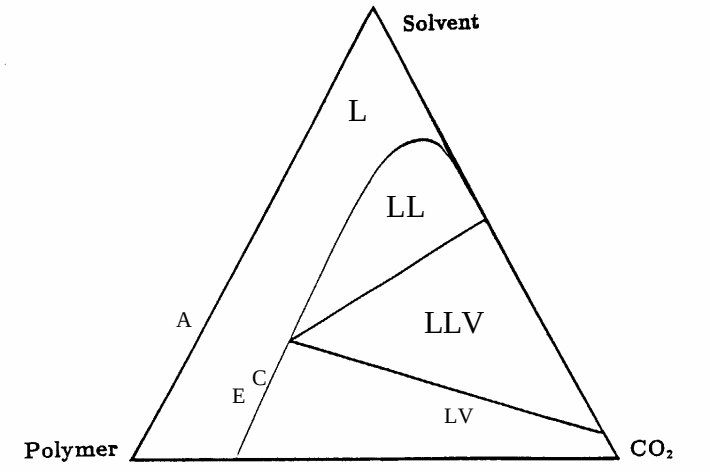

Figure 14.2 Ternary diagram as it relates to the new process. Tie-lines are drawn to relate the liquid mixture composition to the gas phase composition which essentially is a pure gas. Load concentrated adhesive (A) and add SCF (B), mixture sprayed is C; as devices is emptied one would move to D, mixture sprayed is E.

Additionally to the development of the device itself, we performed measurements of ternary phase diagrams for adhesive. This investigation included the separate investigation of each of the three possible binary mixtures and based on the outcome a systematic mapping of the three phase diagram. The temperature and pressure dependence was determined since the pressure in the vessel decreased when adhesive was spayed. The temperature dependence is important because the solubility of the supercritical carbon dioxide fluid in the polymer phase depends on temperature as well. Once operating ranges for prospective adhesives were determined, the second prototype was developed.

The first prototype had a fundamental flaw that was not for seen, it did not possess an internal mixing apparatus. As a result, the adhesive systems separated in the can and did not spray adequately. In order to address this flaw, system 2 was adopted. The system, shown in Figure 14.3 utilizes a circulating pump and a two hose system to both continually mix the system and to avoid any temperature or concentration gradients. System 2 is cart mounted making it highly portable. It also was designed to serve as a filling station for system 3, Figure 14.4, a hand held apparatus similar to system 1 that enabled mixing. System 2 was highly successful and the results of spray testing shown elsewhere in this report are derived from this system.

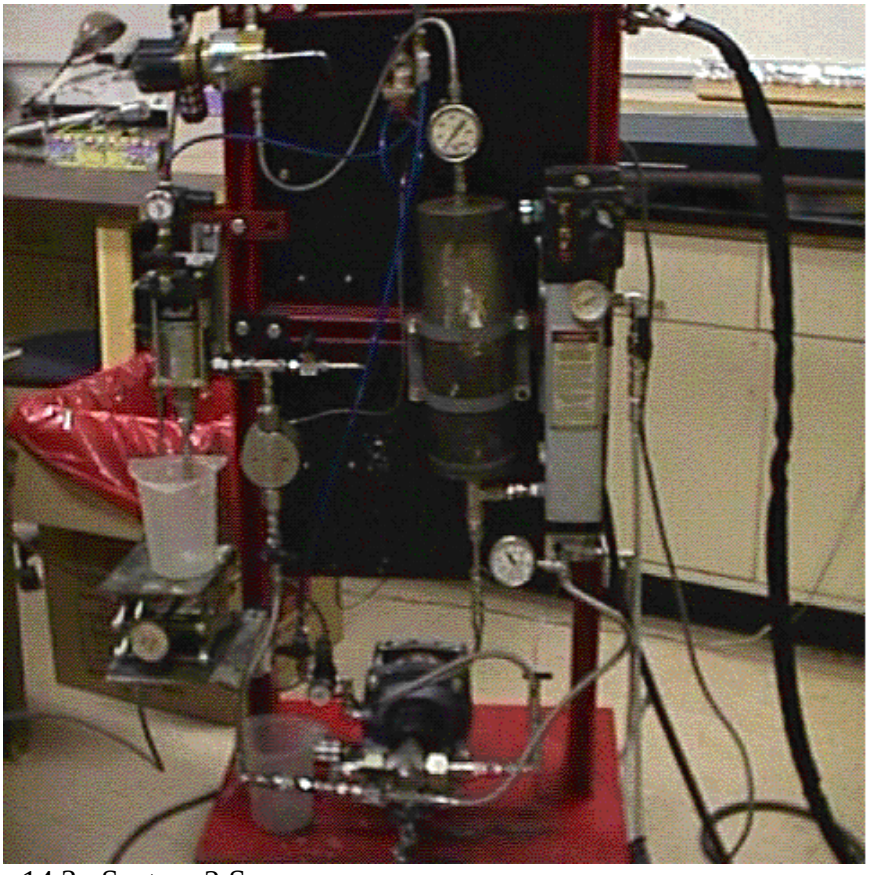

Figure 14.3 –System 2 Sprayer

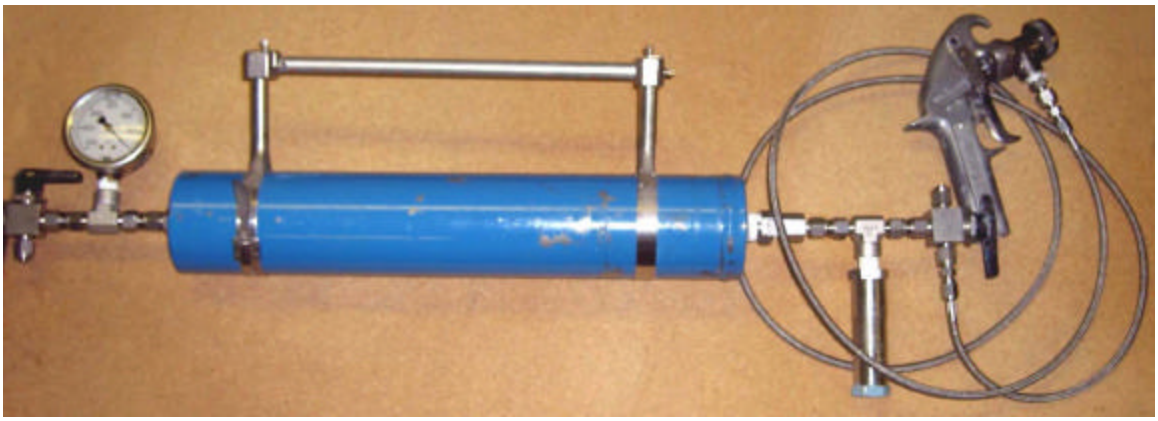

Figure 14.4- System 3 Handheld Sprayer

15. Performance

Adhesive formulation is the optimization of mixtures properties for a specific application. For this project, the focus is on nonstructural (contact) adhesives such as those widely used in repair and maintenance applications. The current products are aerosol can or pressure pot sprayer applied solvent borne products. They typically contain a base polymer, tackifiers, additives, and solvents. The tackifiers serve to modify the applicator's feel or perception of the product while modifying more tangible properties such as open time. The other additives include high temperature modifiers, antioxidants, reaction modifiers, and colorants. Solvents are chosen to either dissolve the other components or to modify the viscosity and evaporate quickly. This leads to the terms slow solvent for the solvent responsible for dissolution of the polymer and other components and fast solvent for the viscosity reducing solvent. In order to investigate the performance of a formulated adhesive, a widely-used formulation served as the starting point.

The base formulation for the commercial adhesive was taken from *Adhesive Technology Handbook* by Noyes (1). It is a widely used starting formulation for neoprene adhesives and contains the following in weight percent:

- Neoprene 14 %
- Toluene (slow solvent) 62 %
- Hexane (fast solvent) 17 %
- Phenolic Resin (high temperature strength) 5%
- Magnesium Oxide (to activate phenolic resin) 1 %
- Zinc Oxide (aids magnesium oxide) 0.7%
- Water 0.1 %
- Antioxidant 0.2 %

In order to determine the effect of various formulation differences, the following samples were tested. The number corresponds to the bar chart shown below.

1. Neoprene dissolve in toluene at 18 weight percent
2. Commercial formulation purchased from a supplier
3. Formulation as described above
4. Formulation as described above without hexane (Suitable for UNICARB application)
5. Formulation as described above without hexane and with 12 % by weight hydrocarbon tackifier added
6. Formulation as described above without hexane and with 3 % by weight hydrocarbon tackifier added
7. Formulation as described above without hexane and with 3 % by weight hydrocarbon tackifier added and a 10% reduction in toluene
8. Formulation as described above without hexane and with 3 % by weight hydrocarbon tackifier added and a 20% reduction in toluene

Lap Shear Test using 2024 T3 Aluminum per ASTM D1002 (2)

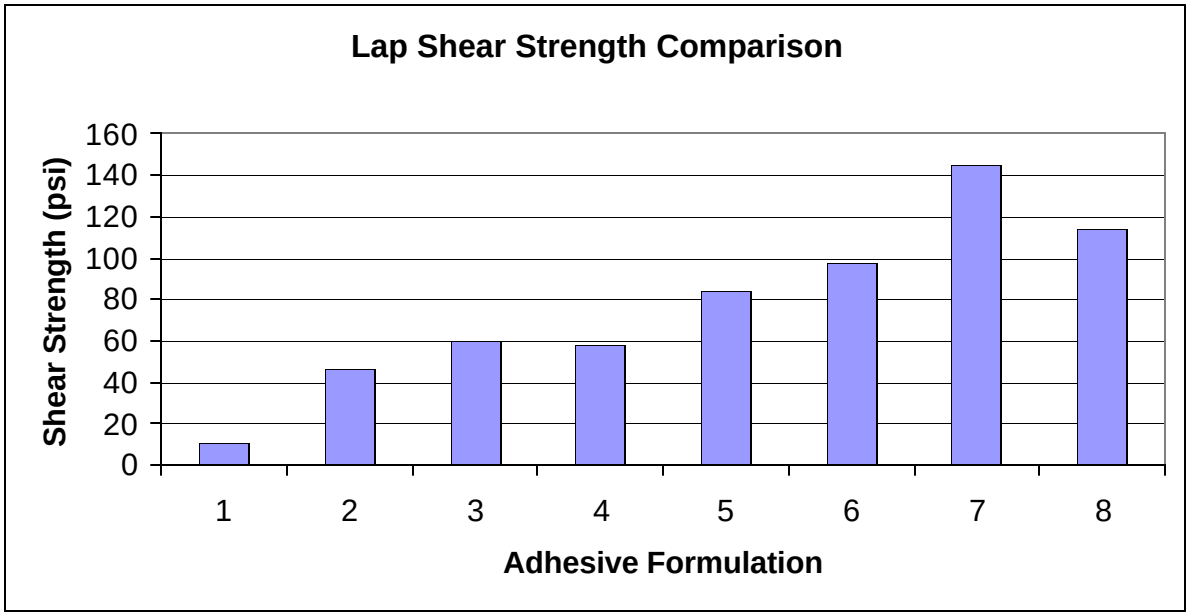

Figure 15.1 – Lap Shear Strength Comparison

As expected, each of the formulated products exhibited an improvement in lap shear strength over neoprene in toluene. The large improvements in performance occurred with the introduction of a tackifier resin. In this case, the resin served to extend open time and enhance the bonding. The optimum ratio appears to be a 10% reduction in slow solvent with 3 weight pecent tackifier. The 100 parts tackifier resulted in a softer final product and reduced lap shear strength and the 10% reduction showed an enhancement over either full slow solvent or a 20% reduction. The reason for this may be two fold; the greater solvent is trapped causing reduced strength while the 20% reduction does not have sufficient solvent for uniform polymer-tackifier interaction.

Performance testing of sprayed test coupons was undertaken to determine the role of multiple passes in the performance of the adhesive. As can be seen from the results, the multiple pass sprayed samples compare very well with the drawn samples. This indicates that we are applying an even and regular coating on the test coupons and can expect to achieve the same results in service.

	SIS			**Neoprene**	
Number of Spray Passes	Stress at Peak Load (psi)	Standard Deviation	**Number of Spray Passes**	Stress at Peak Load (psi)	Standard Deviation
Drawn	33.14	5.74	**Drawn**	51.24	2.77
1	0	0	**1**	41.84	19.07
2	14.59	9.13	**2**	49.58	13.87
3	16.04	2.44	**3**	51.82	6.71
4	Not tested	Not tested	**4**	40.31	13.97
5	35.52	19.65	**5**	44.94	26.11
10	28.98	5.63	**10**	Not tested	Not tested

Figure 15.2 – Impact of Number of Passes on Shear Strength

Data for the other systems studied are shown in Figure 15.3. The values are presented in their raw form since they are not final formulated adhesives. The key for the Figure follows.

15.1 References

1. H Landrock, *Adhesives Technology Handbook*, Noyis Publications, Park Ridge, NJ 1985.
2. *ASTM Book of Standards*. D1002-01,**15**, 2002, 46-50

16. Conclusions

16.1 Summary

In this report, the application of the UNICARB© process to the spraying of adhesives was discussed. Using supercritical carbon dioxide as a viscosity reducer, the UNICARB© process is one of several applications in which carbon dioxide behaves as a solute. The work presented in Chapter 1 was aimed at demonstrating the various ways that supercritical carbon dioxide can behave as a solute, or simultaneously as solute and solvent. It also was intended to clarify the misconception that supercritical carbon dioxide is only useful as a solvent and that its usefulness is limited by its lack of solvent power. When used as solute, the fact that supercritical carbon dioxide is a bad solvent is not important; rather, its main advantages are good diffusivity and low viscosity.

For an adhesive to be sprayed using the UNICARB© process, the adhesive mixture must undergo two phase transitions starting from a single-phase liquid mixture to become a mixture consisting three phases (LLV). Thus, the success of the UNICARB© process is determined largely by the supercritical phase behavior of polymer-solvent-carbon dioxide system. The work in Chapter 3 reviewed the important phase behavior of polymeric mixtures. In addition, data were presented to amend the current understanding of polymeric mixtures by showing an unusual L-LF phase transition at high carbon dioxide concentration.

The work in Chapters 4-9 has demonstrated that UNICARB© process can be applied to the spraying of adhesives through the investigation of the phase behavior of various common adhesive formulations mixed with supercritical carbon dioxide. The

polymers studied included block copolymers, polychloroprene, and polyacrylate. Below are summaries of the conclusions made in Chapters 4-9:

- SIS:Toluene systems formulated at 1:3 and 17:33 ratio exhibited only bubble point transitions in the range of carbon dioxide concentrations and temperatures studied. As carbon dioxide concentration was increased, the vapor pressure curves shifted upward and became slightly steeper. At 2:3 ratio, the SIS:Toluene system showed both bubble point and cloud point transitions. The vapor pressure curve was steeper than the LCST curve, and one possible cause was the high carbon dioxide concentration at 32 wt. %.
- SEBS:Toluene systems formulated at 1:3 and 1:2 ratio exhibited only bubble point transitions in the range of carbon dioxide concentrations and temperatures studied. At 1:2 ratio, bubble points that appeared like cloud points were visually observed. As carbon dioxide concentration was increased, the vapor pressure curves shifted upward and became slightly steeper. At 2:3 ratio, the SIS:Toluene system showed both bubble point and cloud point transitions. The vapor pressure curve was again steeper than the LCST curve, and one possible cause was the high carbon dioxide concentration at 31 wt. %.
- Polychloroprene:Toluene systems formulated at 9:41 and 1:3 ratio exhibited only bubble point transitions in the range of carbon dioxide concentrations and temperatures studied. A phenolic-polychloroeprene adhesive was tested and only showed bubble point transitions, too. As carbon dioxide concentration was increased, the vapor pressure curves shifted upward and became steeper. Because

these systems were cloudy, but no cloud point transition was found over the range of pressures, temperatures, and compositions studied here. It is not clear whether this system will exhibit a decompressive spray in the UNICARB® process.

- The acrylic Morstik® adhesive exhibited both cloud point and bubble transitions. As carbon dioxide concentration was increased, the vapor pressure curves shifted upward and became steeper. At the highest carbon dioxide concentration, 42.2 wt. % and 70 ^{o}C, a cloud point was found. The 8:1 Morstik:Toluene system did not exhibited any cloud point transition over the range of compositions and temperatures studied.

Both cloud points and bubble points were found for two block copolymer systems and one polyacrylate system. These systems could be used as the staring formulation for adhesives that will be sprayed using the UNICARB® process, and the operating condition could be determined from the phase boundaries measured experimentally.

16.2 Future Work

In Chapters 4 through 9, preliminary data showed that the polymeric systems underwent phase transitions at higher pressures when expanded dynamically than statically. However, there were inconsistencies in the data for polychloroprene and polyacrylate systems, and this had resulted in the large uncertainties and the lack of explanation for some results. More importantly, it is inconclusive whether the phase transitions actually occurred at higher pressure when expanded rapidly due to the large uncertainties. Although speculations were made to account for inconsistency in

experimental data, finding and eliminating the cause for inconsistency remained a key aspect of this research. One method of troubleshooting for error is to perform experiments on a system that already has been studied extensively, such as polystyrene. Thus, error can be determined by comparing data obtained with published data. The experimental apparatus also could be improved to eliminate some of the problems encountered. Adding a recirculating pump to the high pressure cell should improve the efficiency of mixing viscous polymeric solutions, and reduce temperature and concentration gradients.

So far, the scope of this work has been limited to developing solvent-borne contact adhesive systems. In the future, the research can be expanded to study hot-melt contact adhesives. Hot-melt adhesive is attractive because it does not require additional viscosity reducer other than supercritical carbon dioxide. As a result, VOC emission caused by the release of conventional organic solvent can be eliminated. One of the obstacles in studying hot-melt adhesives is eliminating cold spots in the apparatus that will cause the polymer to solidify if not hot enough. Another problem that requires careful consideration is the effect of temperature variation on the performance of the adhesive during spraying. Slight temperature variations do not significantly change phase behavior of a solvent-borne adhesive, but the same temperature variations can cause a hot-melt adhesive to solidify before atomization.

In addition to hot-melt adhesives, this research also can be expanded to investigate the potential to apply the UNICARB® process to other spraying applications, such as the spraying of inks. Ink formulation consists three major parts: pigments, vehicles, and solvents. The pigments are carried by liquid vehicles (usually oil), whose

viscosity is reduced by the "solvents". As in paints and adhesives, the solvents are actually viscosity reducers, which thermodynamically behave as "solutes". Thus, it may be possible to replace the conventional viscosity reducers with supercritical carbon dioxide and obtain the environmental benefits and the better performances brought by the UNICARB® process. Some possible ink systems to be reformulated include packaging ink, gravure ink, and metallic ink, all of which uses toluene and/or methyl ethyl ketone as viscosity reducer.

17. Transition Plan and Recommendations

The transition plan for this project has changed several over during the course of research and development. The opportunities for application of the technology are so widespread that many more applications will arise in the future.

The transition plan at the time of the proposal leading to this project predicted that a replacement for all nonstructural adhesives was possible using UNICARB. That has been shown to be correct from a technical standpoint but barriers to the adoption of new technology for niche applications such as adhesives are very high. In applications where only occasional adhesive use is required, a switch to a UNICARB system is not practical due to the changes that occur in the adhesives when they are held at pressure for a long periods and the initial cost of the equipment.

As a result of these findings, opportunities for application of the technology in more appropriate settings have been sought. The settings that have been determined to possess the highest potential for success are short duration, high volume applications and applications in adverse environments where both water and organic solvents are problematic.

The first opportunity to attempt to adapt the system for this type of application is currently underway at NSWC-Indian Head under the leadership of Randy Cramer and Jerry Salan. Their needs meet both of the criteria set forth above, the need for a high volume, short duration application and the presence of an adverse environment. In addition, the spray target is special in that it is energetic, making the possibility of zero solvent very attractive from a safety standpoint. A paper submitted for a recent JANNAF meeting may be found in Appendix B.

As other opportunities for expanding the application of this technology are investigated, we will continue to adapt our work. The flexibility of the system and the vast number of adhesives that can be used means that we have just scratched the surface on potential applications. In addition, the work with melt state polymers that was originally beyond the scope of the project, shows that it is possible to spray zero VOC adhesives using the UNICARB system. It is this opportunity that may have the greatest potential since it would be possible to replace both solvent and water bourne adhesive systems in virtually any application that currently uses sprayable adhesives.

Recommendations for optimal transition of the technology include standardization of adhesive application processes across DoD, elimination of noncompliant adhesives from use, and greater training of technicians and others responsible for adhesive use. The greatest barrier to the use of novel technology is the resistance of both end users and procurement agents to adopt new technology. In this project, it proved to be impossible to replace casual adhesive use, especially aerosol can adhesives, at the depot level because the usage was too low to justify the adoption of the needed equipment. In the future, it will be necessary to determine the overall usage requirements in individual settings prior to attempting integration of the technology.

The best opportunities for adoption of the technology developed by this project are in settings that require either continuous or semicontinuous adhesive spraying where emissions are a concern and the lack of reactivity of the carbon dioxide is an advantage. These settings include system manufacturing, rapid prototyping, and appliqué applications. We are working closely with a new DARPA research center at Johns Hopkins to adapt the UNICARB system for the application of adhesives for appliqué for

DoD applications. These niche opportunities appear to hold the greatest promise for the technology to grow in DoD.

In industrial settings, many opportunities exist for integration of the technology at the OEM level. Since large volumes and continuous processes are more appropriate in these settings, it is possible for UNICARB to be adopted for adhesives in much the same fashion that it has been adopted for paints and coatings. We are currently working with Dow Chemical to identify opportunities for industrial applications.